University of Alberta

STUDIES OF DIRECT - SAMPLE - INSERTION INDUCTIVELY - COUPLED - PLASMA MASS SPECTROMETRY

by

SHIJUN SHENG ©

A thesis submitted to the Faculty of Graduate Studies and Research in partial fulfillment of the requirements for the degree of **Master of Science**.

Department of Chemistry

Edmonton, Alberta

Fall, 1999

National Library of Canada
Acquisitions and Bibliographic Services
395 Wellington Street
Ottawa ON K1A 0N4
Canada

Bibliothèque nationale du Canada
Acquisitions et services bibliographiques
395, rue Wellington
Ottawa ON K1A 0N4
Canada

Your file Votre référence

Our file Notre référence

The author has granted a non-exclusive licence allowing the National Library of Canada to reproduce, loan, distribute or sell copies of this thesis in microform, paper or electronic formats.

L'auteur a accordé une licence non exclusive permettant à la Bibliothèque nationale du Canada de reproduire, prêter, distribuer ou vendre des copies de cette thèse sous la forme de microfiche/film, de reproduction sur papier ou sur format électronique.

The author retains ownership of the copyright in this thesis. Neither the thesis nor substantial extracts from it may be printed or otherwise reproduced without the author's permission.

L'auteur conserve la propriété du droit d'auteur qui protège cette thèse. Ni la thèse ni des extraits substantiels de celle-ci ne doivent être imprimés ou autrement reproduits sans son autorisation.

0-612-47094-6

Canada

University of Alberta

Library Release Form

Name of Author: SHIJUN SHENG

Title of Thesis: STUDIES OF DIRECT-SAMPLE-INSERTION INDUCTIVELY-COUPLED-PLASMA MASS SPECTROMETRY

Degree: MASTER OF SCIENCE

Year this Degree Granted: 1999

Permission is hereby granted to the University of Alberta Library to reproduce single copies of this thesis and to lend or sell such copies for private, scholarly, or scientific research purposes only.

The author reserves all other publication and other rights in association with the copyright in the thesis, and except as hereinbefore provided, neither the thesis nor any substantial portion thereof may be printed or otherwise reproduced in any material form whatever without the author's prior written permission.

Shijun Sheng

11123, 71 Ave. Edmonton
Alberta AB T6G 0K3

Date: Aug , 1999

University of Alberta

Faculty of Graduate Studies and Research

The undersigned certify that they have read, and recommend to the Faculty of Graduate Studies and Research for acceptance, a thesis entitled STUDIES OF DIRECT - SAMPLE - INSERTION INDUCTIVELY - COUPLED - PLASMA MASS SPECTROMETRY submitted by SHIJUN SHENG in partial fulfillment of the requirements for the degree of MASTER OF SCIENCE.

Gary Horlick

Dr. G. Horlick, Supervisor

M. McDermott

Dr. M. McDermott

R. Creaser

Dr. R. Creaser

DATE: July 8, 1999

To my Wife Zhaohui and my parents back home

ABSTRACT

Direct sample insertion for the inductively coupled plasma (DSI-ICP) is a sample introduction technique that can handle both solid and liquid samples. This thesis presents the studies of Direct Sample Insertion Inductively Coupled Plasma Mass Spectrometry (DSI-ICP-MS) technique that combines the advantages offered by both the DSI and ICP-MS.

Characterizing and optimizing the parameters of both DSI and ICP-MS, especially the transient signal acquisition parameters were investigated in the first part of this thesis. The analytical performance of this DSI-ICP-MS technique was demonstrated with liquid standard solutions containing Pb, Bi, In, Ag, Fe, Co, Mn, Cu, Ga, As, Sb, and Se. Analytical curve figures of merit were obtained including relative standard deviation (%RSD), detection limit, calibration function slope, correlation coefficient, linear range, and effect of internal standardization. The analytical ability of this technique was explored with some real biological samples---a series of NIST (USA) and NIES (Japan) botanical standard reference materials (SRMs). Once reliable and stable instrumental conditions were established, the direct measurement of Pb, As, and Sb was investigated in these SRMs with different calibration

methods (internal standardization, external calibration and standard additions), without any labor intensive pretreatment. The results agreed well with the certified values. The research shows that DSI-ICP-MS is a reliable, fast, relatively simple and precise technique for trace element determinations in solid biological samples.

ACKNOWLEDGEMENT

I would like to thank my research director Dr. Gary Horlick for his guidance, support, and patience throughout this work. I would also like to thank Mr. Youbin Shao. I have learnt a lot from him. Financial support provided by the Department of Chemistry at the University of Alberta, and the National Science and Engineering Research Council (NSERC) is also gratefully acknowledged.

TABLE OF CONTENTS

CHAPTER PAGE

1. Introduction

1.1 Inductively Coupled Plasma (ICP) 1

1.2 Sample Introduction System 2

1.3 Direct Sample Insertion (DSI) 4

1.3.1 Device development 4

1.3.2 Materials and designs for the sample carrying Probe 8

1.3.2.1 Graphite Cup 8

1.3.2.2 Wire- loop DSI 13

1.3.3 Applications of DSI 14

1.4 Thesis Outline 19

References 21

2. Effect of Operating Parameters on Analytical Signals in DSI-ICP-MS

2.1 Introduction 25

2.1.1 Inductively coupled plasma mass spectrometry (ICP-MS) 25

2.1.2 ICP-MS instrumentation 26

2.1.3. DSI as a sample introduction system for ICP-MS 29

2.1.4. Operating parameters of DSI-ICP-MS 31

2.2 Experimental 32

2.3 Results and Discussion 34

2.3.1 ICP-MS parameters 34

2.3.1.1 Forward power 34

2.3.1.2 Gas flow rates 35

2.3.1.3 Other ICP-MS parameters 37

2.3.2 DSI parameters 38

2.3.2.1 Drying position 38

2.3.2.2 Atomizing position 38

2.3.3 Transient signal acquisition 40

2.3.3.1 Effect of dwell time on data acquisition points/s 40

2.3.3.2 Effect of dwell time on background baseline noise and detection limits 49

2.4 Conclusion 53

References 55

3. Measurement of Pb, Bi, Ag and In By DSI-ICP-MS

3.1 Analytical Performance of DSI-ICP-MS for Pb, Bi, Ag and In 57

3.1.1 Introduction 57

3.1.2 Experimental 58

3.1.3 Results and discussion 59

3.1.3.1 Analyte and background signals 59

3.1.3.2 Internal standardization 64

3.1.3.3 Analytical curve figures of merit 66

3.1.4. Conclusion 70

3.2 Measurement of Pb in Solid Biological Samples 70

3.2.1 Introduction 70

3.2.2 Experimental 73

3.2.3 Results and discussion 74

3.2.3.1 Matrix effect 74

3.2.3.2 Calibration methods for Pb measurement in powdered plant tissues 77

3.2.4 Conclusion 87

References 88

4. Measurement of Fe, Co, Mn and Cu by DSI-ICP-MS

4.1 Introduction 91

4.2 Experimental 93

4.3 Results and Discussion 96

4.3.1 Signal time profiles 96

4.3.2 Analytical curve figures of merit 98

4.4 Conclusion 102

References 105

5. Measurement of As, Sb and Se by DSI-ICP-MS

5.1 Measurement of As, Sb and Se in Standard Solutions 106

5.1.1 Introduction 106

5.1.2 Experimental 108

5.1.3 Results and discussion 111

5.1.3.1 Signal time profiles 111

5.1.3.2 Effect of Pd/Mg chemical modifier 113

5.1.3.3 Analytical curve figures of merit 116

5.1.3 Conclusion 120

5.2 Measurement of As and Sb in Solid Biological Samples 123

5.2.1 Introduction 123

5.2.2 Experimental 124

5.2.3 Results and discussion 125

(1) External calibration by liquid standard Solutions 125

(2) Standard addition 130

(3) External calibration by different SRMs 136

(3) External calibration by same SRM with different masses 138

5.2.4 Conclusion 140

References 141

6. Conclusion and future work 143

LIST OF TABLES

TABLE PAGE

2.1 Parameter settings for the acquisition of transient Signals 41

2.2 Summary of DSI-ICP-MS instrumental parameters 54

3.1 Summary of analytical curve figures of merit 67

3.2 Measurement of Pb concentration in SRMs 81

4.1 Summary of DSI-ICP-MS instrumental parameters 94

4.2 Summary of analytical curve figures of merit 101

5.1 Summary of DSI-ICP-MS instrumental parameters 109

5.2 Summary of analytical curve figures of merit 119

5.3 Measurement of As and Sb in plant samples 129

LIST OF FIGURES

FIGURE PAGE

1.1 Graphite cup configurations 10

1.2 Graphite sample probe geometries 12

2.1 Schematic diagram of the Perkin-Elmer/SCIEX ELAN 250/500 ICP-MS system 27

2.2 Schematic diagram of DSI device for ICP-MS 30

2.3 Schematic illustration of DSI-ICP-MS 33

2.4 Signals for 1 ppm Cu and Ga (10 uL) (5 consecutive insertions) at a power of 1.5 kW.....36

2.5 Time profiles of 1ppm Pb, Bi, Ag and In with different dwell times 45

2.6 Effect of dwell time on data acquisition points/s 47

2.7 Effect of dwell time on signal intensities (peak area) for 1ppm Pb, Bi, Ag, and In (10 uL) 48

2.8 Signal and baseline of 0.01ppm Pb with different dwell times 50

2.9 Effect of dwell time on background standard deviation

For Pb, Ag and In 51

2.10 Effect of dwell time on detection limits for Pb, Ag and In 52

3.1 Time profiles of 1 ppm Pb and In, 0.5 ppm Bi and 2 ppm Ag by DSI-ICP-MS 61

3.2 Low level signals for (a) 20pg Pb, (b) 20 pg Bi, (c) 80 pg Ag, and (d) 60 pg In 63

3.3 Instrument stability of DSI-ICP-MS (a) without internal standard, (b) with Bi as internal standard 65

3.4 Calibration curves (log-log) of Pb, Ag, and In (5 ng Bi as internal standard) 69

3.5 Time profiles of 1 ppm Pb and Bi in (a) water solution, and (b) CSF matrix 76

3.6 Pb signals in solid plant SRMs: (a) 4 mg spinach, (b) 2 mg tomato leaves, (c) 2 mg pine needles, (d) 1.5 mg orchard leaves, and (e) 2 mg pepperbush 80

3.7 Calibration curve of Pb using solid plant SRMs with 5 ng Bi as internal standard 83

3.8 Calibration curve of Pb using solid plant SRMs (without internal standard) 86

4.1 Signal time profiles of 1 ppm Fe, Co, Mn and Cu

in DSI-ICP-MS 97

4.2 Low level signal time profiles for (a) 1000 pg Fe, (b) 200 pg Co, (c) 100 pg Mn, and (d) 200 pg Cu 100

4.2 Calibration curves (log-log) of Fe, Co, and Mn with 10 ng Cu as internal standard 104

5.1 Signal time profiles of 1 ppm As, Sb and 10 ppm Se by DSI-ICP-MS 112

5.2 Low level signal time profiles of (a) 100 pg As, (b) 100 pg Sb and (c) 1000 pg Se78 115

5.3 Effect of Pd/Mg chemical modifier on the signal intensities (peak area) of 1 ppm As and Sb 117

5.4 Signal time profiles of 1 ng As and Sb (a) without modifier, and (b) with 500 ng Pd/Mg midifier 118

5.5 Calibration curves (log-log) of (a) As, (b) Sb, and (c) Se78 with 5 ng In as internal standard 122

5.6 As and Sb signal time profiles of (a) 6.2 mg spinach, (b) 6.0 mg tomato leaves, (c) 6.1 mg pine needles, (d) 2.2 mg orchard leaves and (e) 5.0 mg pepperbush 128

5.7 As and Sb signal time profiles in (a) 1 ppm As and Sb liquid solution, (b) 2.5 mg orchard leaves, (c) 2.5 mg orchard leaves spiked with 60 ng As and 20 ng Sb 133

5.8 Calibration curves of (a) As and (b) Sb in orchard leaves by standard addition method 134

5.9 Calibration curves of (a) As and (b) Sb in pepperbush by standard addition method 135

5.10 Calibration curve of As containing four SRMs: spinach, pine needles, tomato leaves, and orchard leaves 137

5.11 Calibration curves of (a) As, and (b) Sb containing different weights of orchard leaves 139

Chapter 1

Introduction

1.1 Inductively Coupled Plasma (ICP)

Since its introduction by Greenfield et al. [1] and Wendt and Fassel [2] in 1964, the ICP has become the most powerful source for elemental analysis. It has been used as a source for techniques such as Atomic Emission Spectrometry (AES) [1, 2], Atomic Fluorescence Spectrometry (AFS) [3, 4] and Mass Spectrometry (MS) [5, 6]. These ICP based techniques have been used for trace element determinations in a wide variety of fields. These fields include the analysis of natural and industrial waters, metals, agricultural materials, biological materials (fluids and solids), geological solids (rocks, ores and soil) and environmental materials. Compared to other sources, such as flame, arc, and spark based techniques, the ICP is an almost ideal source for vaporization, atomization, ionization and excitation. Excellent features of ICP spectrometers include [7]:

- Simultaneous multielement analysis for most (70) elements (qualitative and quantitative)
- Low detection limits (ppb for emission and ppt for mass spectrometry)

- Relative freedom from matrix interference
- Wide linear dynamic range (4 to 6 orders of magnitude concentration range)
- Precision of measurement (%RSD: 1-3%)
- Rapid analysis

1.2 Sample Introduction System

ICP determinations are normally restricted to solution samples as pneumatic nebulization is the most widespread method for sample introduction. The popularity of this system owes much to its simplicity, rapid sample change over, relatively good stability and low cost. But it also has important drawbacks:

(1) Low sample transport efficiency.

The use of a pneumatic nebulizer and spray chamber results in low sample transport efficiency. Typically only 1-2% of the sample eventually reaches the plasma through this introduction system.

(2) The need for relatively large sample amounts.

The required volume is at the milliliter level. This requirement restricts the analysis of small samples, for example, micro or nanoliter size samples.

(3) Solution and solvent limitation.

When sample solutions contain high quantities of salts or dissolved solids, clogging of the nebulizer and the MS interface may occur. Also, the analysis of samples in organic solvents is impossible because carbon can condense on the sampler, skimmer, and lenses, causing significant contamination to the instrument.

Because the pneumatic nebulizer is the most common sample introduction method, analysis of solid samples generally requires the use of some form of sample pre-treatment (i.e. digestion or extraction). Many problems are associated with these procedures, such as contamination from acids, solvents, or reagents; dilution or even loss of already low level analyte concentrations; formation of polyatomic matrix-related species due to the addition of acids and other reagents; and large sample quantity requirements. Therefore, it is desirable that a method for the direct analysis of solid materials be established.

There have been a number of sample introduction methods proposed for the direct analysis of solid samples by ICP spectrometers, including electrothermal vaporization (ETV) [8, 9], laser ablation [10, 11], and arc

nebulization [12]. In these sample introduction techniques, the generated dry solid aerosol is transported into the plasma with a stream of carrier gas and transport losses may occur. Loss of the sample during transport to the plasma commonly causes poor precision and memory effects from run to run. This problem can be overcome when inserting the sample directly into the ICP.

1.3 Direct Sample Insertion (DSI)

1.3.1 Device development

The DSI technique was first introduced to ICP spectrometers by Salin and Horlick [13] in 1979. By its name, DSI is a technique that allows for the direct insertion of a small amount of sample (powders, solids, or desolvated liquids) into the central core of the ICP. In their device, conventional dc arc undercut graphite cups containing samples were inserted manually into a modified ICP torch. The plasma was ignited by the graphite electrode with a power of 2.5 kW on each insertion. In their preliminary research, desolvated liquids, powder samples (Spex graphite powder), and solid samples (NIST coal and Orchard leaves) were tested, and some qualitative and

semiquantitative results were obtained. Their results proved that the DSI technique had the potential to significantly expand the overall analytical capability of the ICP. The main disadvantage of this initial design was that the plasma had to be ignited and extinguished on each insertion.

Later, continuous plasma operation was achieved by Sommer and Ohls [14]. In their device, a graphite crucible containing samples was inserted into a 3 kW argon-nitrogen plasma using a pneumatic elevator device. Detection limits were improved by one order of magnitude using their device compared with solution nebulization. But their device was only practical using a high-power ICP.

Kirkbright and coworkers [15, 16] were able to introduce sample into a low power (<1.5 kW), continuously running ICP supported on a demountable torch. They used an axial flat-ended graphite rod onto which 5 uL of sample solution could be applied with a micropipet. Both volatile elements and refractory elements were tested. An Argon-0.1% Freon 23 gas mixture was used to improve the volatilization of refractory carbide-forming elements.

Pettit and Horlick [17, 18] developed a new automated DSI device, in which the sample-carrying cups were sequentially and automatically inserted into the ICP using a pneumatic controlled transport system, without disturbing ICP operation. This device allowed for sample cup location (relative to the plasma) to be programmed through "dry", "ash" and "vaporize" cycles. The system was applicable to the analysis of both small volumes of liquid (10 uL) and small amounts (10 mg) of powders.

A microprocessor-controlled DSI and accompanying software design were developed by Zhang et al. [19]. The insertion of the rod, and the desolvation and ashing of sample solutions were controlled by a microprocessor-controlled stepper motor. The precision was improved by the programmed drying and ashing stages (a relative standard deviation (%RSD) for 7 measurements of 50 ppb Mg was 2%).

An automated DSI for ICP-AES was developed by Horlick and coworkers [20, 21, 22]. An elegant improvement in the mechanical design of DSI was made by Shao and Horlick [20], and it was further developed by addition of a computer-controlled stepper motor to allow more flexible control over cup insertion position. A computer-controlled stepper-motor-driven DSI with

full software support was introduced by Karanassios and Horlick [21]. In this approach, a 24-position autosampler carousel was modified to accommodate sample probe assemblies. The computer controlled system allowed for precise positioning of the probe in or outside (below) the plasma. The thermal gradient below the plasma could be used for sample drying and ashing before the atomizing step. An extensive window-based software package was developed to support this system. A four-channel direct reader system for transient spectral signal acquisition was also developed for this device. An alternative approach to automated DSI was reported by Chan and Horlick [22]. In addition to a computer-controlled stepper motor, a small robot arm was used to automate exchange of the graphite cup sample probes, yielding improved analytical performance.

Karanassios and Horlick [23] extended DSI to ICP-MS in 1989. A mechanical, stepper-motor-driven, computer-controlled DSI device and a full software support system were designed and developed to interface to the Sciex Elan 250 ICP-MS. Compared to its AES counterparts, it was a more elaborate design. A unique feature was the ability of the probe to swing from the vertical plane, where the sample loading took place, to the horizontal plane, which was required for probe insertion. The translation platform also

allowed precise alignment of the probe with the sample orifice of mass spectrometer. Software was also developed to acquire the multielement transient signals generated by DSI for ICP-MS. Background spectral characteristics in this "dry plasma" were documented [24], and some spectral interferences and matrix effects were discussed [25].

1.3.2 Materials and designs for the sample carrying probe

1.3.2.1 Graphite Cup

In the first report on DSI by Salin and Horlick [13], the sample container was a conventional undercut graphite cup used in dc arc emission spectrometry. The graphite cup was mounted on the end of a quartz rod. The authors found it necessary to desolvate liquid samples prior to insertion. This was accomplished by inductively heating the electrode before igniting the plasma. Inductive heating might also be useful for ashing solid samples directly in the cup. Due to the inert Ar atmosphere of the plasma, essentially no consumption of the electrode occurred, and the cup could be reused.

Kirkbright and his colleagues [26] investigated four different graphite cup designs (Fig. 1.1) in order to improve the performance of the DSI cup. All cups were supported by alumina rods. The first design (A) looked similar to a standard dc arc graphite electrode. The remaining designs (B, C, D) were different from the first in that the undercut portions extended much further and connected to the alumina rod directly (no graphite rod between the cup and alumina rod). Design C had a glassy carbon undercut portion. Design D had a very narrow undercut portion and therefore the smallest mass of graphite. After comparing the heating and cooling curves with respect to time for the four designs, and the signal responses for Ni, Cr, Mn, and Pb with the cup configurations investigated, they concluded that design D had the best performance. The reason seemed to be its small heat capacity which resulted in rapid heating allowing for the efficient removal of the sample from the cup. This produced a relatively high transient and localized concentration of the analyte, thus resulting in high sensitivity.

Shao and Horlick [20] investigated quantitatively the effects of different cups on the performance of DSI. They used three different sizes of cup (diameter 3 mm, 4.5 mm, and 6 mm), among which, the 4.5-mm-diameter cup exhibited the best precision, with an overall %RSD of 3.3%. The

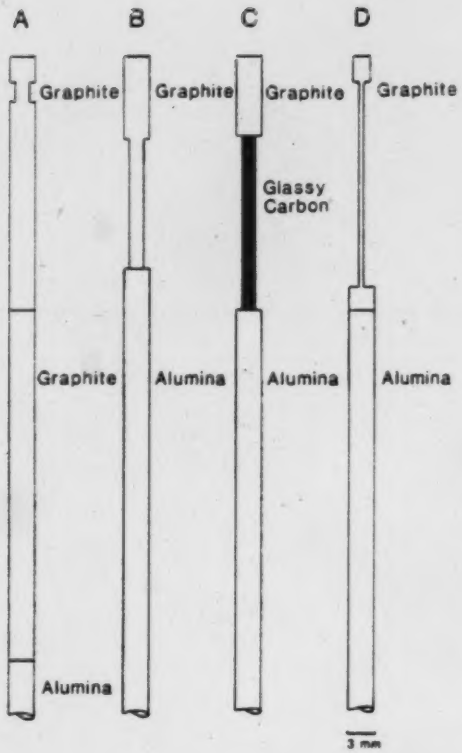

Fig. 1.1 Graphite cup configurations

poorer precision for the smaller cup was thought to be a result of the shorter signal time behavior exhibited by this cup size. On the other hand, the larger cup was somewhat more disruptive of the plasma shape when it was inserted into the plasma, making the signals less reproducible.

Karanassiors et al. [27] investigated the effect of probe geometry on transient signal characteristics. Four probe geometries were chosen for their study, in which the first three were standard commercial available dc arc electrodes from SPEX Industries, and the fourth was a custom made long undercut cup machined out of the corresponding regular electrode (Fig. 1.2). The long undercut cup yielded the strongest signal and the shortest appearance time. The smallest signals and larger appearance times resulted from the larger diameter electrodes. The long undercut geometry should be one of the best in rapidly attaining its maximum temperature in the plasma.

Skinner and Salin [28] modified the cup design further. The basic design of their cup was that there was a hole through the base of the cup, and the stem (glass shaft). Carrier gases could be introduced into the cup via the hollow stem, resulting in a reduction in the background signal in axial viewing AES. When 1000 ppm Freon-12 in Argon was used as a carrier gas through the

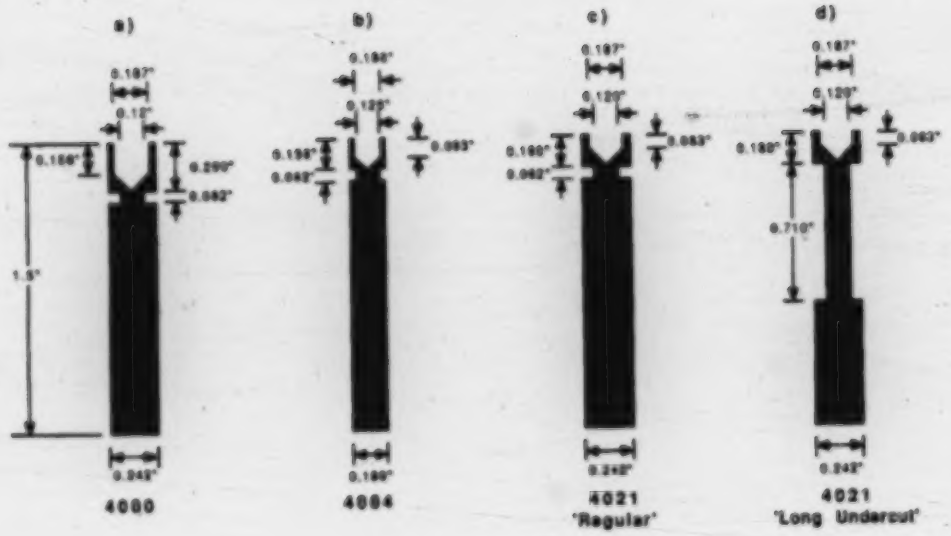

Fig. 1.2 Graphite sample probe geometries

center of the cup, refractory elements were vaporized easily.

Graphite is a favored material for cups due to its heating characteristics, its ease of machining, and the relative simplicity of background spectral features in ICP-AES and MS [24]. A drawback of graphite is carbide formation for some elements. Pettit and Horlick discussed the analytical character of cups made of Ta, Mo, and W. The use of a metal cup enhanced significantly the signal intensity of refractory elements (e.g. Ni) as there was no carbide formation utilizing these metal cups. With about 1% H_2 in the coolant gas (outer plasma gas), the metal cups remained clean and were reusable several hundred times. The highest signal intensities and the best signal precisions (%RSD of 1.8%-4.5%) were obtained with a W cup with 1%H_2/Ar coolant. Background spectral characteristics of Ta, Mo, and W metal cups in ICP-MS have been documented by Karanassios and Horlick [24].

1.3.2.2 Wire- loop DSI

In 1984 Salin and Sing [29] described a wire-loop DSI technique. The graphite electrode was replaced by a 4-cm length of 0.46-mm-diameter

tungsten wire with two vertical side-by-side 2-mm loops on the end. A 10 uL liquid sample was injected manually onto the loop(s). The most striking feature of this system was its high signal sensitivity, and then, a much lower detection limit, due to the low mass of the tungsten wire and the exposure of the analyte species directly to the plasma, resulting in a rapid atomization and a high transient atom population. The lifetime of the tungsten wire loop was approximately 100 insertions. Salin et al. [30] also extended the wire-loop DSI to ICP-MS. Tantalum was used by Sing and Salin [31] as a wire-loop material to overcome the spectral overlap created by emission lines from W. Tantalum provided better temporal resolution but suffered from a short lifetime.

1.3.3 Applications of DSI

Direct analysis by DSI shows advantages over conventional nebulization:

(1) Volume of solution required.

Routinely, a 10-uL aliquot of solution is used for DSI determinations. This feature of only requiring uL rather than mL volumes of sample solution makes DSI particularly attractive for the analysis of biological fluids and other small volume samples. If greater sensitivity is required, replicate

aliquots may be added utilizing multiple drying steps before insertion. DSI coupled with preconcentration techniques, such as electrochemical proconcentration [30, 31, 32], flow injection preconcentration [33], and aerosol deposition [34, 35] can achieve significant improvement in sensitivity and detection limits over conventional nebulization techniques.

(2) Ease of analysis of organic solutions.

In DSI, the sample is desolvated before insertion into the plasma. Thus, analytes can be easily separated from an organic matrix or solvent (e.g. samples from the petroleum industry), minimizing carbon condensation on the instrumental interface and background spectra due to carbon species.

(3) Reduced oxide and hydroxide formation.

Because the sample has been desolvated before analysis in DSI, the population of oxide and hydroxide species is low [24], thus, isobaric interferences from oxides and hydroxides of matrix elements are rare. Hence direct determinations of ^{56}Fe (interference from $^{40}Ar^{16}O^{+}$) and ^{75}As (interference from $^{40}Ar^{35}Cl^{+}$) to detection limits of pg are possible.

(4) Direct analysis of solid samples.

The most important feature of the DSI technique is its ability to accomplish direct analysis of solid samples. A sample amount of up to 10 mg can be inserted directly into the plasma. No sample pretreatment is needed, hence,

contamination and dilution from reagents are minimized. As well, the ashing step in DSI can remove most of the matrix (i.e. organic content), thus giving the benefit of relative freedom from matrix effects.

The analytical ability of DSI combined with ICP-AES and ICP-MS has been proved for a wide range of sample categories including botanical, geological, metallurgical, and refractory materials.

Abdullah et al. [36] measured 15 elements in digested spinach and orchard leaf samples by DSI-ICP-AES. Calibrated with multielement standard solutions, the results agreed with certified values, except for Pb, Ni, Co, and Cd which were present at trace levels. Later on, Abdullah et. al. [37] carried out the direct analysis of orchard leaves without digestion. The elements were determined by calibrating the system with the NIST (USA) and NIES (Japan) standard reference plant materials (pepperbush, spinach, orchard leaves, tomato leaves, and pine needles) and with a cellulose standard prepared for matrix matching. Some results obtained agreed with the certified values, but large errors existed for certain elements. The recovery for Pb was 129%, and the recovery for As was 136%. The authors assumed

that the difference might be caused by errors in preparation of the standards and in weighing the samples.

Monasterios et al. [38] demonstrated the determination of Cu and Zn in human hair by DSI-ICP-AES. Single strands of hair from different donors were inserted into the plasma by DSI without digestion. Solution based Flame Atomic Absorption (FAA) and ICP-AES methods were used to determine Zn and Cu in human hair. There was a significant difference between the values by DSI-ICP-AES with the values by FAA or ICP-AES, indicating that aqueous standards could not be used directly for high accuracy standardization unless a correction factor was determined.

The direct determination of volatile trace elements in nickel-base alloys was studied using DSI-ICP-AES by McLeod et al. [39]. The technique exploited the difference in volatility between volatile trace elements and nonvolatile matrix elements, and a low power (1.0 kW) was used to minimize the potential spectral interferences from matrix elements. It was established that aqueous multielement standard solutions (no-matrix match) could be used for calibration for some elements, but for Pb, a large error (up to 30% relative) existed. Umemoto et al. [40] determined As and Sb in iron and

steels by digestion-DSI-ICP-AES, and the direct determination of trace elements in U_3O_8 powders [41] and Al_2O_3 powder [42] without the need for labor intensive dissolution was also achieved.

Trace elements in three marine sediment reference materials were measured by pellet-DSI-ICP-AES by Blain and Salin [43]. The powdered samples were mixed with graphite and pressed to pellets which were then inserted into the plasma. The graphite cups were modified [44] to hold the pellets. The direct insertion of pellets resulted in sharp signals for volatile elements like Cd, Cu, Hg, Mn, Pb, and Zn. The authors found that internal standardization could compensate for variations in volatilization interferences and changes in excitation conditions between sediment standards, for elements of high and intermediate volatility. They also found that the standard addition method allowed accurate calibration of the technique. The results agreed with the certified values except for Zn.

Mixed-gas ICP techniques have also been used in conjunction with DSI. Pettit and Horlick [20] established a calibration curve for Zn using both geological (coal and coal fly ash) and botanical (orchard leaves, spinach, and tomato leaves) materials with 1%O_2/Ar coolant DSI-ICP-AES. Liu and

Horlick [45] have used mixed-gas plasmas to enhance the volatilization of refractory materials and carbide forming elements. With the use of an Ar-O_2 mixed-gas plasma, volatile, refractory, and carbide forming elements could all be determined. The mixed-gas plasma not only facilitated the release of non-volatile elements from the matrix but also increased the emission signal of volatile elements. For more refractory elements, an Ar-O_2 (20%) mixed-gas plasma was used to further improve volatilization. Successful analyses were carried out for the direct insertion of Al_2O_3, Al metal, oil, and botanical samples.

1.4 Thesis Outline

For a number of years in this laboratory, we have been developing the DSI technique. Most of the work has focused on DSI-ICP-AES. Since Karanassios and Horlick extended DSI to ICP-MS, no further work has been done on this system which can combine the advantages offered by both the DSI and ICP-MS. The objectives of this research are to further develop the analytical performance of DSI-ICP-MS, and explore the analytical ability of this technique with some real samples.

Characterizing and optimizing the parameters of both DSI and ICP-MS, especially the transient signal processing parameters, in order to obtain the best multielement signal characteristics, make up the first part of the thesis. The analytical performance of this technique was investigated with liquid standard solutions containing Pb, Bi, In, Ag, Fe, Co, Mn, Cu, Ga, As, Sb, and Se in different combinations. Analytical curve figures of merit were obtained including relative standard deviation (%RSD), detection limit, calibration function slope, correlation coefficient, linear range, and effect of internal standardization. On the basis of the excellent performance for liquid solutions, the technique was extended to the direct analysis of real solid biological samples---a series of NIST (USA) and NIES (Japan) botanical standard reference materials (SRMs). Once reliable and stable instrumental conditions were established, the direct measurement of Pb, As, and Sb was investigated in these SRMs with different calibration methods, without any labor intensive pretreatment. The results agreed well with the certified values. The research shows that DSI-ICP-MS is a reliable, fast, relatively simple and precise technique for trace element determinations in solid biological samples.

References

1. Greenfield, S., Jones, I. L., and Berry, C. T., **Analyst**, 1964, *89*, 713-720

2. Wendt, R. H., and Fassel, V. A., **Anal. Chem.**, 1965, *37*, 920-922

3. Montaser, A., and Fassel, V. A., **Anal. Chem.**, 1976, *48*, 1490-1499

4. Demers, D. R., and Allimand, C. D., **Anal. Chem.**, 1981, *53*, 1915-1921

5. Houk, R. S., Fassel, V. A., Flesh, G. D., Svec, U.J., Gary, A. L., and Taylor, C. E., **Anal. Chem.**, 1980, *52*, 2283-2289

6. Houk, R. S., Svec, H. J., Fassel, V. A., **Appl. Spectrosc**. 1981, *35*, 380-384

7. Montaser, A., and Golightly, D. W., **Indctively Coupled Plasma In Analytical Atomic Spectrometry**, VCH, New York, 1987

8. Hull, D. R., and Horlick, G., **Spectrochim. Acta.**, 1984, *39B*, 843-850

9. Wang, J., Carey, J. M., and Caruso, J. A., **Spectrochim. Acta.**, 1993,*49B*, 193-203

10. Arrowsmith, P., **Anal. Chem.**, 1987, *59*, 1437-1444

11. Carr, J. W., and Horlick, G., **Spectrochim. Acta.**, 1982, *37B*, 1-15

12. Jiang, S-J., and Houk, R. S., **Anal. Chem.**, 1986, *58*, 1739-1743

13. Salin, E. D., and Horlick, G., **Anal. Chem.**, 1979, *51*, 2284-2286

14. Sommer, D., and Ohls, K., **Fresenius Z. Anal. Chem.**, 1980, *304*, 97-103

15. Kirkbright, G. F., and Walton, S.J., **Analyst,** 1982, *107*, 276-281

16. Kirkbright, G. F., and Zhang, L-X., **Analyst**, 1982, *107*, 617-620

17. Pettit, W. E., and Horlick, G., Pittsburgh Conference and Exposition, 1983, Atlantic City, NJ, USA, No. 151

18. Pettit, W. E., and Horlick, G., **Spectrochim. Acta**., 1986, *41B*, 699-712

19. Zhang, L-X., Kirkbright, G. F., Cpoe, M. J., and Watson, J. M., **Appl. Spectrosc**., 1983, *37*, 250-254

20. Shao, Y., and Horlick, G., **Appl. Spectrosc**., 1986, *40*, 386-393

21. Karanassios, V., and Horlick, G., **Spectrochim. Acta**., 1990, *45B*, 85-104

22. Chan, W. T., and Horlick, G., **Appl. Spectrosc**., 1990, *44*, 380-390

23. Karanassios, V., and Horlick, G., **Spectrochim. Acta**., 1989, *44B*, 1345-1360

24. Karanassios, V., and Horlick, G., **Spectrochim, Acta**., 1989, *44B*, 1361-1385

25. Karanassios, V., and Horlick, G., **Spectrochim. Acta**., 1989, *44B*, 1387-1396

26. Barnett, N. W., Cope, M. J., Kirkbright, G. F., and Taobi, A. A. H., **Spectrohcim. Acta**., 1984, *39B*, 343-348

27. Karanassios, V., Horlick, G., and Abdullah, M., **Spectrochim. Acta**.,

1990, *45b*, 105-118

28. Skinner, C. D., and Salin, E. D., **J. Anal. At. Spectrosc.**, 1997, *12*, 725-732

29. Salin, E. D., and Sing, R. L. A., **Anal. Chem.**, 1984, *56*, 2598-2600

30. Salin, E. D., and Habib, M. M., **Anal. Chem.**, 1984, *56*, 186-1188

31. Salin, E. D., and Habib, M. M., **Anal. Chem.**, 1985, *57*, 2055-2059

32. Abdullah, M., Fuwa, K., and Haraguchi, H., **Appl. Spectrosc.**, 1987, *41*, 715-721

33. Moss, P. and Salin, E. D., **Appl. Spectrosc.**, 1991,*45*, 1581-1586

34. Rattray, R. Minoso, J., and Salin, E. D., **J. Anal. At. Spectrosc.**, 1993, *8*, 1033-1036

35. Rattray, R. and Salin, E. D., **J. Anal. At. Spectrosc.**, 1995, *10*, 829-836

36. Abdullah, M., Fuwa, K., and Haraguchi, H., **Spectrochim. Acta.**, 1984, *39B*, 1129-1139

37. Abdullah, M., and Haraguchi, H., **Anal. Chem.**, 1985, *57*, 2059-2064

38. Monasterios, C. V., Jones, A. M., and Salin, E. D., **Anal. Chem.**, 1986, *58*, 780-785

39. McLeod, C. W., Clarke, P. A., and Monthorpe, D. J., **Spectrochim. Acta.**, 1986, *41B*, 63-71

40. Umemoto, M., and Hubota, M., **Spectrochim. Acta.**, 1987, *42B*,

491-499

41. Page, A. G., Godbole, S. V., Madraswale, K. H., Kulkarni, M. J., Mallapurkar, V. S., and Joshi, B. D., **Spectrochim. Acta**., 1984,*39B*, 551-557

42. Zaray, G., Broekaert, J. A. C., and Leis, F., **Spectrochim. Acta**., 1988, *43B*, 241-253

43. Blain, L., and Salin, E. D., **Spectrochim. Acta**., 1992, *47B*, 205-217

44. Blain, L., Salin, E. D., and Boomer, D. W., **J. Anal. At. Spectrosc**., 1989, *4*, 721-725

45. Liu. X., and Horlick, G., **J. Anal. At. Spectrosc**., 1994, *9*, 833-840

Chapter 2
Effect of Operating Parameters on Analytical Signals in DSI-ICP-MS

2.1 Introduction

2.1.1 Inductively coupled plasma mass spectrometry (ICP-MS)

Since the reports by Houk et al. [1] and Date and Gray [2], followed by the introduction of commercial systems in 1983, inductively coupled plasma mass spectrometry (ICP-MS) has developed into an accurate and sensitive technique for trace and ultra-trace multielemental determinations. The rapid growth and acceptance of the ICP-MS is the result of its superior measurement capabilities for elemental analysis. Included in these are:

(1) Very low detection limits. Current detection limits for the Perkin-Elmer/Sciex Elan 6000 ICP-MS for the direct analysis of solution samples are in the range of 1 to 100 pg/ml for most elements (reported by Eric Denoyer of Perkin-Elmer/Sciex Corporation, October 31, 1996). These detection limits are broadly achieved for almost all elements across the periodic table and they are 1-3 orders of magnitude lower than those achieved by inductively coupled plasma atomic emission spectrometry (ICP-AES) and atomic fluorescence spectrometry (AFS) under comparable conditions.

(2) Wide dynamic range. Currently most ICP-MS instruments offer a dynamic range of nearly 4-8 orders of magnitude, which is much wider than offered by ICP-AES. A large linear response range decreases analysis times by lessening the demand for sample dilution or preconcentration.

(3) Spectral Simplicity. The mass spectra of the elements are very simple and unique, containing a maximum of 250 masses, including all elements, their isotopes, and possible polyatomic species [3], compared to the thousands of lines found in ICP-AES spectra.

(4) Rapid isotope measurement ability. The natural isotope abundance pattern provides quick and very specific evidence for the qualitative identification for an element. This has facilitated the development of ICP-MS as a powerful technique for automated qualitative and semi-quantitative elemental analysis. The inherent capability to measure elemental isotope ratios allows the routine utilization of isotope ratio data and the isotope dilution technique [4] to study and solve analytical problems.

2.1.2 ICP-MS instrumentation

A schematic diagram of the Perkin-Elmer/Sciex Elan 250/500 ICP-MS system, which was used to acquire the data in this thesis, is presented in Fig. 2.1. The main components of the instrument include the ICP, an interface system (consisting of a sampling cone, a differentially pumped zone, and a skimming cone), ion lenses, a quadrupole mass spectrometer, and a detector.

In principle, the ICP system is identical to that used for ICP-AES. After the plasma is ignited, the sample aerosol introduced by the sample introduction system is desolvated, atomized, and ionized in the central channel of the plasma which exhibits a temperature of 7000-8000 K. Ions generated in the ICP are transferred into the mass spectrometer through a two-stage, differentially pumped MS interface. The first cone (sampler) of the interface

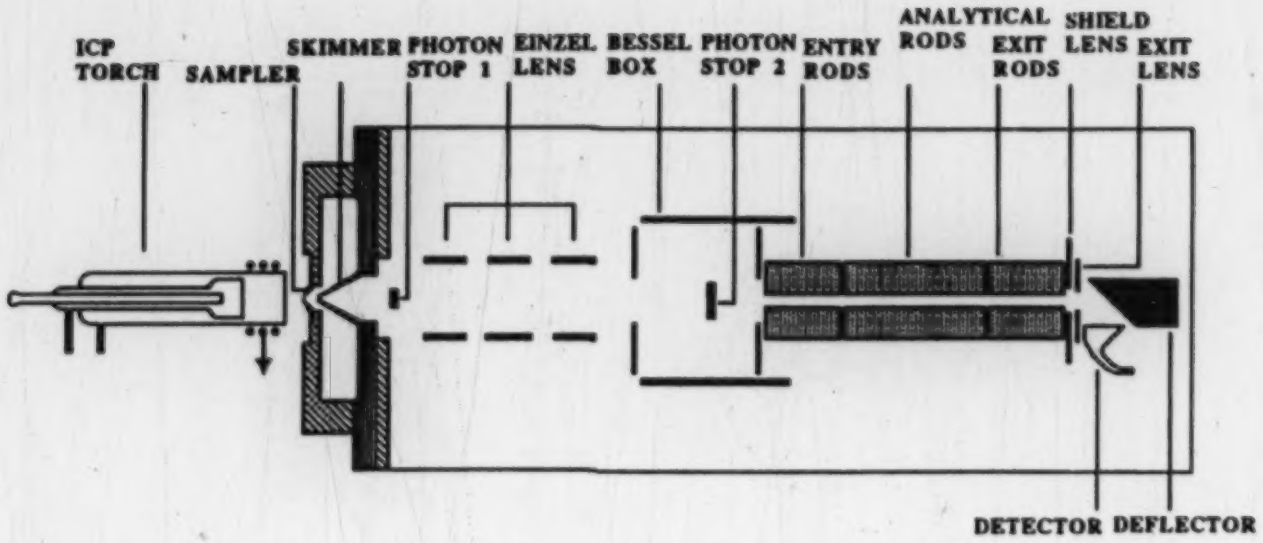

Fig. 2.1 Schematic diagram of the Perkin-Elmer/SCIEX ELAN 250/500 ICP-MS system

is used to sample the atmospheric-pressure plasma. The second cone (skimmer) in the interface samples the expansion zone formed behind the sampler. The skimmer orifice must be located in the expansion zone (~2 mm from the sampler) for optimal extraction of the analyte ions. The differentially pumped zone provides an intermediate region to interface to the vacuum required by the mass analyzer.

Ions are transferred to the mass analyzer via the ion optics, which consist of an Einzel lens and a Bessel box. The Bessel box contains a central stop to block passage of undesirable photons to the detector. Also a preliminary photon stop is placed just behind the skimmer. The basic trajectories of ions through this system have been presented by Vaughan and Horlick [5]. The path of ions through electrostatic lenses depends on ion kinetic energy, and can be altered significantly by space charge effects.

Almost all work in ICP-MS has been conducted using a quadrupole mass analyzer. Such a system offers two major advantages: ease of use with an ion source near ground potential and low cost of manufacture. The major drawback is its intrinsically low mass resolution, typically 0.5 to 1 atomic mass unit (amu), with resolution defined as the peak width at 10% peak height. A cryopump provides a running vacuum of almost 3.8×10^{-5} Torr.

After separation according to mass-to-charge ratio in the mass analyzer, ions are collected at the detector. The detector is mounted off-axis to reduce the chance of photons reaching the detector. When photons reach the detector, the background signal level is raised, which can degrade detection limits.

2.1.3. DSI as a sample introduction system for ICP-MS

The DSI device was constructed and interfaced to a Sciex Elan 250 ICP-MS by Karanassios and Horlick [6] in 1989. DSI-ICP-MS combines the advantages offered by both DSI and ICP-MS, such as the ability to handle small samples, reduction or even elimination of a number of spectral interferences as the plasma is dry [7], and relative freedom from matrix effects by removal of most of the matrix. A schematic diagram of the automatic DSI system for ICP-MS is presented in Fig. 2.2.

The basic components required for the DSI system include: the torch support assembly, the platform/probe assembly, the DSI device base and the drive mechanism.

The torch support assembly consists of a plexiglass base, the torch support, the torch and the shutter. The plexiglass base can be easily adjusted horizontally in the x-direction, and the torch support can be easily adjusted in both the y-direction and the z-direction, allowing precise alignment of torch with respect to the sampler orifice of the mass spectrometer. The torch is a modified Fassel torch with a wider central tube, and the shutter is placed directly on the end of the torch. The shutter is opened and closed electromechanically. When igniting the plasma, the shutter must be closed.

The platform consists of the probe assembly and its support, and a vertical and horizontal probe assembly position adjusting mechanism. The probe assembly is a quartz rod with a sample carrying probe on the top. The two

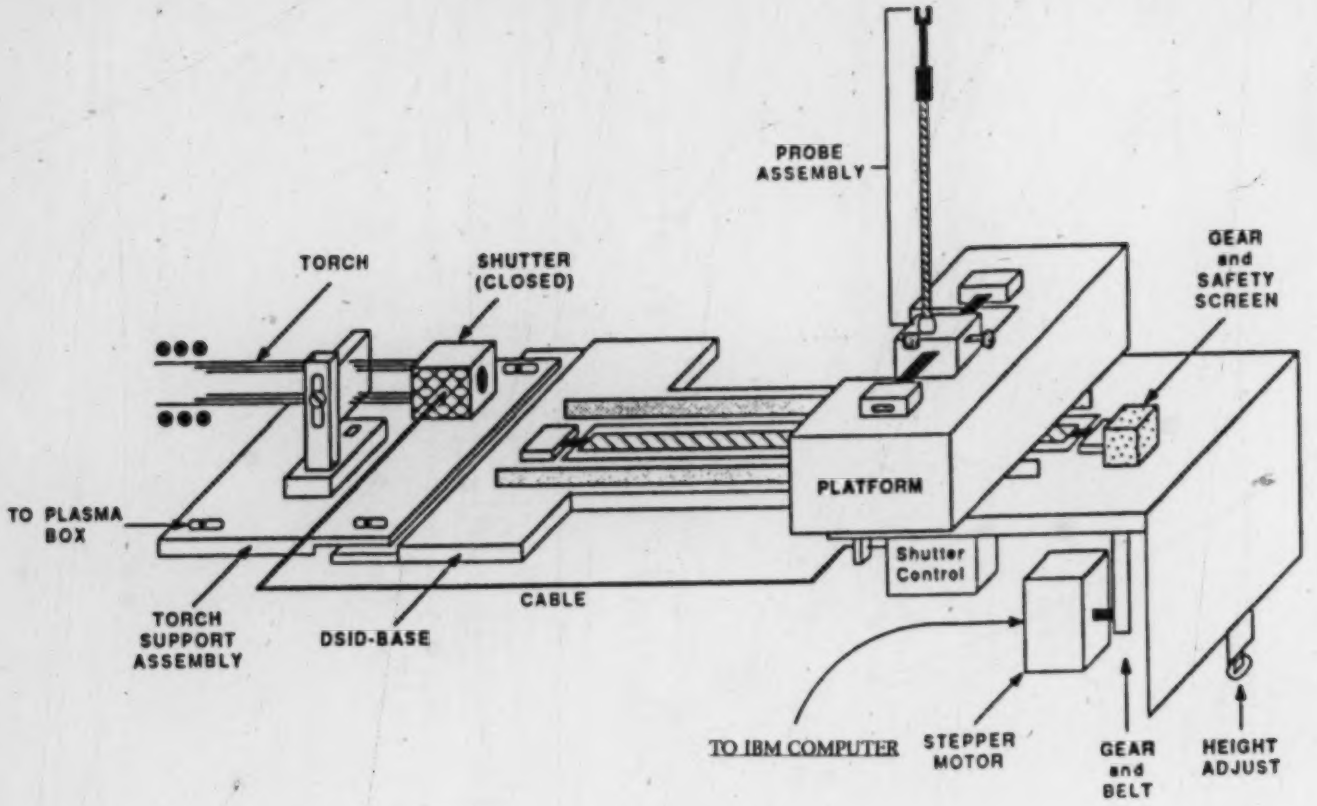

Fig. 2.2 Schematic diagram of DSI device for ICP-MS [6]

position adjusting mechanisms allow both the horizontal and the vertical adjustment of the center of the sample probe with respect to the sampler orifice. The probe assembly rotates between 0^0 (horizontal), which is required for probe insertion, and 90^0 (vertical), where sample probe replacement takes place.

The probe assembly is driven by a computer-controlled stepper motor. A window-based software was written for an IBM PRO-SPEC 386 computer to drive the stepper motor. The insertion of the sample carrying probe is accomplished by sending the appropriate data and instructions to the stepper motor. The insertion positions can also be controlled by the computer so that in situ drying and ashing can take place before the probe is inserted into the plasma.

2.1.4. Operating parameters of DSI-ICP-MS

In order to use DSI-ICP-MS efficiently and to take full advantage of its capability, it is necessary to know the effect of instrument operating parameters on the analytical signals. The instrumentation involved in DSI-ICP-MS is quite complicated and a great number of variables affect the analytical signal. The parameters of both DSI and ICP-MS must be considered together to obtain the best instrumental performance. The key parameters include the sample carrying probe insertion (ashing and atomizing) positions, forward power, gas flow rates, lens settings, and most important, the transient signal acquisition parameter settings. The effect of these parameters on analyte signals will be discussed separately in this chapter.

2.2 Experimental

The Perkin-Elmer/SCIEX Elan 250 ICP-MS coupled with the DSI device just described was used in this work. A schematic illustration of the DSI-ICP-MS is shown in Fig. 2.3. The precise alignment of the sample carrying probe with the sampler orifice was done by moving the probe close to the sampler and adjusting the x and y direction by the horizontal drive knob and the vertical drive knob on the front panel of the ICP-MS, so that the crater of the graphite cup and the tip of sampler were at the same position. The sampler and the skimmer were made of nickel. The effect of sampler and skimmer orifice size on analyte signals in ICP-MS was discussed by Vaughan and Horlick [8]. They concluded that the large sampler orifice yielded large signals, and the effect of orifice size of the skimmer was not as dramatic as the effect of the sampler orifice size. In this work, a larger sampler orifice with a diameter about 1 mm was used, in order to obtain higher signal intensity.

The undercut graphite electrodes utilized in this work were purchased from Bay Carbon, Inc., Bay City, Michigan. Two types of electrodes with different tip length and diameter were used in this work without any modification, and no signal difference was found between the two types of electrodes. When solid samples were analyzed, the bigger electrode was preferred because more sample could be loaded. In order to reduce the amount of impurities contained in the sample probe, the graphite electrodes were treated according to the procedure recommended by Abdullah et al. [9] and were pre-burned in the plasma 3-5 times prior to their use [10].

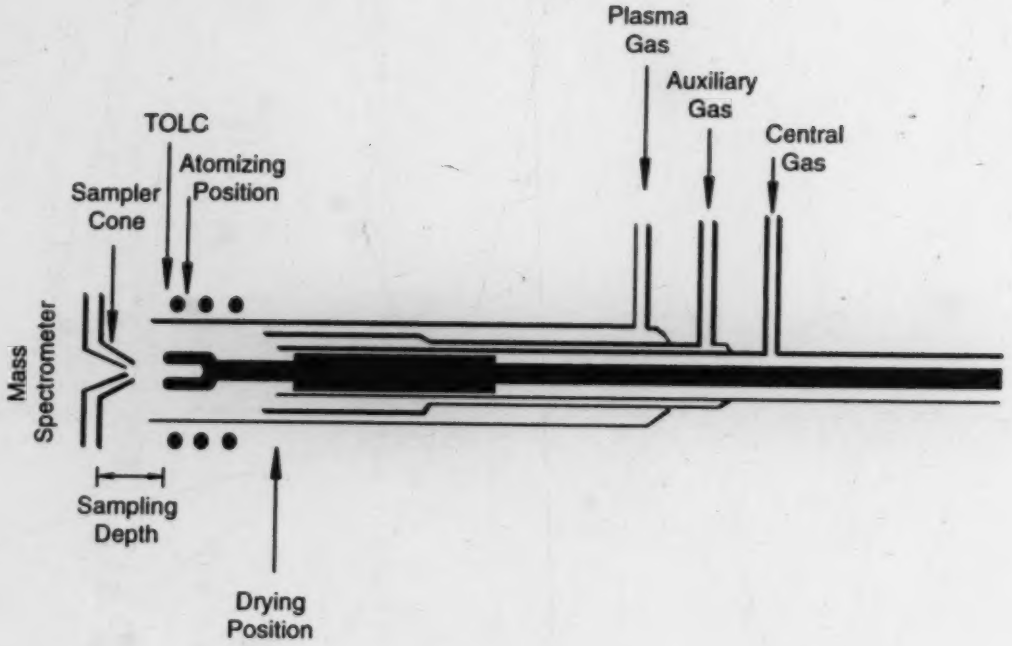

Fig. 2.3 Schematic illustration of DSI-ICP-MS

All solutions were prepared by serial dilution with distilled/deionized water from 1000 ppm standard stock solution (SPEX Industries Inc., Edison, NJ or LECO Instruments Ltd., Mississauga, ON) of the respective element. The distilled/deionized water was produced in a Millipore Super-Q apparatus (Millipore, Milford, MA). A 10uL volume of solution was transferred to the sample carrying probe with a Eppendorf micropipette. Solution transferred into the cups was dried by heating the electrodes in an aluminum holder under an infrared lamp for 2-3 minutes prior to insertion into the plasma.

2.3 Results and Discussion

2.3.1 ICP-MS parameters

2.3.1.1 Forward power

In DSI, the temperature of the electrode after insertion depends on forward power, and the size and geometry of the graphite cup. Barnett et al. [11] measured the temperature of different types of graphite cups after insertion using a radiation thermometer. With a forward power of 1.5 kW as used in their work, they found that the maximum temperature of the cup was about 2000 K. Page et al. [12] found that the temperature of the cup with a cup lid was 1400 K at a power of 1.4 kW determined using melting point tests. A temperature of 3600 K was reported by Umemoto et al. [13] with a small cup (low heat capacity) at a power of 1.5 kW, but a temperature of only 3000 K was found at a power of 3 kW in a nitrogen/Ar plasma by Zaray et al. [14]. In summary, quite different values of cup temperature have been reported.

A solution containing 1 ppm each of Cu and Ga was used to investigate the effect of forward power on signal intensity. Signals were measured at powers of 1.0 kW, 1.25 kW, 1.5 kW, 1.75kW, and 2.0 kW. The signals increased with increasing power. When the power was lower than 1.5 kW, the signals for Cu and Ga were low, and unstable. At low power the temperature of the sample cup is likely not high enough to completely vaporize and ionize the analytes. The boiling points of Cu and Ga are 2567°C and 2403°C respectively [15]. It is possible that the temperature of the cup is lower than 2500°C when the power is below 1.5 kW. The signals for 10 uL of the 1ppm Cu and Ga solution with 5 consecutive insertions at a power 1.5 kW are shown in Fig. 2.4. The signals are quite reproducible and the relative standard deviation (%RSD) of peak areas is less than 2%. It can be concluded that because of the cooling effect of the insertion of the graphite cup, a high power (at least 1.5 kW in this work) should be used in DSI-ICP-MS in contrast to that for pneumatic nebulization where 1.2 kW is generally sufficient.

2.3.1.2 Gas flow rates

Among the many ICP-MS instrumental parameters available for optimization, central gas flow rate (nebulizer flow rate) is the parameter that has the most significant effect on signal intensity. Parameter plots (intensity vs central gas flow rate at a given power setting) have become a frequent scene in the ICP-MS literature [16]. In this study, the effect of central gas flow rate was investigated with 1ppm Cu and Ga (10 uL) solution residues at a power of 1.5 kW. With a variation of the central gas flow rate from 0.5

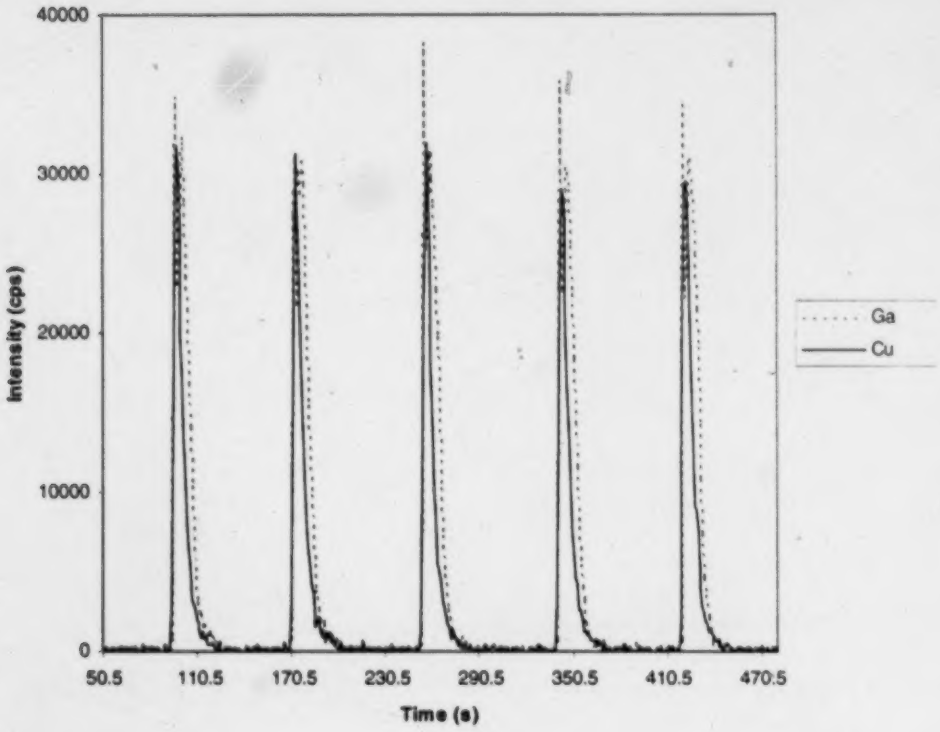

Fig. 2.4 Signals for 1 ppm Cu and Ga (10 uL) (5 consecutive insertions) at a power of 1.5 kW

L/min to 2.5 L/min, the results are quite unlike those with a conventional pneumatic nebulizer system [16]. It was found that the central gas flow rate had little effect on the signal intensities (peak height). However, the central gas is essential to sustain a continuously operating plasma and to prevent air entrainment in the torch, so a 1 L/min central gas flow rate was chosen for all studies.

The effect of plasma and auxiliary gas flow rates were investigated in the same way as central gas flow rate. To sustain a stable running plasma, a 13 L/min plasma gas and 0.2 L/min auxiliary gas were used. When too high or too low a plasma or auxiliary gas flow rate was used, the plasma was unstable, and could extinguish.

2.3.1.3 Other ICP-MS parameters

Because there is no continuously aspirating solution to assist optimization in a DSI system, the ion lens settings used in DSI were established using a pneumatic nebulizer system. A 1 ppm multielement standard solution containing the elements to be studied by DSI was run and the analyte signals were maximized before installing the DSI system. The effects of these ion lens settings on analyte signals have already been studied for the pneumatic nebulization ICP-MS by Vaughan et al. [16].

Finally, unless otherwise stated, the typical sampling depth (distance from the sampling cone to the top of load coil (TOLC)) [6] used in this work was 10 mm .

2.3.2 DSI parameters

2.3.2.1 Drying position

One of the operational aspects of the DSI technique is its capability of in situ desolvation and drying, by which most of the matrix and solvent can be removed. Zhang et al. [17] found that the drying position should range from 34 to 56 mm below the top of the load coil (TOLC). When the cup position was lower than 56 mm, desolvation was not complete, and when the cup position was higher than 34 mm the sample was desolvated immediately and the plasma was typically extinguished during this drying stage. They also stated that the drying position depended on power. Chan and Horlick [18] used a position of 35 mm below the load coil (BLC) as the desolvation position (without external desolvation), and 18 mm BLC as a drying position. For the studies presented in this thesis, as part of the insertion sequence, a pre-insertion position of 45 mm below the top of the load coil was used (5 seconds) to insure that the sample was dry before actual insertion into the plasma.

2.3.2.2 Atomizing position

The insertion position of the graphite cup during the atomizing stage is a relatively critical parameter in its effect on analyte signal intensity. Various atomizing positions have been reported. Zhang et al. used 2 mm below TOLC [17], Shao and Horlick [19] used 0 mm below TOLC, while other values such as 2 mm [20], 4 mm [21], 6 mm [14], and 8 mm [9] above

TOLC have also been reported. Karanassios and Horlick decided that the "0 mm" insertion position (TOLC) was a good compromise for multielement analysis [10]. Karanassios and Horlick also used this "0 mm" position in their DSI-ICP-MS system [6].

A multielement solution containing 1 ppm Pb, Bi, Ag and In was used to establish an optimum cup insertion position value for this work. Analyte signals were recorded simultaneously for all elements and measured for a range of final insertion positions: 26 mm, 16 mm, 8 mm, 3 mm below TOLC, 0 mm, and 6 mm above TOLC. It was found that the highest signals were obtained at an insertion position 3 mm below TOLC for all the four elements. Much lower signals were obtained at the other positions. This 3-mm-below-TOLC atomizing position was used for all further work in this study.

Atomizing time is determined primarily by the evaporation character of the elements. A shorter time is needed for volatile elements, and a longer time for non-volatile and refractory elements. It has been found that high power increases the signal intensity but has little effect on atomizing time [10], if no chemical modifier is used [22]. The best atomizing time for each element should be determined empirically, and a compromise should be made for multielement analysis. For Pb, Bi, Ag and In which have similar evaporation characteristics, a 15 seconds atomizing time was sufficient to cover the complete atomization of all the four analytes.

2.3.3 Transient signal acquisition

Unlike pneumatic nebulization, where the solution is continuously aspirated into the plasma, the signals generated by a DSI device are peak-like and transient in nature. But a quadrupole-based mass spectrometer is sequential in nature. In order to fulfill the multielement analysis capability of DSI-ICP-MS, a way to overcome this limitation is by making intensity measurements at one mass for a given period of time (referred to as a "dwell time") and then rapidly switching (via electronic means) to another mass. This can be done by utilizing the transient signal acquisition mode provided by Elan 250 ICP-MS. The parameter settings used for acquisition of transient signals are listed in Table 2.1. The "peak-hopping" mode provides some multielement capacity, the extent of which depends upon dwell time, and the number of elements(masses) scanned. These considerations will be discussed in detail in this section.

2.3.3.1 Effect of dwell time on data acquisition points/s

A multielement standard solution containing 1 ppm Pb, Bi, Ag and In was used for these measurements and the power setting was 1.5 kW. Results obtained for Pb, Bi, Ag and In by peak-hopping with dwell times of 50, 100 and 250 ms, and 1 measurement/peak are shown in Fig. 2.5. Note that the word "peak" here refers to signal from a m/z position and peak hopping is scanning the quadrupole from one mass to another mass, i.e. 208 for Pb, 209 for Bi, 107 for Ag and 115 for In. Also, 1 measurement/peak refers to making one measurement at the peak of the mass position for each element.

Table 2.1 Parameter settings for the acquisition of transient signals

Resolution		L		
Ion Multiplier	HV	4000		
Rod Offset	Volts	0.0		
Plasma RF Power	Watts	1250		
Auxiliary Flow	L/min	1.8		
Plasma	L/min	15.0		
Nebulizer Pressure	psi	30.0		
Sample Flow		0		
Measurements/Peak		1		
Scanning Mode		E		
Measurement mode		T		
Dwell time	ms	100		
Preheat Temp	C	0	Time s	0.00
Ash Temp	C	0	Time s	0.00
Main Heat Temp	C	0	Time s	0.00
Initial Measurement	Delay	s		1.00
Final Measurement	Delay	s		50.00

Note that:

- Preliminary Transient Scan = Yes
- Data Buffered = Yes (optional)

This use of the term "peak" should not be confused with the DSI signal peaks shown in Fig. 2.5 which result from the vaporization of sample out of the DSI cup. It can be seen in Fig. 2.5 that for DSI signals, dwell time is critical in defining analyte temporal behavior. Less data points are obtained for a more volatile element (i.e. Pb) than for a less volatile element (i.e. In). Beyond a time of 250 ms, there are not enough data points to define the analyte signal, especially for volatile elements. In order to acquire and assess the multielement transient signals adequately and accurately, dwell time must be chosen carefully.

The effects of different dwell times on the number of acquired points/s when 2, 3, and 4 masses are scanned are summarized in Fig. 2.6. From the results, it is clear that the number of data points/s is dependent on both the dwell time and the number of the masses scanned. Less data points/s are obtained when longer dwell times are used. For a given dwell time, a smaller number of data points is acquired when more elements(masses) are scanned. In order to simultaneously measure multiple elements and to adequately define analyte temporal behavior, a compromise choice of the dwell time and the number of the elements(masses) scanned must be made. From Fig. 2.6, it can be determined that a 100 ms dwell time is sufficient to acquire an adequate number of data points/s. When four elements(masses) are scanned, more than two points/s can be acquired at the 100 ms dwell time which is sufficient to define the signal time profiles.

The effect of dwell time on signal intensity (peak area) is shown in Fig. 2.7. The signal intensity (peak area) remains constant when dwell time is changed, making it less susceptible than peak height to dwell time effects.

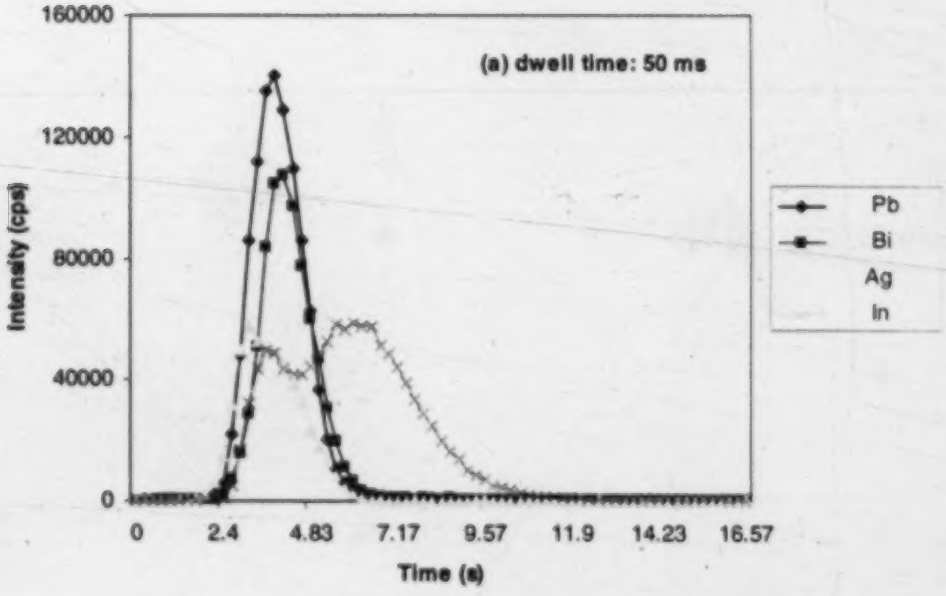

Fig. 2.5 Time profiles of 1ppm Pb, Bi, Ag and In with different dwell times

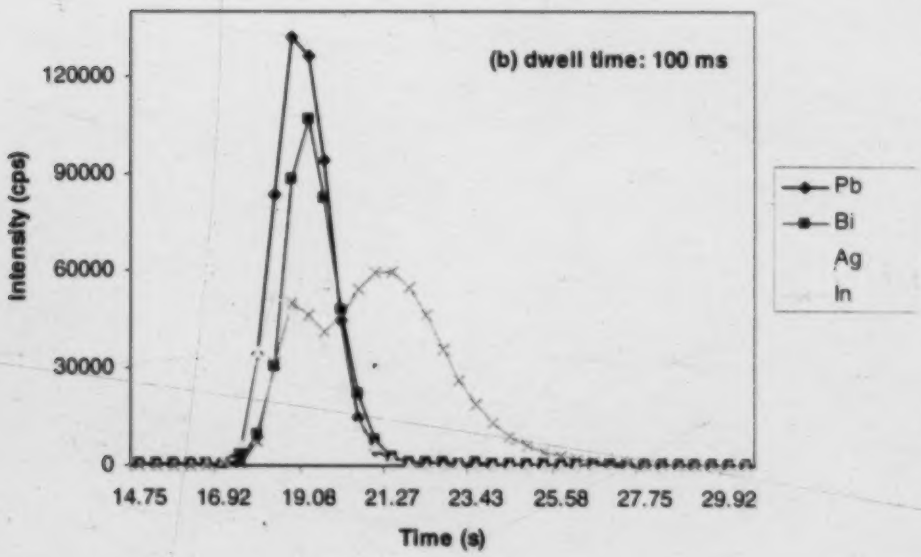

Fig. 2.5 (cont.) Time profiles of 1ppm Pb, Bi, Ag and In with different dwell times

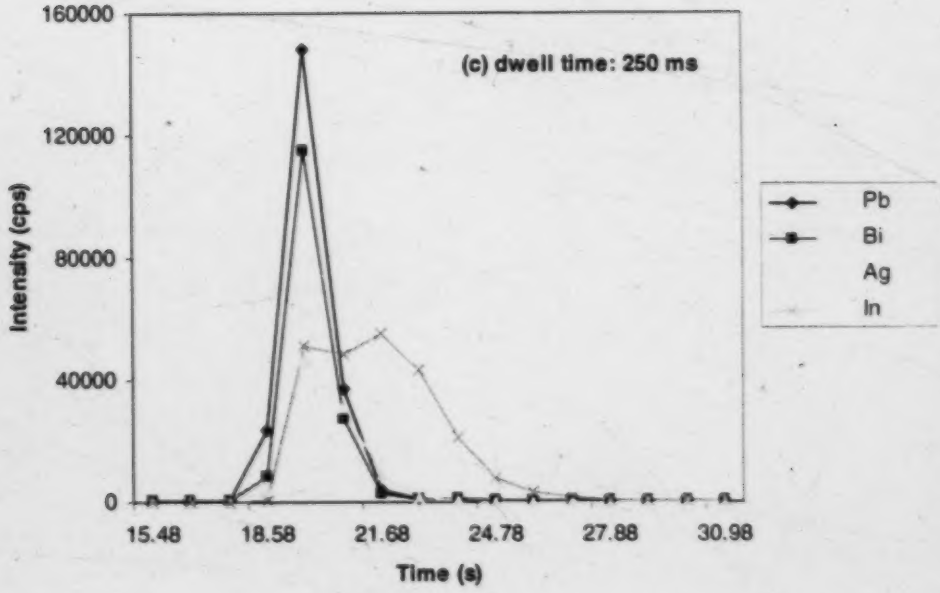

Fig. 2.5 (cont.) Time profiles of 1ppm Pb, Bi, Ag and In with different dwell times

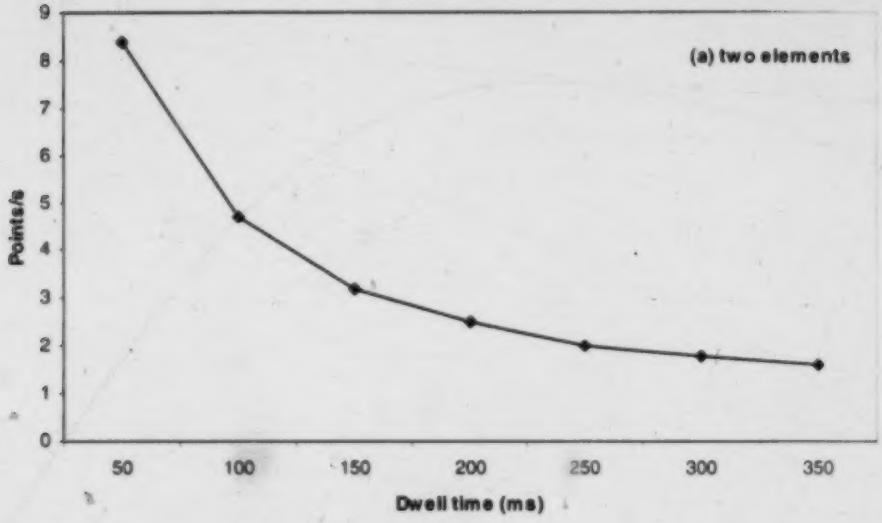

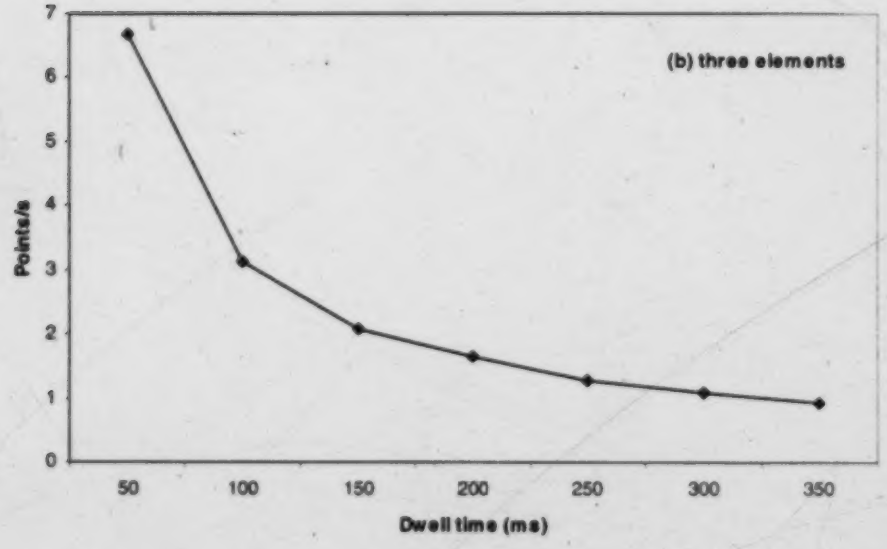

Fig. 2.6 Effect of dwell time on data acquisition points/s

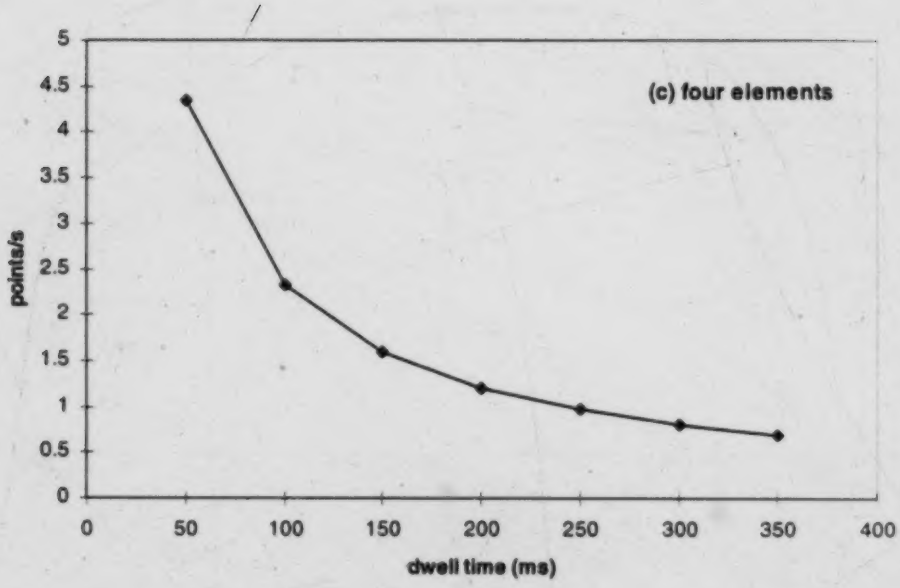

Fig. 2.6 (cont.) Effect of dwell time on data acquisition points/s

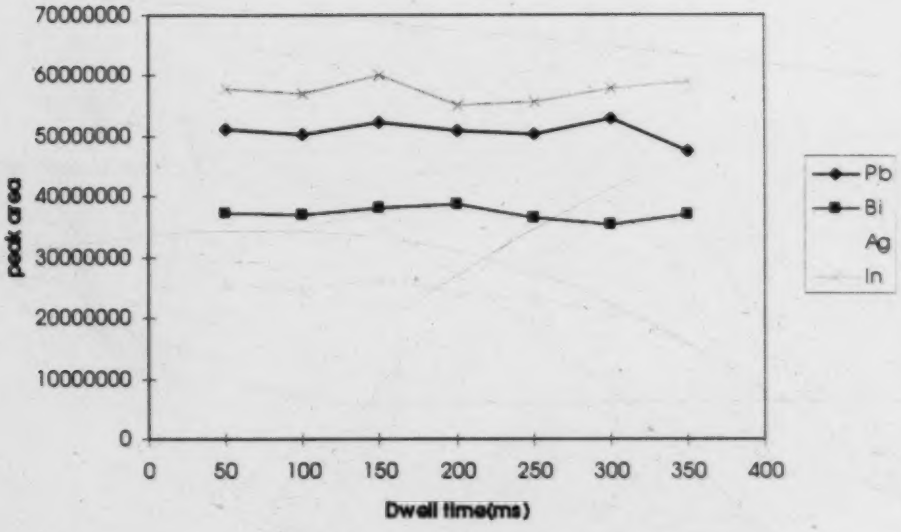

Fig. 2.7 Effect of dwell time on signal intensities (peak area) for 1ppm Pb, Bi, Ag, and In (10 uL)

2.3.3.2 Effect of dwell time on background baseline noise and detection limits

Background spectral interferences result from isobaric overlaps of polyatomic species originating from argon and entrained air, from sample matrix or solvent, from other isotopes with the same mass-to-charge ratio and from doubly charged species. Noise from instrument electronics and photons can also contribute some of the background signal level.

The signals for 0.01 ppm Pb (10 uL) and the background baseline before and after insertion when 100 ms and 300 ms dwell time are used are shown in Fig. 2.8. The baseline is cleaner (lower background standard deviation) when the longer dwell time (300 ms) is used. Low baseline noise is an advantage in obtaining low detection limits. The effect of dwell time on the background standard deviation for 1 ppm Pb, Ag, and In is shown in Fig. 2.9. It can be seen that the background standard deviation decreases when dwell time increases. However, there is little change after 100 ms, thus this dwell time should not compromise detection limits. In keeping with the change of background standard deviation with dwell time, the detection limits are lower when longer dwell times are used. A detection limit is defined as the concentration providing a signal equivalent to three times the background standard deviation. It is roughly the lowest concentration that the instrument can statistically detect. The effect of dwell time on the detection limits for Pb, Ag and In is shown in Fig. 2.10. As seen for the effect of dwell time on background standard deviation, lower detection limits can be obtained when the dwell time is longer than 100 ms, but there is little gain after 100 ms.

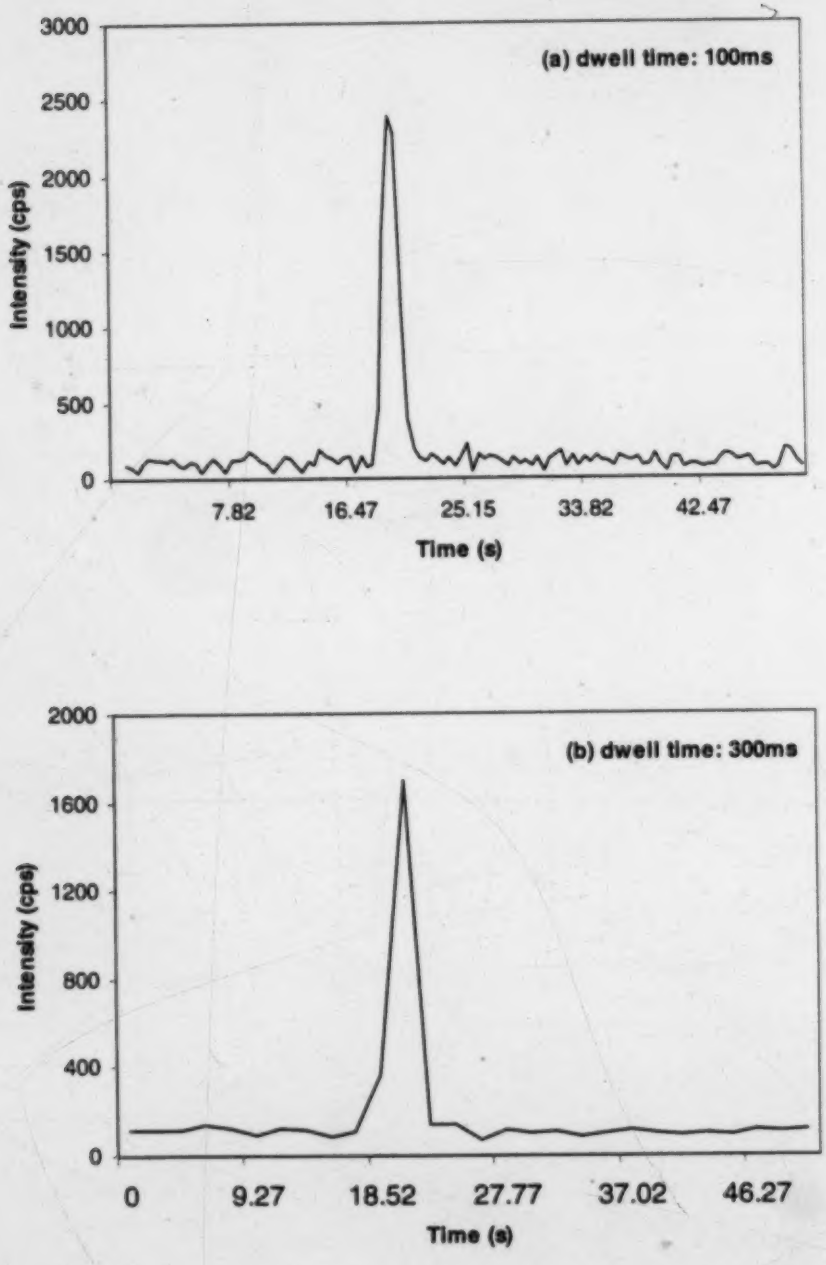

Fig. 2.8 Signal and baseline of 0.01ppm Pb with different dwell times

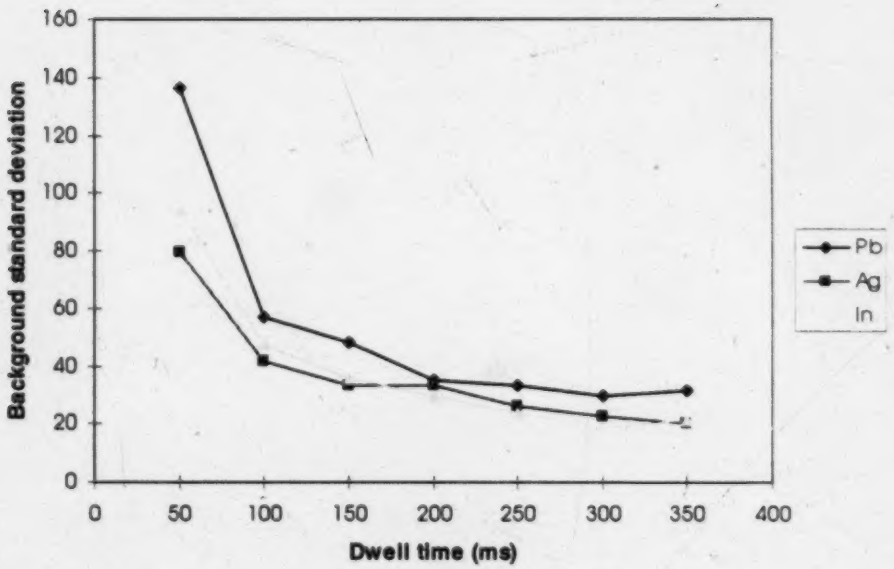

Fig. 2.9 Effect of dwell time on background standard deviation for Pb, Ag and In

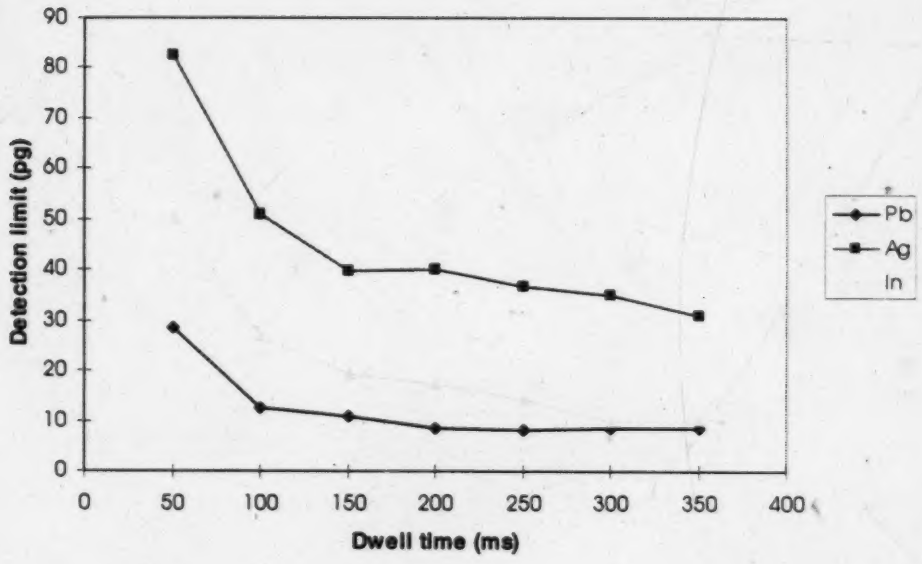

Fig. 2.10 Effect of dwell time on detection limits for Pb, Ag and In

In summary, the peak-hopping mode can provide reasonable capability for the measurement of multi-element transient signals generated by the DSI technique. The critical parameters are the dwell time and the number of elements(masses) scanned. A compromise must be made between dwell time and the number of elements(masses) scanned. When four elements(masses) are determined simultaneously, a 100 ms dwell time is a suitable compromise to define the transient signal behavior properly in the time domain with an adequate number of data points and low detection limits.

2.4 Conclusion

Several measurement parameters that affect analyte signal intensity and that determine the transient signal acquisition capability of the mass spectrometer were discussed in this chapter. The basic running conditions that have been determined are summarized in Table 2.2. With these measurement conditions, simultaneous multielement analyses can be carried out for up to 4 elements at a time.

Table 2.2 Summary of DSI-ICP-MS instrumental parameters

A. DSI device:	
Drying Position:	45 mm below TOLC
Time:	5 s
Atomizing Position:	3 mm below TOLC
Time:	Depends on volatility
B. ICP-MS:	
Power :	At least 1.5 kW
Sampling Depth:	10 mm
Carrier Gas Flow Rate:	1 L/min
Plasma Gas Flow Rate:	13 L/min
Auxiliary Gas Flow Rate:	0.2 L/min
Lens Setting:	Decided by pneumatic system
C. Transient Signal Acquisition	
Dwell Time:	100 ms
Measurement/peak:	1

References

1. Houk, R. S., Fassel, V. A., Flesh, G. D., Svec, H. J., Gray, A. L., and Taylor, C. E., **Anal. Chem.**, 1980, *52*, 2283-2289
2. Date, A. R., and Gray, A. L., **Analyst**, 1981, *106*, 1255-
3. Zhu, G., andBrowner, R. F., **Appl. Spectrosc.**, 1987, 349-
4. Longerich, H. P., **Atomic spectrosc.**, 1989,*10*, 112-115
5. Vaughan, M. A., and Horlick, G., **Spectrochim. Acta.**, 1990, *45B*, 1301-1311
6. Karanassios, V., and Horlick, G., **Spectrochim. Acta.**, 1989, *44B*, 1345-1360
7. Karanassios, V., and Horlick, G., **Spectrochim. Acta.**, 1989, *44B*, 1361-1385
8. Vaughan, M. A., and Horlick, G., **Spectrochim. Acta.**, 1990, *45B*, 1289-1299
9. Abdullah, M., Fuwa, K., and Harahuchi, H., **Spectrochim. Acta.**, 1984, *39B*, 1129-1139
10. Karanassios, V., Horlick, G., and Abdullah, M., **Spectrochim. Acta.**, 1990, *45B*, 105-118
11. Barnett, N. W., Cope, M. J., Kirkbright, G. F., and Taobi, A. A. H., **Spectrochim. Acta.**, 1984, *39B*, 343-348
12. Page, A. G., Godbole, S. V., Madraswala, K. H., Kulkarni, M. J., Mallapurkar, V. S., and Joshi, B. D., **Spectrochim. Acta.**, 1984, *39B*, 551-557
13. Umemoto, M., and Hubota, M., **Spectrochim. Acta.**, 1987, *42B*, 491-499

14. Zaray, G., Broekaert, J. A. C., and Leis, F., **Spectrochim. Acta**., 1988, *43B*, 241-253

15. Weast, R. C., and Astle, M. J., Eds, **Handbook of Chemitry and Physics**, *60th edn*., C.R.C. Press, Cleveland, U.S.A.

16. Vaughan, M., Horlick, G., and Tan, S. H., **J. Anal. At. Spectrosc.**, 1987,*2*, 765-772

17. Zhang, L-X., Kirkbright, G. F., Cope, M. J., and Watson, J. M., **Appl. Spectrosc.**, 1983, *37*, 250-254

18. Chan, W. T., and Horlick, G., **Appl. Spectrosc.**, 1990, *44*, 525-530

19. Shao, Y., and Horlick, G., **Appl. Spectrosc**., 1986, *40*, 386-393

20. Abdullah, M., and Haraguchi, H., **Anal. Chem**., 1985, *57*, 2059-2064

21. Kirkbright, G. F., and Zhang, L-X., **Analyst**, 1982,*107*, 617-620

22. Karanassios, V., and Horlick, G., **Spectrochim. Acta.**, 1989, *44B*, 1387-1396

Chapter 3
Measurement of Pb, Bi, Ag and In By DSI-ICP-MS

3.1 Analytical Performance of DSI-ICP-MS for Pb, Bi, Ag and In

3.1.1 Introduction

Almost all preliminary investigations of the DSI technique are done first with liquid samples, and then expanded to other types of sample such as powders and solids. The DSI technique has some advantages for the direct analysis of liquid samples, such as a 100% sample introduction efficiency, capability to handle small quantities of samples, and removal of sample matrix before insertion. The analytical performance of DSI devices has been reported extensively for ICP-AES by many researchers. In general, the precision (% RDS) reported ranged from 1-25% [1, 2, 3], with a typical value somewhat between 5% and 10%. This is worse than the 2% routinely achieved with a conventional pneumatic nebulizer system. The reported detection limits vary widely [4, 5, 6], depending on instrumental optimization and the sample and probe types in use. However, most detection limits are in the ng to pg range, superior, or at least comparable to those achieved by a pneumatic nebulization system. Calibration curves have been constructed for liquid samples, and calibrations are linear over at least three orders of magnitude [7, 8, 9].

However, not much work has been done for DSI-ICP-MS since its first introduction by Karanassios and Horlick [10]. The aim of the present study is to investigate and characterize the basic analytical performance of DSI-

ICP-MS for the quantitative analysis of liquid samples using multielement standard solutions containing Pb, Bi, Ag and In. In this part of the thesis, internal standardization will be discussed, calibration curves will be presented, %RSD will be determined, and detection limits will be established for the selected elements.

3.1.2 Experimental

The Perkin-Elmer/SCIEX Elan 250 ICP-MS coupled to the DSI device described previously was used in this research. The method for alignment and the experimental procedure were mentioned in Chapter 2, and used in this part without any change. The operating parameters were summarized in Table 2.2 of last chapter. A forward power of 1.5 kW was used for all measurements. It should be noted that the plasma is extinguished upon insertion if liquid samples are used without drying or ashing. Thus liquid samples were dried under an infrared lamp for 2-3 minutes before insertion. The drying and atomizing parameters are:

	Drying	Atomizing	Cooling
Position/mm (below TOLC)	45	3	180
Time/s	5	15	5

Considering the relatively high volatility of the elements Pb, Bi, Ag and In, an atomizing time of 15 seconds is adequate to completely evaporate the 10 uL multielement liquid solution residue in the graphite cup.

As mentioned in Chapter 2, the ion lens settings used in DSI were established using a pneumatic nebulizer system, by running a 1 ppm multielement standard solution and by maximizing for the Pb signal before installing the DSI system. The ion lens settings are:

Lens	Setting
Bessel Box Barrel (B)	94
Bessel Box Plates (P)	58
Einzel Lens (E1)	97
Photon Stops (S2)	65

The undercut graphite electrodes ASTM# S-15 were purchased from Bay Carbon, Inc., Bay City, Michigan. In order to reduce the amount of impurities contained in the sample probe, the graphite electrodes were pre-burned in the plasma 3-5 times under regular insertion sequence prior to their use.

All solutions were prepared by serial dilution with distilled/deionized water of 1000 ppm standard stock solution (SPEX Industries Inc., Edison, NJ or LECO Instruments Ltd., Mississauga, ON) of the respective element. The distilled/deionized water was produced in a Millipore Super-Q apparatus (Millipore, Milford, MA).

3.1.3 Results and discussion

3.1.3.1 Analyte and background signals

The signals for 1 ppm Pb and In, 0.5 ppm Bi, and 2 ppm Ag measured with the DSI-ICP-MS are shown in Fig. 3.1 for the insertion of a desolvated aqueous sample (10uL). The analyte time behavior is element dependent with the more volatile elements observed first. The basic volatility of an element is related to its boiling point. The boiling points [11] of the four elements are:

	Pb	Bi	Ag	In
Boiling Points (°C)	1740	1560	2212	2080

As shown in Fig. 3.1, the Pb and Bi signals are sharper (shorter evaporation time) than In, most likely because of their lower boiling points. The evaporation times for Pb and Bi are 7-8 seconds, whereas the signal for In has a duration of almost 15 seconds. The tailing is significant for Ag and In, and it is necessary to measure the peak area rather than peak height for quantitative analysis [12].

There is no measurable signal on a second burn of the same cup, showing that the analytes are evaporated completely during the first insertion. So the same cup can be used directly for the next determination without any cleaning procedure, and the graphite cups used with non-carbide forming analytes are re-usable for over 20 insertions [13].

Low level signals for 20 pg Pb, 20 pg Bi, 80 pg Ag and 60 pg In and their respective background time profiles are shown in Fig. 3.2.

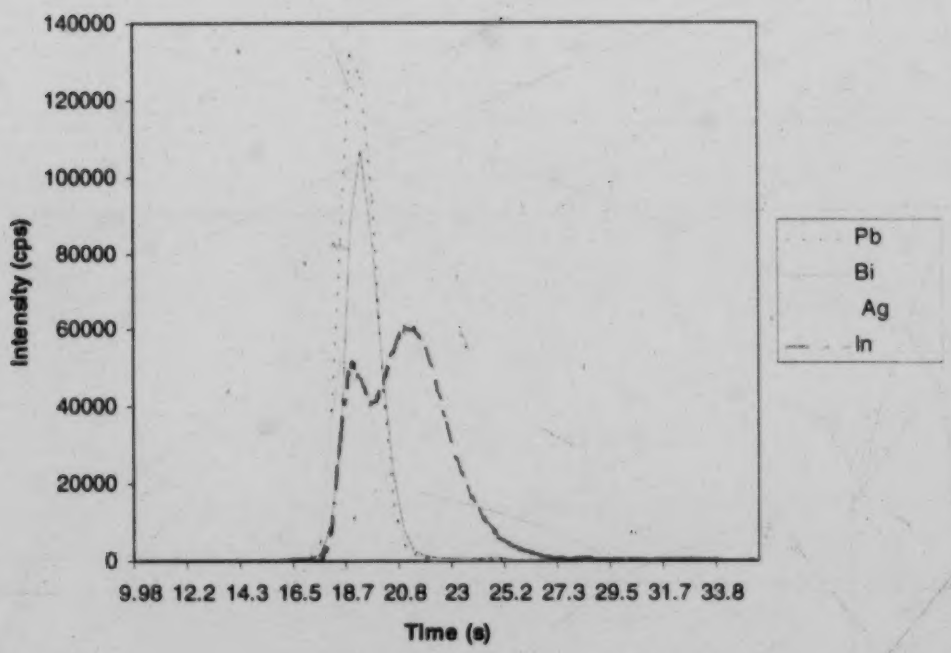

Fig. 3.1 Time profiles of 1 ppm Pb and In, 0.5 ppm Bi and 2 ppm Ag by DSI-ICP-MS

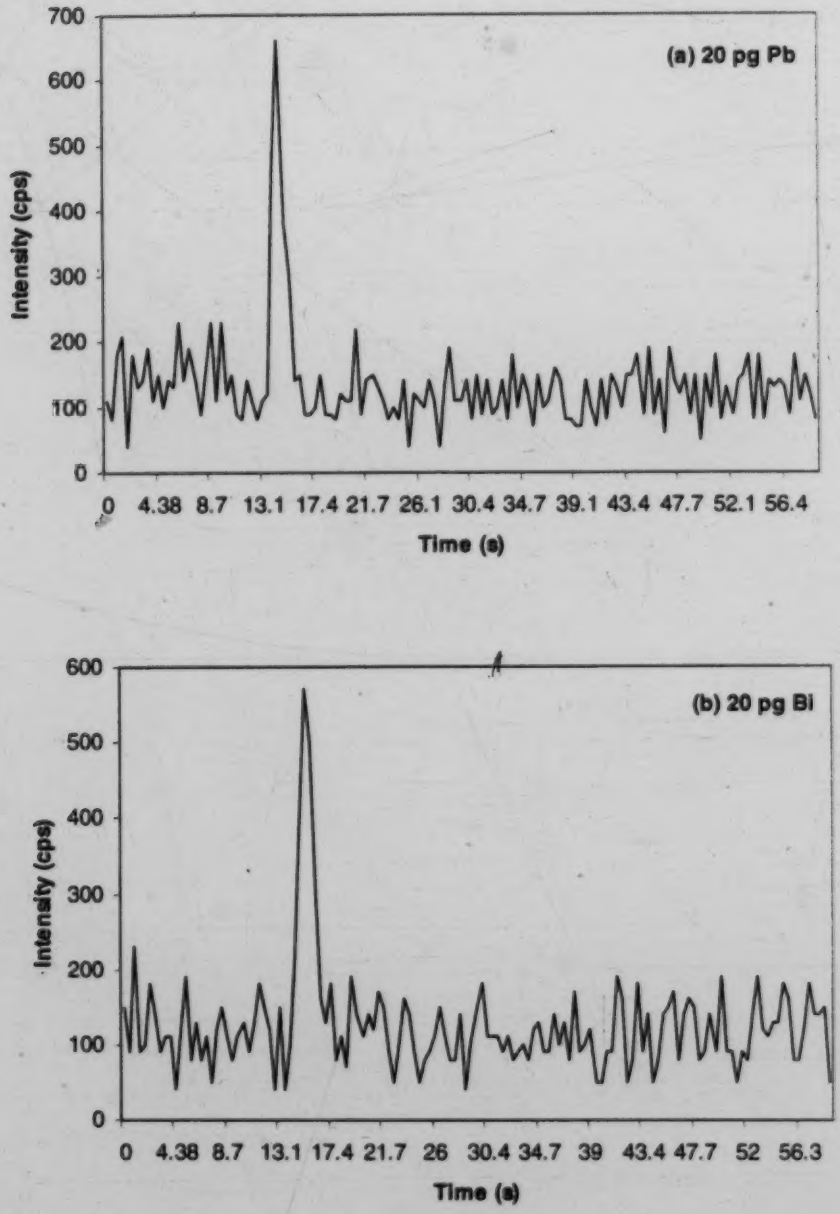

Fig. 3.2 Low level signals for (a) 20pg Pb, (b) 20 pg Bi, (c) 80 pg Ag, and (d) 60 pg In

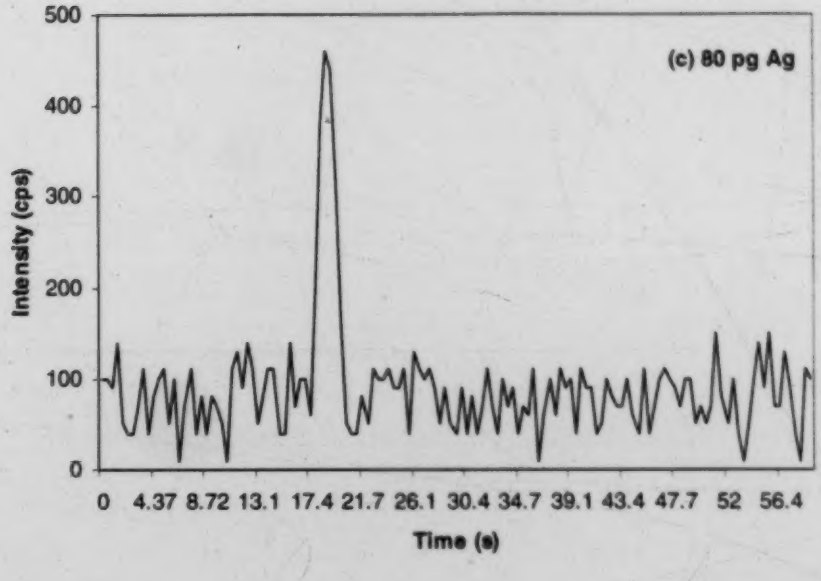

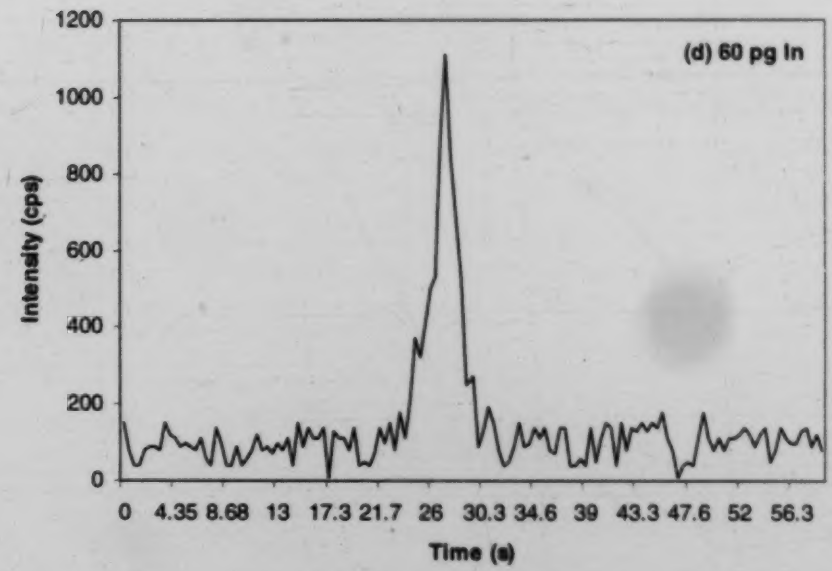

Fig. 3.2 (cont.) Low level signals for (a) 20pg Pb, (b) 20 pg Bi, (c) 80 pg Ag, and (d) 60 pg In

3.1.3.2 Internal standardization

Essentially all quantitative analysis procedures reported for ICP-MS have involved the use of internal standardization [14,15, 16]. In general, internal standardization is important for the compensation of drift, 1/f noise, and multiplication noise [17, 18, 19]. The general consensus is that internal standardization is most effective when the analytes and internal standards are closely matched in terms of mass and first stage ionization potential. Other important considerations in the choice of a suitable internal standard included: low natural abundance in the sample, freedom from significant spectral interference and negligible memory effects in the spectrometer system. An internal standard should also not be a source of spectral interference on the analytes, thus the monoisotopic elements are preferred if possible.

In the measurement of Pb, Bi, Ag and In as a group, Bi is a suitable choice of internal standard for the other three elements in consideration of these criteria. To each sample insertion the same amount of Bi is added and the signal of the analyte is divided by that of the internal standard.

The long-term instrument precision was evaluated using 1 ppm Pb and 0.5 ppm Bi standard solution, with measurements of a total of 18 runs in three hours. The results are shown in Fig. 3.3. Without an internal standard, the relative standard deviation (% RSD) of the 18 measurements of 1 ppm Pb was 15%. The high %RSD is attributed to both run-to-run differences and the instrument instability. The signal intensities (peak area) of Pb exhibit

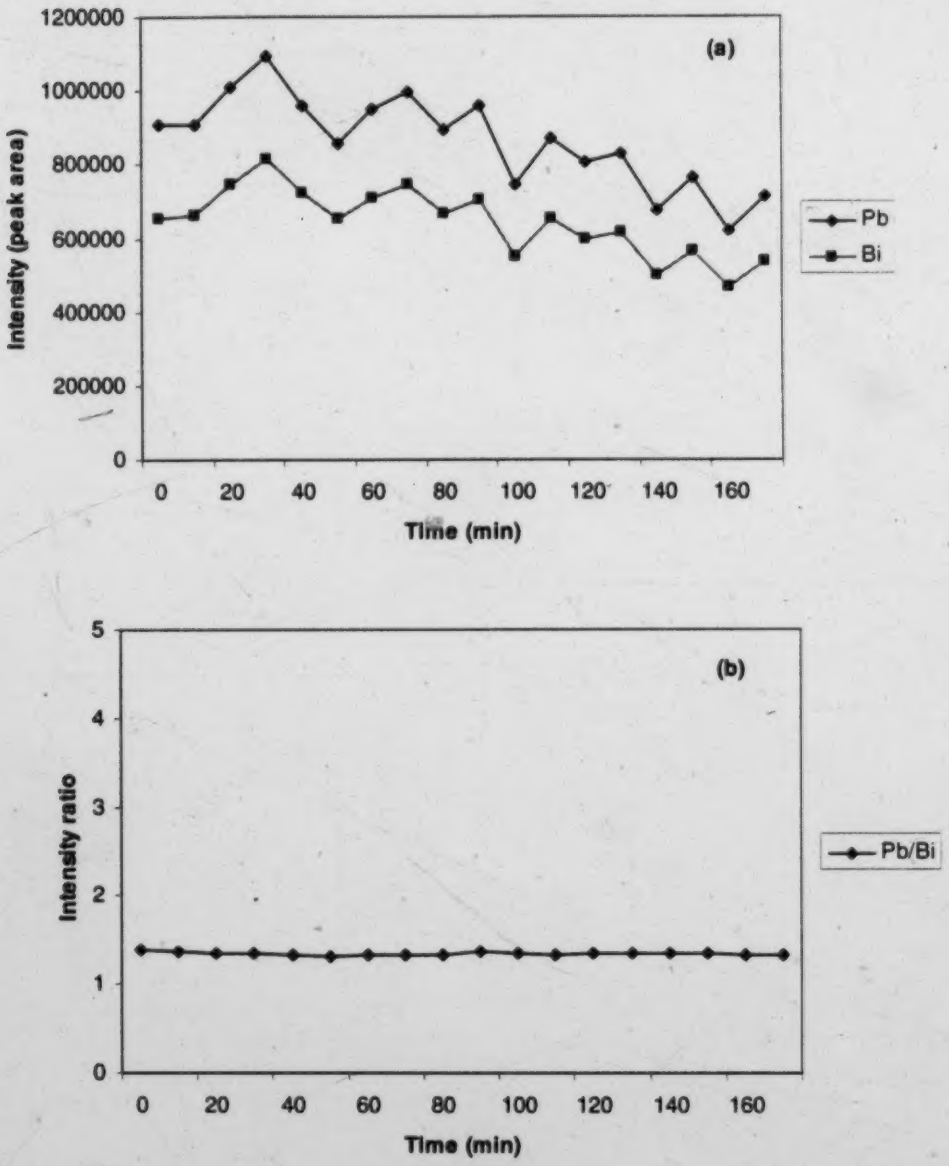

Fig. 3.3 Instrument stability of DSI-ICP-MS (a) without internal standard, (b) with Bi as internal standard

obvious drift over time. With 0.5 ppm Bi as internal standard (measured with Pb simultaneously), the peak area ratios of Pb and Bi exhibit a %RSD of only 1.4%. The significant overall improvement in the precision of the results clearly indicates that the internal standard provides excellent compensation of run-to-run differences and instrument drift. Clearly an internal standard is important for precise and accurate measurements in DSI-ICP-MS.

3.1.3.3 Analytical curve figures of merit

The quantitative performance of the DSI system for the analysis of aqueous solution sample residues is summarized in Table 3.1. The analytical curve figures of merit are obtained under the optimized instrument conditions, with 10 uL aliquots of the multielement standard solution containing Pb, Bi, Ag and In.

(1) Detection limits

After optimizing the instrumental operating conditions for DSI-ICP-MS, the detection limits for Pb, Bi, Ag and In in solution aliquots were determined. The detection limit is defined as the analyte concentration corresponding to the signal intensity equal to three times the standard deviation of the blank. The insertion of an empty cup was used for the calculation of background standard deviation. The detection limits in Table 3.1 are given on the basis of peak height. Peak area can also be used to calculate detection limits, as suggested by Chan and Horlick [12], but peak height detection limits were slightly better in this case. The detection limits obtained by DSI-ICP-MS are

in the low-pg range, significantly better than those obtained by DSI-ICP-AES [12, 20, 21], which are in the 100 pg range.

Table 3.1 Summary of analytical curve figures of merit

Element	Detection limit (pg)	Calibration function slope	Correlation coefficient	Internal standard	linear range
Pb 208	4.49	1.0082	1.000	5ng Bi	100
Ag 107	13.03	1.0834	0.999	5ng Bi	100
In 115	1.72	1.0378	1.000	5ng Bi	100

(2) Relative standard deviation (%RSD)

The internal standard decreases the %RSD of the analytes from about 10% to less than 3%. The internal standard used was Bi with a fixed amount of 5 ng (10 uL x 0.5 ppm) in each insertion. The relative intensity is the ratio of analyte peak area to Bi peak area.

(3) Calibration curve

The calibration curves for quantitative measurements of Pb, Ag and In are shown in Fig. 3.4. All calibration curves were established with 5 ng Bi as the internal standard. Each point on the calibration curves represents an average value based on 6 replicates. It can be seen that excellent calibration curves were established over a dynamic range of at least two orders of magnitude, with correlation coefficients of 0.999-1.000. The calibration function slope is the slope of the log-log plot, which should be 1.00 for linear response.

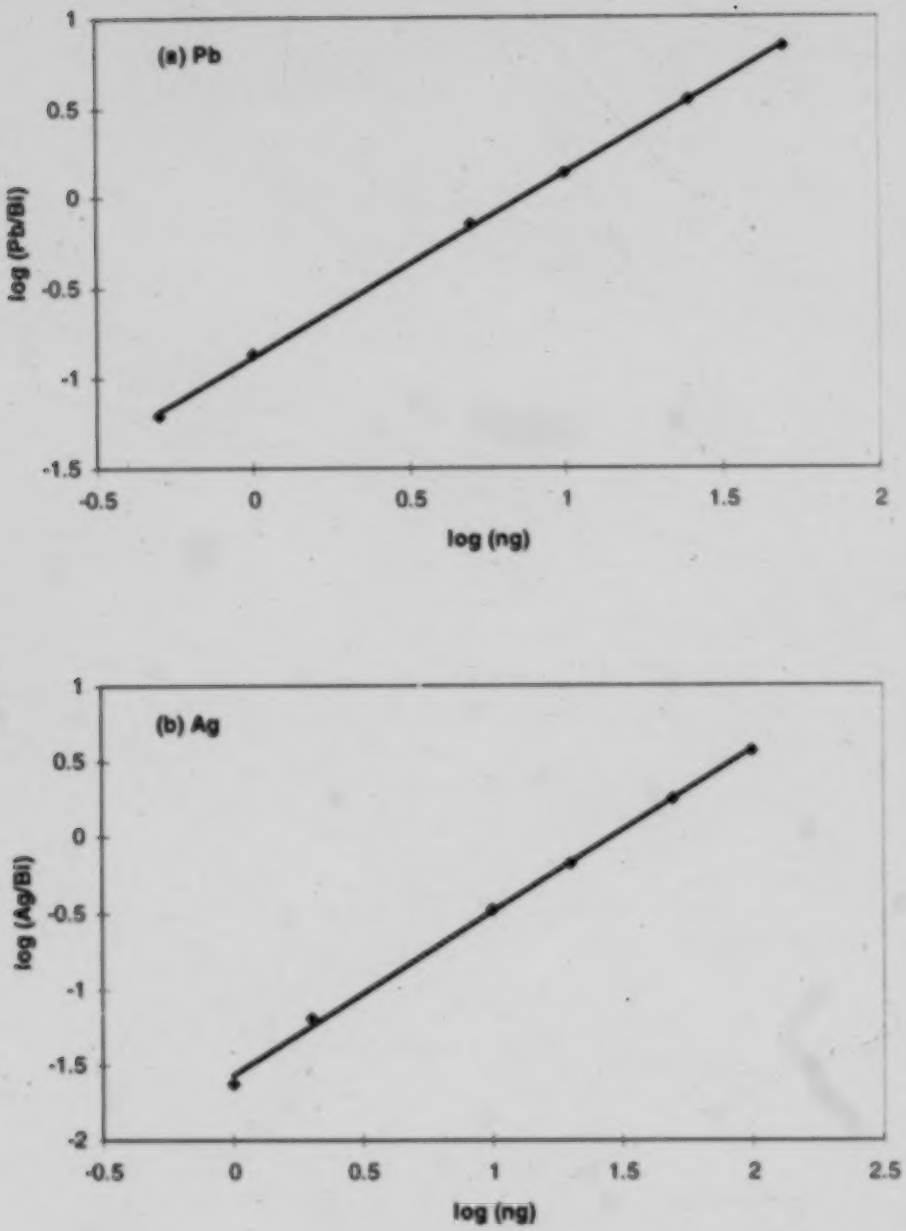

Fig. 3.4 Calibration curves (log-log) of Pb, Ag, and In (5 ng Bi as internal standard)

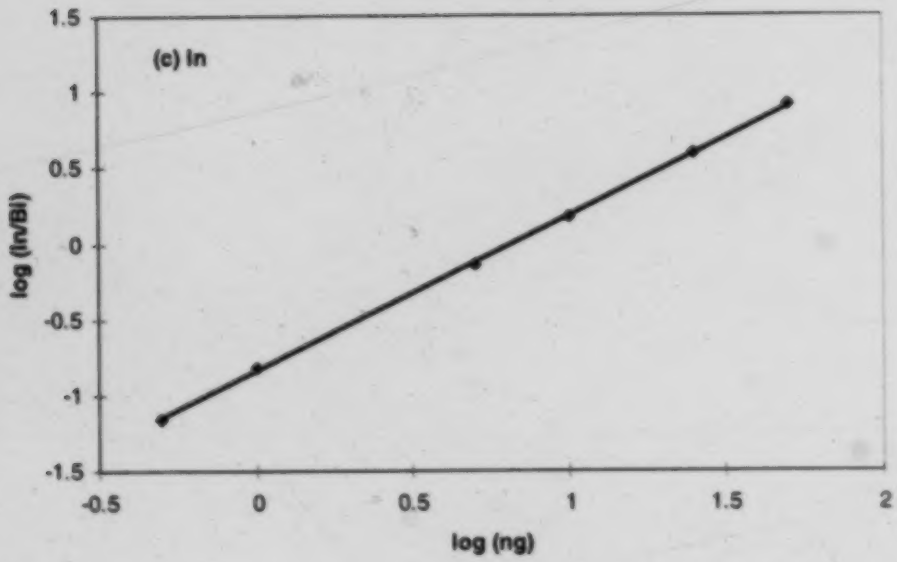

Fig. 3.4 (cont.) Calibration curves (log-log) of Pb, Ag, and In (5 ng Bi as Internal standard)

Calibration curves without internal standardization were also established for comparison (not shown), and their calibration function slope and correlation coefficient are all worse than those obtained with an internal standard.

3.1.4. Conclusion

The basic analytical performance of DSI-ICP-MS was investigated using Pb, Bi, Ag and In standard solutions. Good quantitative results can be obtained for these elements with good precision and low detection limits with the use of 10 uL of solution sample. Excellent calibration curves were established for these elements with the use of an internal standard.

3.2 Measurement of Pb in Solid Biological Samples

3.2.1 Introduction

Lead (Pb) poisoning is a significant health problem. The historical widespread use of Pb in paint and gasoline has distributed Pb throughout the environment. Lead is probably the most studied toxic element in occupational and environmental medicine. Exposure to lead occurs through inhalation of particles containing lead and ingestion of food, drinking water, settled indoor dust, and soil contaminated with lead. Lead is absorbed through the lungs or the gastrointestinal tract into the blood. Environmental exposure to lead can be hazardous to human health. The adverse effects of chronic long-term exposure to lead include gastrointestinal disturbances, anemia, insomnia, weight loss, motor weakness, muscle paralysis, and nephropathy [24, 26, 36]. The problem of Pb toxicity is complicated because

Pb affects different people unequally. Many experts believe that Pb has no threshold, but instead has a continuum of toxicity. Due to the health threats posed by lead, The National Research Council has reduced the acceptable lead level in blood several times to the current level of concern of 10 ug/dL.

Lead has been measured in different types of biological samples, including: (1) human or animal tissue and body fluids, which includes organs, hair, muscle, bone, blood, feces, and urine [15, 22, 23, 24]; (2) plant tissue, which includes samples of terrestrial plants, aquatic plants, and humic materials [2, 3, 4, 25]; and food products and related substances [26, 27, 28, 29]. The analysis of plant tissues is of major significance in biogeo-chemical and agronomic studies, and is a direct and inexpensive method for mineral exploration. This type of survey establishes the relationship between metal concentration in the soil and plants growing in an area. Knowledge of the mineral elements present in the different plant organs is basic to an understanding of plant physiology, and valuable for determining the amount of harmful elements (e.g. Pb) found in plants that are used for animal and human consumption.

As the risk of exposure to potentially toxic elements continues to grow, the need for analytical systems to monitor such species at low levels increases. Different analytical methods have been employed for analyzing Pb in biological samples, such as atomic absorption spectrometry (AAS) [30, 31], X-ray fluorescence (XRF) [32, 33], inductively coupled plasma atomic emission spectrometry (ICP-AES) [25, 34] and inductively coupled plasma mass spectrometry (ICP-MS) [35, 36].

In spite of the variety of analytical methods and materials, a common problem exists with respect to sample preparation. Sample preparation is often more time-consuming than the instrumental measurement itself. Due to the solution sample state requirement of ICP, the most conventional approach to sample preparation involves decomposition of the sample by thermal or chemical means, followed by dissolution and dilution of the residue to a specific volume prior to analysis. Of the various procedures, microwave oven acid digestion [25, 37] is commonly used and an effective method for biological analyses. Digestion may cause some analytical problems such as contamination from reagents, dilution and even loss of analytes already at a low level. In addition to digestion, separation and preconcentration steps might be required during sample preparation in order to improve detection capability and eliminate interferences.

The alternative sample introduction methods for ICP spectrometry that have been used in the trace element analysis of biological samples includes electrothermal vaporization (ETV) [23, 28], graphite furnace (GF) [24,38), and laser ablation (LA) [39, 40]. These methods can provide direct analysis of biological samples, but they have relatively complicated and expensive instrumentation. An ideal analytical instrument would detect trace amounts of the elements in biological samples, at low cost, with little sample pretreatment. The aim of this work is to develop an analytical procedure for the direct analysis of trace element Pb in powered plant tissue by DSI-ICP-MS.

3.2.2 Experimental

The DSI-ICP-MS instrumentation was described previously. The undercut graphite electrodes ASTM# S-14 (Bay Carbon, Inc., Bay City, Michigan) were used for solid samples because their deeper tip crater can hold more samples and reduce sample spattering. In order to reduce the amount of impurities contained in the sample probe, the graphite electrodes were pre-burned in plasma 3-5 times under regular insertion sequence prior to their use.

The solid samples including spinach NIST SRM 1570, tomato leaves SRM 1573, pine needles SRM 1575, orchard leaves SRM 1571, and pepperbush NIES SRM No.1 were used directly without further treatment. The solid samples were weighed on a micro-balance and placed in a graphite cup.

The addition of internal standard was performed by adding 10 uL of 0.5 ppm Bi (5 ng) standard solution onto a graphite cup, and drying it under a infrared lamp for 2-3 minutes, before weighing the solid sample.

One of the aspects of DSI-ICP-MS instrumentation is the horizontal insertion of the sample probe required by the mass spectrometer interface. It causes problems for solid sample introduction because a powdered solid sample may fall out during the horizontal movement of the probe into the plasma. One of the suggested resolutions is the use of a boiler cap (i.e. a lid on the probe) [1, 41]. But the use of a boiler cup produces a broader peak of lower intensity. This can be attributed to the increase in probe mass, which results in a decrease in the probe heating rate [42]. Another approach

developed in this lab is to coat the solid sample with a sugar solution. In this work, 20 uL of a 1% sugar solution was applied on the top of the solid sample, and then dried under an infrared lamp for 3 minutes. The sugar coating after drying prevents the loss of sample during the insertion procedure.

It should be noted that the plasma is extinguished upon insertion if solid samples are used without ashing. It was determined that an ashing time of 30 seconds was required for these samples. No visible signals were detected during ashing stage, indicating that no analyte loss occurs. The ashing and atomizing parameters are:

	Ashing	Atomizing	Cooling
Position/mm (below TOLC)	45	3	180
Time/s	30	15	5

With an ashing time of 30 seconds at the designated position, most if not all of the organic contant of the powdered botanicals is removed before insertion.

3.2.3 Results and discussion

3.2.3.1 Matrix effect

A matrix effect is a non-spectroscopic interference, in which a high concentration of a concomitant species induces changes in the signal

intensity of an analyte. Although suppression is most often observed, signal enhancement is also possible. These interference effects are generally believed to be due to the physical and chemical behavior of the matrix elements (and analytes) in the sample introduction system, the plasma, the interface region and the ion optics. The consequence of these non-spectroscopic interferences is a difference in signal strength for a given concentration of analyte in the presence and absence of matrix elements. Such generalized matrix effects are normally relatively minor in ICP-AES [43], but matrix effect occurs in ICP-MS and has been intensively investigated by Tan and Horlick [44].

A brief investigation of matrix effects in DSI-ICP-MS was performed by comparing the Pb and Bi signals in a water matrix to those in a biological matrix---artificial cerebrospinal fluid (CSF). 1 ppm Pb and Bi were prepared both in water solution and in CSF solution. The CSF solution, provided by Dr. Norm Dovichi's research group, contains high concentrations of alkaline salts (NaCl, Na_2CO_3, KCl, and Na_2HPO_4), other salts ($CaCl_2$, and $MgCl_2$), acid (HCl), and glucose (dextrose anhydrous) in distilled water. The time profiles of 1 ppm Pb and Bi in water solution and in CSF solution are shown in Fig. 3.5. The signals of Pb and Bi in water are smooth and only single peaks can be seen. But the signals of Pb and Bi are quite different in the CSF matrix, in which asymmetric double peaks are obtained. The first peaks are probably due to the formation and earlier vaporization of the more volatile chloride of Pb and Bi, whose melting and boiling points are relatively low. The shape of the double peak is also changed with the insertion position. Quantitative calculations show that even though the peak shapes and peak heights are changed, the peak areas of Pb and Bi and then the peak area ratio

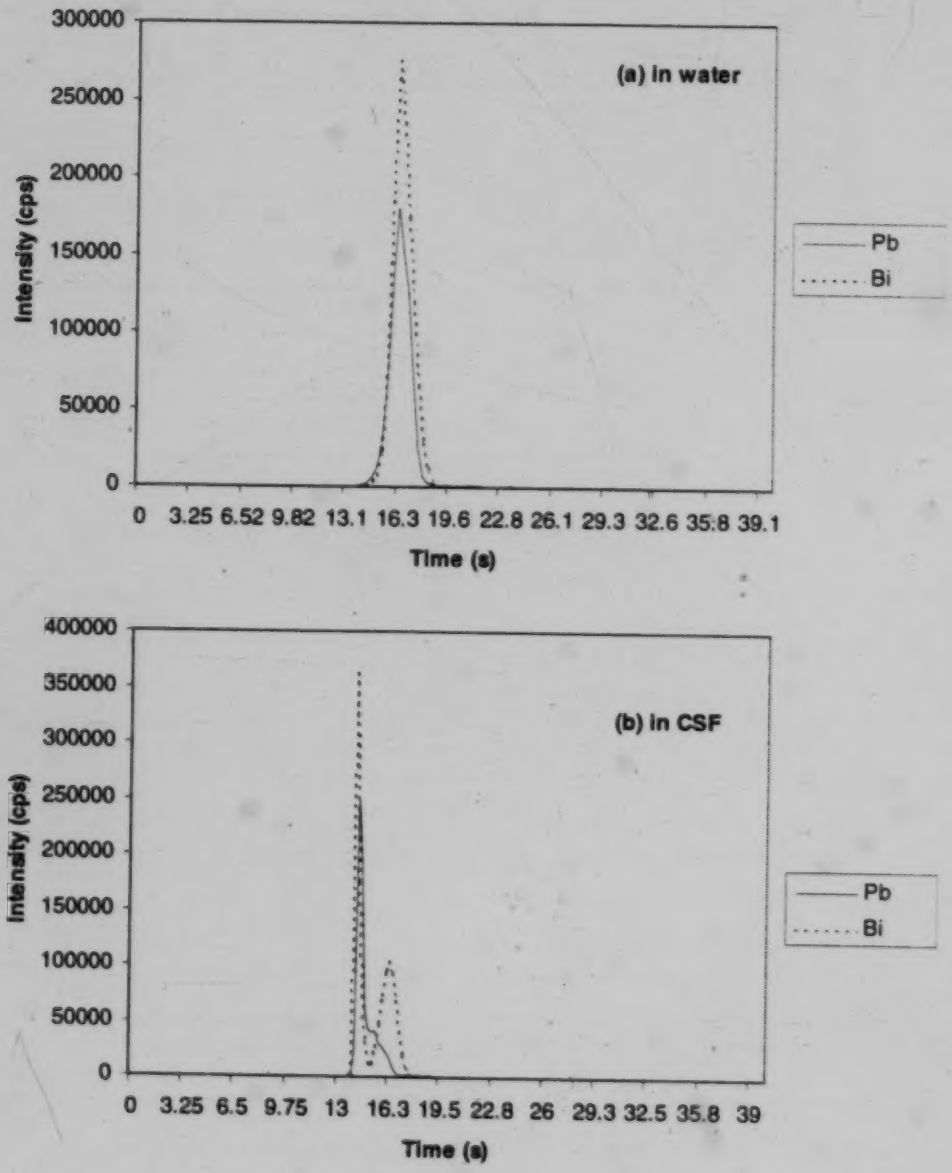

Fig. 3.5 Time profiles of 1 ppm Pb and Bi in (a) water solution, and (b) CSF matrix

(Pb/Bi) in CSF matrix are roughly the same as those in the water matrix. The observation that peak shape changes while the peak area remains constant indicates that the concomitant alters the volatilization characteristics of the analyte but does not alter the overall residence time of the analyte in the plasma nor does it significantly alter the excitation conditions. Thus the DSI-ICP-MS demonstrates some freedom from matrix interference. The result is encouraging in that it shows the possibility to quantitatively analyze a biological sample, at least a biological fluid, directly by calibration with aqueous standard solutions.

3.2.3.2 Calibration methods for Pb measurement in powdered plant tissues

The Pb signals for 4 mg spinach NIST SRM 1570, 2 mg tomato leaves SRM 1573, 2 mg pine needles SRM 1575, 1.5 mg orchard leaves SRM 1571, and 2 mg pepperbush NIES SRM No.1 are shown in Fig. 3.6. The measured Pb concentrations in SRMs are summarized in Table 3.2. The results are based on three calibration methods: external calibration by liquid standard solutions, external calibration by different SRMs with internal standard, and external calibration by different SRMs without internal standards.

(1) External calibration by liquid standard solutions

ICP-MS is considered to be more susceptible to matrix effects than ICP-AES [45]. One way to solve this problem is by the introduction of an internal standard to the sample. In addition to compensating for run-to-run differences and instrument drift, an internal standard is also known to be

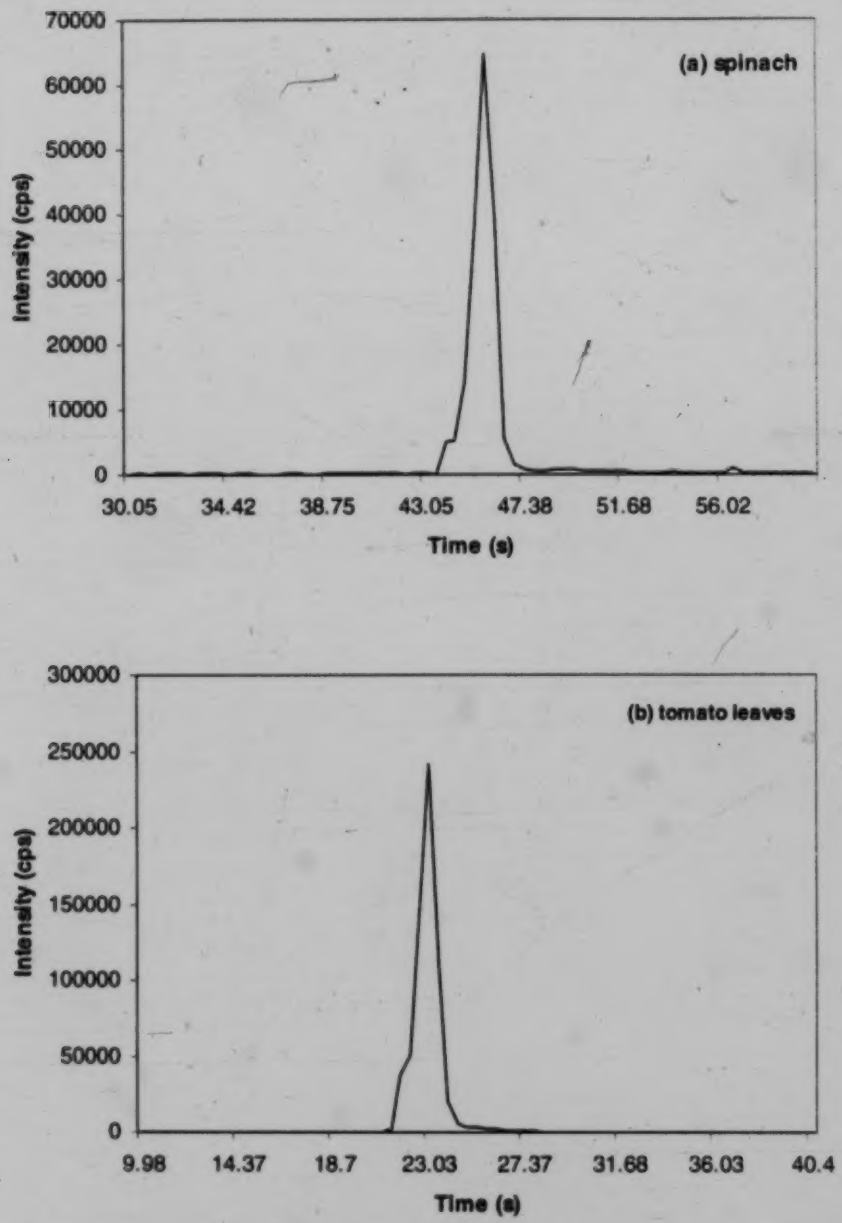

Fig. 3.6 Pb signals in solid plant SRMs: (a) 4 mg spinach, (b) 2 mg tomato leaves, (c) 2 mg pine needles, (d) 1.5 mg orchard leaves, and (e) 2 mg pepperbush

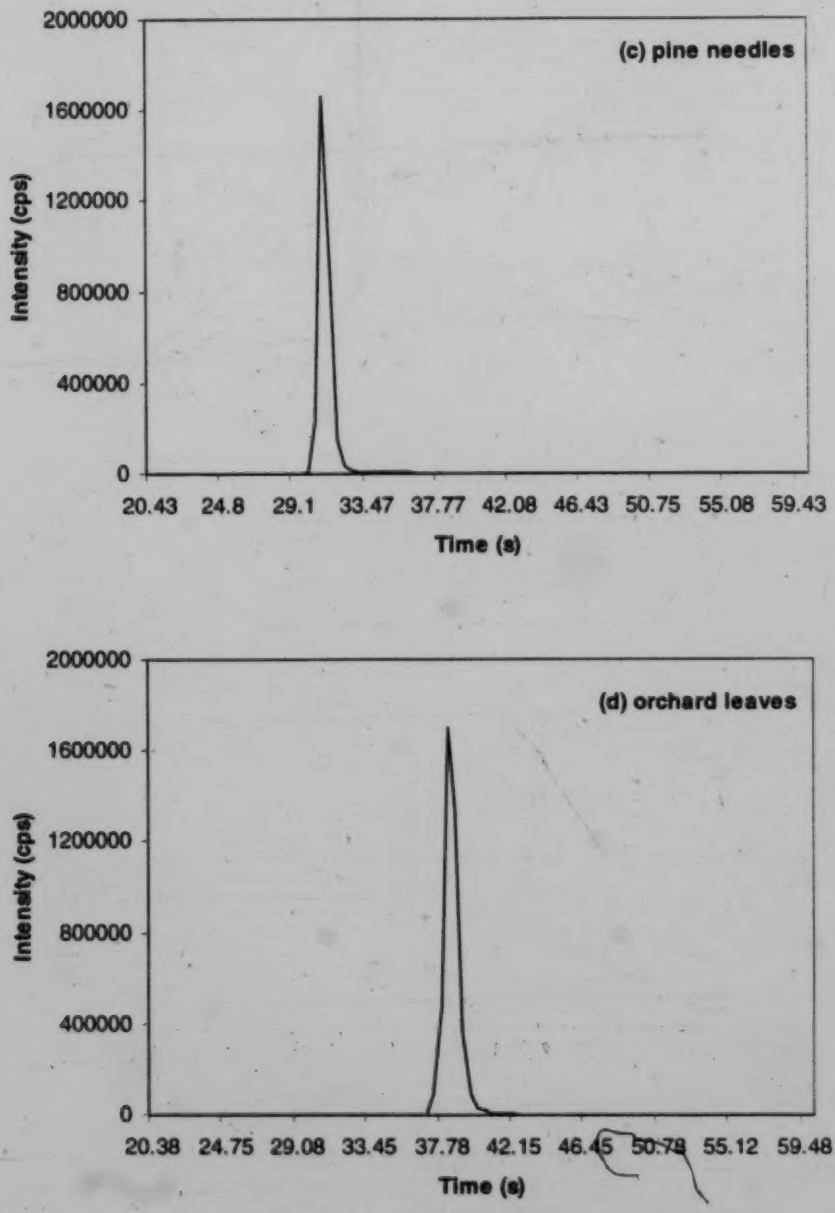

Fig. 3.6 (cont.) Pb signals in solid plant SRMs: (a) 4 mg spinach, (b) 2 mg Tomato leaves, (c) 2 mg pine needles, (d) 1.5 mg orchard leaves, and (e) 2 mg pepperbush

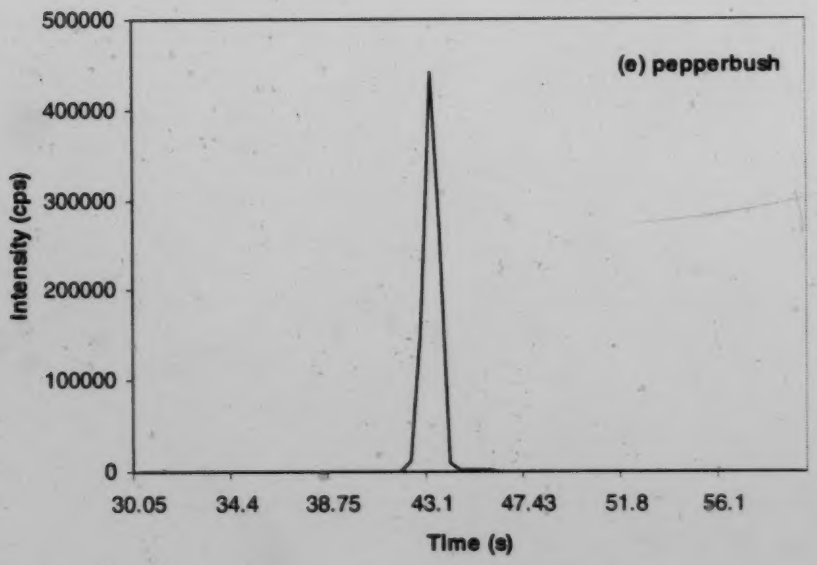

Fig. 3.6 (cont.) Pb signals in solid plant SRMs: (a) 4 mg spinach, (b) 2 mg Tomato leaves, (c) 2 mg pine needles, (d) 1.5 mg orchard leaves, and (e) 2 mg pepperbush

Table 3.2 Measurement of Pb in Plant Samples

Calibration method	correlation coefficient	SRM	Certified value(ug/g)	Measured value(ug/g)	recovery
external calibration using standard solutions(Bi as internal standard)	0.9999	pine needles	10.8	14.2	131.4%.
external calibration using SRMs (Bi as internal standard)	1.0000	pepperbush	5.5	3.65 3.39 3.49	66.3% 62.0% 63.3%
external calibration using SRMs (without internal standard)	0.9995	pepperbush	5.5	5.52 5.58 4.85	100.4% 101.4% 88.2%

RSD%: 1%-15% of 5 measurements each sample (with or without internal standard)

important in correcting matrix effects in ICP-MS. It would be ideal to measure Pb concentrations in solid botanical SRMs by calibration with liquid standard solutions. The concentrations of aqueous standards were carefully chosen so that the value in the unknown solids are within the calibration curve range. An internal standard of 5 ng Bi was used for both the calibration standards and the sample. Unfortunately the results shown in Table 3.2 are not good. A large error (> 30%) exists for the Pb concentration in pine needles, even with the use of an internal standard. Although not tested, it can be assured that a similar error would occur with other SRMs because of their similar matrix. The data indicate that aqueous standards cannot be used directly for this determination. The positive error indicates that the major components in botanicals---NaCl, KCl, $CaCl_2$, $MgCl_2$---enhance the signal intensity of Pb. The effects caused by the major components are likely the result of changes in analyte volatilization. Therefore, an alternative calibration approach is necessary for accurate results.

(2) External calibration by different SRMs with internal standard

One approach to the direct analysis of plant materials which contain Na, K, Ca, and Mg as major components is to establish calibration curves with a reference standard having similar concentrations of the major components (similar matrix) or a synthetic standard prepared by matrix matching.

A calibration curve for Pb using 2.05 mg spinach SRM 1570, tomato leaves SRM 1573, pine needles SRM 1575, and orchard leaves SRM 1571, spiked with 5 ng Bi as internal standard, is shown in Fig. 3.7. Three random weighs

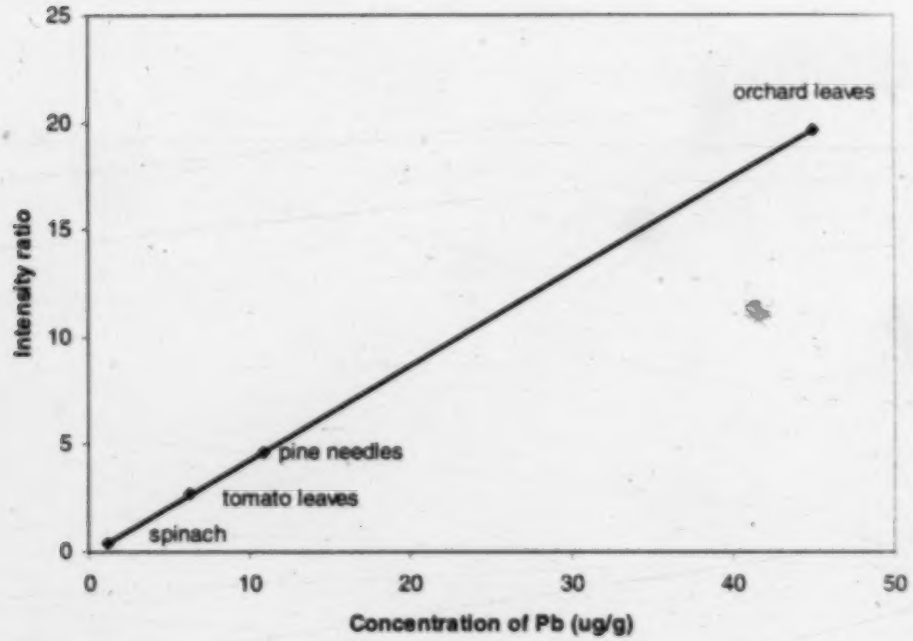

Fig. 3.7 Calibration curve of Pb using solid plant SRMs with 5 ng Bi as internal standard

of pepperbush sample (2 - 6 mg) spiked with 5 ng Bi as internal standard were measured as an unknown sample. For each data point, five replicate burns were made and the average intensity values were used. The measured Pb concentration, shown in Table 3.2. is still not what we expected, and a negative error exists in this case. A careful investigation showed that although there is no detectable Bi signal in the American standards (spinach, tomato leaves, pine needles, and orchard leaves), a relatively high Bi signal was found in the Japanese standard pepperbush, probably due to different geo-environments in the two countries. The high Bi signal in pepperbush is one of the reasons for the low Pb recovery in the sample. Thus a different internal standard would have to be used for Pb measurement.

It would again be necessary to match carefully the physical and spectroscopic properties of the internal standard with those of the elements of interest. The selection of another element having the same volatility and ionization characteristics as Pb is made difficult by the fact that most of the suitable elements are analytes as well and are found in real samples. Indium was tried as the internal standard for the determination of Pb, but it didn't work, probably due to its higher boiling point.

In addition to the difficulties in finding a suitable internal standard, the different physical and chemical states of the internal standard and the real sample also make the internal standard less effective to compensate for matrix effects. The water solution residue used as the internal standard in this method is quite different from the botanical samples to be determined. The internal standard elements (Bi or In) could certainly experience different matrix effects than the analyte Pb in the samples. The method of

compensating for a matrix effect is effective only if the analyte and the internal standard experience the same matrix effect. The liquid internal standards do not allow for the adequate correction for the matrix effect. The use of solid internal standard may be a solution to this problem.

(3) External calibration by different SRMs without internal standard

A calibration curve for Pb established using 4 mg spinach SRM 1570, 2 mg tomato leaves SRM 1573, 2 mg pine needles SRM 1575, and 1.5 mg orchard leaves SRM 1571 without the use of an internal standard, is shown in Fig. 3.8. Different masses of SRMs were weighed for calibration in order to keep the Pb signal intensities in the proper dynamic range of the mass spectrometer, because spinach has a low Pb concentration, whereas orchard leaves has a rather high Pb content (about 45 times higher than that in spinach). Three random weighs of pepperbush sample (about 2 mg) were measured as an unknown sample. For each data point, four or five replicate burns were made and the average intensity values were used. The measured Pb concentrations are shown in Table 3.2. The results now agree well with the NIES certified value.

Without the use of an internal standard, the correlation coefficient of the Pb calibration curve is 0.9995, slightly worse than that with the internal standard, but acceptable for the accurate quantitative analysis. The relative standard deviation (%RSD) of four or five replicate measurements of the solid SRMs is in a range of 1% - 15%. The relatively poor precision is probably because of the reproducibility of weighing, the physical condition of the sample carrying probe (i.e. cup porosity), the nature of the residue

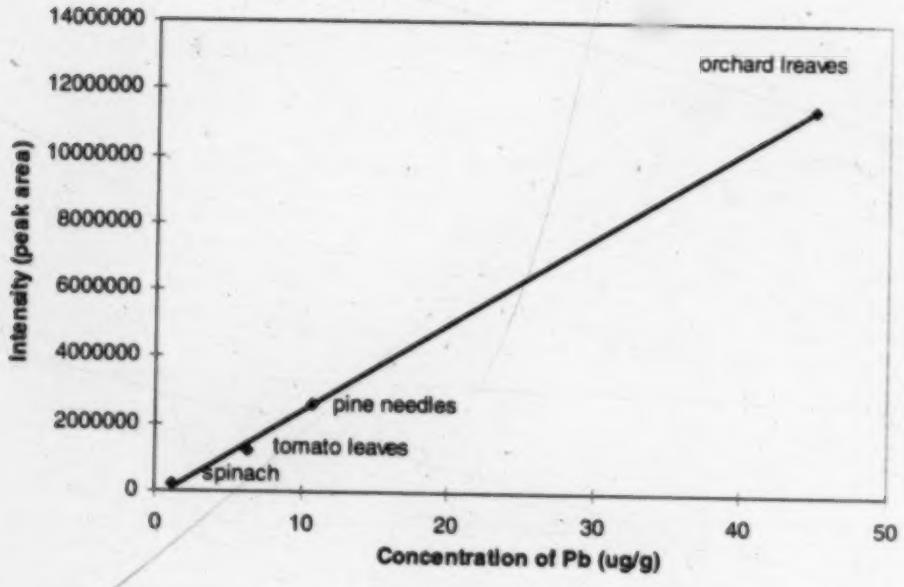

Fig. 3.8 Calibration curve of Pb using solid plant SRMs (without internal standard)

remaining in the probe after ashing or at the initial stages of atomizing, instrumental drift or noise (no internal standard correction), and most likely, the solid sample inhomogeneity due to the small amount of sample in use. In consideration of all these factors, the obtained %RSD is quite reasonable.

3.2.4 Conclusion

Lead continues to be an important element for environmental monitoring due to health effects. Assessment of potential hazards and monitoring of remediation effects are essential to providing a safe environment. DSI-ICP-MS is a rapid and useful method for monitoring lead in solid biological samples, such as botanicals. In comparing three calibration methods, external calibration by SRMs with similar organic origin was found to be a reliable method for the accurate measurement of Pb concentration in a similar sample. This method can also be used to measure lead content in other types of samples including food and agricultural products, human blood and serum, soil, paint, and dust. Additionally, the use of solid internal standardization might be effective in future work.

The work described was performed using SRMs, which can be considered to be "ideal" produced samples. When this method is used for real samples, care must be taken with regard to sampling and sample preparation. It should also be noted that the composition of plant tissues is strongly dependent on biological and environmental factors including the local climate.

References

1. Salin, E. D., and Horlick, G., **Anal. Chem.**, 1979, *51*, 2284-2286
2. Abdullah, M., and Haraguchi, H., **Anal. Chem.**, 1985, *57*, 2059-2064
3. Shao, Y., and Horlick, G., **Appl. Spectrosc.**, 1986, *40*, 386-393
4. Abdullah, M., Fuwa, K., and Haraguchi, H., **Spectrochim. Acta.**, 1984, *39B*, 1129-1139
5. Pettit, W. E., and Horlick, G., **Spectrochim. Acta.**, 1986, *41B*, 699-712
6. Chan, W. T., and Horlick, G., **Appl. Spectrosc.** 1990, *44*, 525-530
7. Haraguchi, H., Abdullah, M., Hasegawa, T., Kurosawa, M., and Fuwa, K., **Bull. Chem. Soc. Jap.**, 1984, *57*, 1839-1842
8. Abdullah, M., Fuwa, K., and Haraguchi, H., **Appl. Spectroec.**, 1987, *41*, 715-721
9. Salin, E. D., and Sing, R. L. A., **Anal. Chem.**, 1984, *56*, 2596- 2600
10. Karanassios, V., and Horlick, G., **Spectrochim. Acta.**, 1989, *44B*, 1345-1360
11. Weast, R. C., and Astle, M. J., Eds, **Handbook of Chemitry and Physics**, *60th edn.*, C.R.C. Press, Cleveland, U.S.A.
12. Chan, W.T., and Horlick, G., **Appl. Spectrosc.**, 1990, *44*, 380-390
13. Karanassios, V., and Horlick, G., **Spectrochim. Acta.**, 1990, *45B*, 105-118
14. Igarashi, Y., Kawamura, H., and Shiraishi, K., **J. Anal. At. Spectrosc.**, 1989, *4*, 571-576
15. Vandecasteele, C., Vanhoe, H., and Dams, R., **J. Anal. At. Spectrosc.**, 1993, *8*, 781-786
16. Vanhaecke, F., Boonen, S., Moens, L., and Dams, R., **J. Anal. At. Spectrosc.**, 1995, *10*, 81-87

17. Vaughan, M. A., and Horlick, G., **J. Anal. At. Spectrosc.**, 1989, *4*, 45-50

18. Moherty, W., **Spectrochim. Acta.**, 1989, *44B*, 263-280

19. Stroh, A., and Vollkopf, U., **Atom. Spectrosc**. 1993, *14(3)*, 76-79

20. Umemoto, M., and Kubota, M., **Spectrochim. Acta.**, 1989, *44B*, 713-723

21. Liu, X. R., and Horlick, G., **J. Anal. At. Spectrosc.**, 1994, *9*, 833-840

22. Bergdahl, I. A., and Schutz, A., **J. Anal. At. Spectrosc.**, 1996, *11*, 735-738

23. Chang, C-C., and Jiang, S-J., **J. Anal. At. Spectrosc.**, 1997, *12*, 75-80

24. Baranowska, I., **Occup. Environ. Med.**, 1995, *52*, 229-232

25. Madeddu, B., and Rivoldini, A., **Atom. Spectrosc**. 1996, *17(4)*, 148-154

26. Dean, J. R., Ebdon, R., and Massey, R. C., **Food Addit. Contam**. 1990, *7*, 109-116

27. Dean, J. R., Massey, R. C., and Ebdon, L., **J. Anal. At. Spectrosc.**,1987, *2*, 369-374

28. Wang, J., Carey, J. M., Caruso, J. A., **Spectrochim. Acta.**, 1994, *49B*, 193-203

29. Ying, L., M. Sc. thesis, Univ. of Alberta, 1992

30. Krug, F. J., Silva, M. M., Oliveira, P. V., Nobrega, J. A., **Spectrochim. Acta**. 1995, *50B*, 1469-1474

31. Sanford, C. L., Thomas, S. E., and Jones, B. T., **Appl. Spectrosc.**, 1996, *50*, 174-181

32. Cake, K. M., Chettle, D. R., Webber, C. E., Gordon, C. L., Bowins, R. J., McNutt,R. H., and Vaillancourt, C., **Adv. X-Ray Anal.**, 1995, *38*, 601-606

33. Kovala, T., Matikainen, E., Mannelin, T., Erkkila, J., Riihimaki, V.,

Hanninen, H., and Aitio, A., **Occup. Environ. Med.**, 1997, *54(7)*, 487-493

34. Kimbrough, D. E., and 'mel'Suffet, I. H., **Analyst**, 1996,*121*, 309-315
35. Mauras, Y., Premel-Cabic, A., Berre, S., and Allain, P., **Clinica Chim. Acta**, 1993, *218*, 201-205
36. Schutz, A., bergdahl, I. A., Ekholm, A., and Skerfving, S., **Occup. Environ. Med.**, 1996, *53(11)*, 736-740
37. Sheppard, B. S., Heitkemper, D. T., and Gaston, C. M., **Analyst**, 1994, *119*, 1683-1686
38. Yen, C-C., Chen, W-K., Hu, C-C., Wei, B-L., Chung, C., and Kuo, S-C., **Atom. Spectrosc.**, 1997, *18(2)*, 64-69
39. Wang, S., Brown, R., and Gray, D. J., **Appl. Spectrosc.**, 1994, *48*, 1321-1325
40. Roberts, N. B., Walsh, H. P. J., Klenerman, L., Kelly, S. A., and Helliwell, T. R., **J. Anal. At. Spectrosc.**, 1996, *11*, 133-138
41. Page, A. G., Godbole, S. V., Madraswala, K. H., Kulkarni, M. J., Mallapurkar, V. S., and Joshi, B. D., **Spectrochim. Acta.**, 1984, *39B*, 551-557
42. Barnett, N. W., Cope, M. J., Kirkbright, G. F., and Taobi, A. A. H., **Spectrochim. Acta**, 1984, *39B*, 343-348
43. Lepla, K., Vaughan, A., and Horlick, G., **Spectrochim. Acta.**, 1991, *46B*, 967-973
44. Tan, S. H., and Horlick, G., **J. Anal. At. Spectrosc.**, 1987, *2*, 745-763
45. Houk, R. S., **Anal. Chem.**, 1986, *58*, 97A

Chapter 4
Measurement of Fe, Co, Mn and Cu by DSI-ICP-MS

4.1 Introduction

Since the earliest studies in ICP-MS [1], background polyatomic species derived from the plasma gas, water from the sample aerosol and the entrainment of air in the plasma have all been accepted features of the resulting ICP-MS spectra [2, 3]. The polyatomic species derived from argon, water and air present in the plasma, such as ArH^+, ArN^+ and ArO^+, are believed to be formed in the plasma. One of the most troublesome spectral interferences observed in the ICP-MS is that caused by argon polyatomic species, such as $^{40}Ar^{16}O^+$, which make it almost impossible to determine iron by the most abundant isotope $^{56}Fe^+$ (91.2%). Because the interference appears at the most abundant isotope of the element to be determined, the analyst may have to resort to measurements at a less abundant isotope, with a concomitant loss of sensitivity. But the determination of Fe is still a problem because the next most abundant isotope, $^{54}Fe^+$ (2.15%), also suffers from severe interference due to $^{40}Ar^{14}N^+$ and $^{38}Ar^{16}O^+$.

A number of investigators have made attempts to reduce the effects of polyatomic ion interferences. An method for reducing the polyatomic species is the use of mixed gas addition to either the carrier or the plasma gas flow [4, 5, 6]. Various studies have been described using gases such as N_2, H_2, CH_4 and Xe to attenuate the polyatomic ions by means of gas-phase collisions and reactions, and all have reported success to some extent, but usually with accompanying attenuation of the analyte signal, and enhanced

polyatomic signals resulting from the combination of Ar with the added gas. Addition of N_2 to the plasma gas can substantially reduce the interference at m/z=56 caused by ArO^+, but increases the interference at the less abundant isotope $^{54}Fe^+$ by ArN^+.

A so called cold plasma is considered to be a solution to some polyatomic problems for certain elements. This approach is to operate the plasma source under conditions of lower power and higher nebulizer flow (and perhaps increased sampling depth and aerosol desolvation). Under these conditions, the background mass spectrum is changed from one dominated by Ar^+ species to one dominated by NO^+. The decrease in the Ar^+ signal as the injector flow is increased and the plasma power is decreased is due to the cooling of the plasma. It was suggested that the cold plasma gas kinetic temperature was about 1450 K at a power of 600 W [7]. The major source of NO^+ is from the nitric acid in the solution. A cold plasma was first reported by Jiang et al. [8] for the determination of K isotope ratios. The lower signal level of ArO^+ also allows for the determination of Fe [7, 9]

Removing the water in the sample aerosol prior to introduction into the plasma, has been found to reduce the ArO^+ background. A number of approaches have been used, such as sample desolvation [10, 11], and ETV [12, 13]. These methods have all achieved varying degrees of success, but still give some ArO^+ background.

An important characteristic of DSI is that it results in a "dry plasma". The sample is dried and desolvated during the drying stage, and no water is introduced into plasma during the final insertion. Thus, in the DSI-ICP-MS

system, solvent-dependent background species are significantly reduced. The complete elimination of water and the simple spectrum of the sample carrying probes results in a remarkable reduction and even elimination of numerous background species normally associated with ICP-MS when solution samples are nebulized into the plasma. The interference-free determinations of many elements including Fe that were previously thought to be impossible when a conventional pneumatic nebulizer system is utilized, have now become feasible by DSI-ICP-MS. In this chapter, the simultaneous determination of Fe, Co, Mn and Cu in standard solutions by DSI-ICP-MS will be demonstrated, and the analytical curve figures of merit will be discussed.

4.2 Experimental

The Perkin-Elmer/SCIEX Elan 250 ICP-MS coupled with the DSI device described previously was used in this research. The operating parameters are summarized in Table 4.1.

A forward power of 1.5 kW was initially used for the simultaneous determination of Fe, Co, Mn and Cu, but low and board signal time profiles were obtained for Fe, Co, and Cu. The boiling points of Fe, Co, Mn, and Cu [14] are:

	Fe	Co	Mn	Cu
Boiling Point ($^{\circ}$C)	2750	2870	1962	2567

Table 4.1 Summary of DSI-ICP-MS instrumental parameters

A. DSI device:	
Ashing Position:	45 mm below TOLC
Time:	5 s
Atomizing Position:	3 mm below TOLC
Time:	Depends on volatility
B. ICP-MS:	
Power :	2 kW
Sampling Depth:	10 mm
Carrier Gas Flow Rate:	1 L/min
Plasma Gas Flow Rate:	13 L/min
Auxiliary Gas Flow Rate:	0.2 L/min
Lens Setting:	Decided by pneumatic system
C. Transient Signal Acquisition	
Dwell Time:	100 ms
Measurement/peak:	1

Considering their high boiling points, a higher forward power should be used to atomize the relatively refractory elements Fe, Co, and Cu, in order to obtain sharper peaks with less tailing. With the use of a power setting of 2.0 kW, higher signal sensitivities and better signal shapes were obtained for these elements. Due to the relatively low volatility of these elements, an atomizing time of 50 seconds was necessary to completely evaporate the 10 uL multielement liquid solution residue of Fe, Co, Mn and Cu in the graphite cup. The liquid sample was dried under an infrared lamp for 2-3 minutes before insertion. The drying and atomizing parameters are:

	Drying	Atomizing	Cooling
Position/mm (below TOLC)	45	3	180
Time/s	5	50	5

As mentioned previously, the ion lens settings used in DSI were established using a pneumatic nebulizer system, in this case, by running a 1 ppm multielement standard solution and by maximizing for the Cu signal before installing the DSI system. The ion lens settings are:

Lens	Setting
Bessel Box Barrel (B)	86
Bessel Box Plates (P)	35
Einzel Lens (E1)	99
Photon Stops (S2)	53

The undercut graphite electrodes ASTM# S-15 were purchased from Bay Carbon, Inc., Bay City, Michigan. In order to reduce the amount of impurities contained in the sample probe, the graphite electrodes were pre-burned in the plasma 3-5 times under regular insertion sequence prior to their use.

All solutions were prepared by serial dilution with distilled/deionized water of 1000 ppm standard stock solution (SPEX Industries Inc., Edison, NJ or LECO Instruments Ltd., Mississauga, ON) of the respective element. The distilled/deionized water was produced in a Millipore Super-Q apparatus (Millipore, Milford, MA).

4.3 Results and Discussion

4.3.1 Signal time profiles

The signal time profiles of 1 ppm Fe (m/z=56), Co (m/z=59), Mn (m/z=55) and Cu (m/z=63) measured with the DSI-ICP-MS are shown in Fig. 4.1 for the insertion of a desolvated multielement aqueous sample (10uL), under the optimized running conditions. The analyte time behavior is element dependent with more volatile elements coming off rapidly. As shown in Fig. 4.1, Mn has a much sharper signal (shorter evaporation time) than Fe and Co because of its lower boiling point. Fe and Co have a longer atomization time with significant tailing, in that the signals of Fe and Co have post-insertion base-line levels of approximately equal magnitude of that observed during pre-insertion in about 50 seconds. It is believed that a further increase of forward power should increase the signal intensities and reduce the tailing of

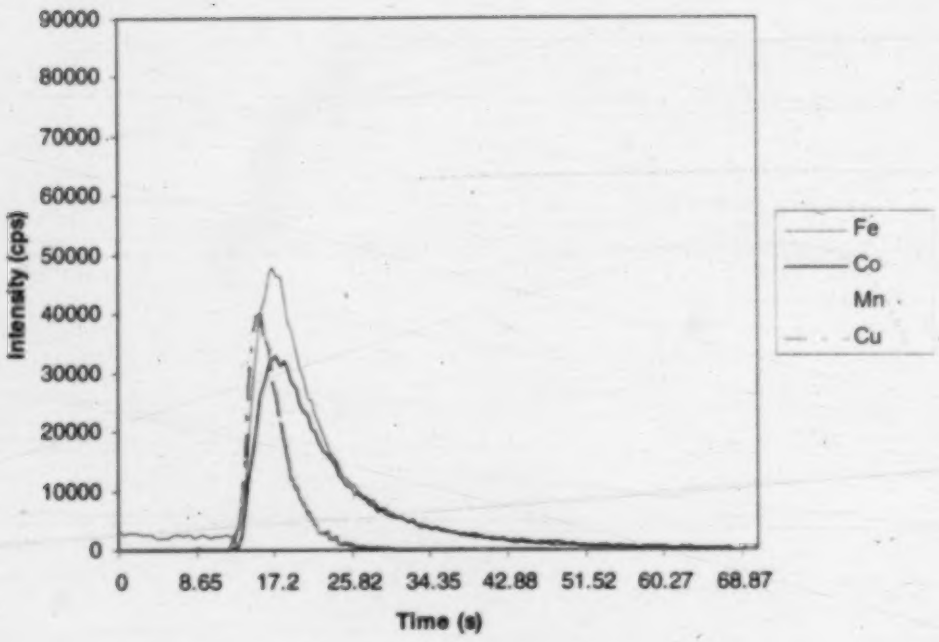

Fig. 4.1 Signal time profiles of 1 ppm Fe, Co, Mn and Cu in DSI-ICP-MS

elements like Fe and Co. This was not tested in consideration of the lifetime of the torch. No measurable signal could be observed on the second burn of the same cup, showing that the analytes were evaporated completely during the first insertion.

Low level signal time profiles for 1000 pg Fe, 200 pg Co, 100 pg Mn and 200 pg Cu and their respective background time profiles are shown in Fig. 4.2. The preinsertion signal level of ArO^+ is about 2500 counts/s (see Fig. 4.2(a)), whereas with conventional nebulization, the background count rate is from 10000 to 30000 counts/s. The intensity of ArO^+ is reduced significantly in this dry plasma. From Fig. 4.2(a), it also can be seen that the base line of Fe shifts to a lower value with the inserted cup. The postinsertion level of ArO^+ is approximately 500 counts/s. This is attributed to a reduction in energy available to the plasma due to energy coupling with the graphite probe. The decreased plasma temperature due to the insertion of the probe reduces the ionization efficiency for higher ionization potential elements, such as Ar. So the actual background level of ArO^+ is about 500 counts/s, at least 20 times lower than that in a pneumatic nebulization system. The background spectrum with DSI sample introduction is therefore simplified and spectral overlap problems are curtailed, and Fe can be determined at trace levels with minimal interference.

4.3.2 Analytical curve figures of merit

The analytical curve figures of merit obtained under the optimized instrument conditions, with 10 uL aliquots of the multielement standard solution containing Fe, Co, Mn and Cu, are listed in Table 4.2.

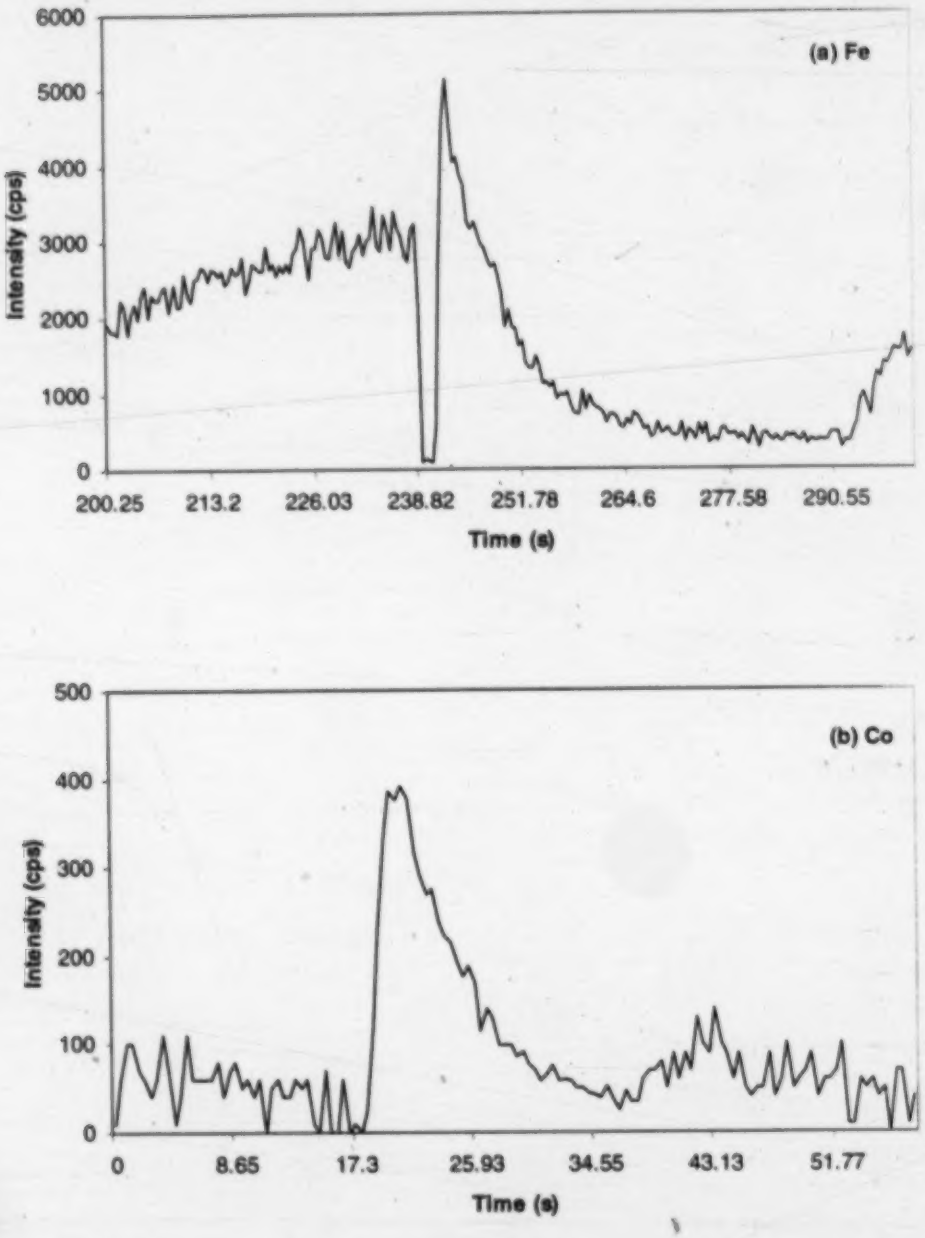

Fig. 4.2 Low level signal time profiles for (a) 1000 pg Fe, (b) 200 pg Co, (c) 100 pg Mn, and (d) 200 pg Cu

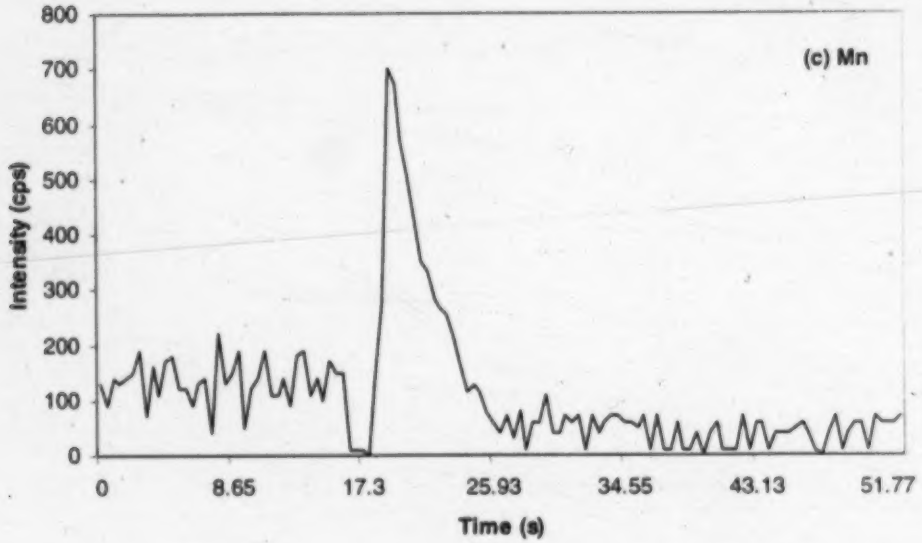

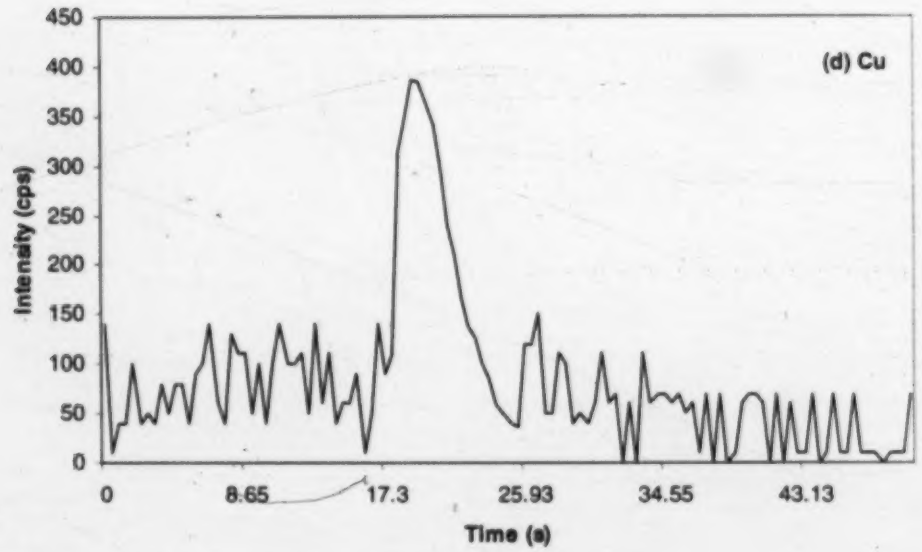

Fig. 4.2 (cont.) Low level signal time profiles for (a) 1000 pg Fe, (b) 200 pg Co, (c) 100 pg Mn, and (d) 200 pg Cu

Table 4.2 Summary of analytical curve figures of merit

Element	Detection limit (pg)	Calibration function slope	Correlation coefficient	Internal standard	linear range
Fe 56	30.12	1.0517	0.999	10ng Cu	100
Co 59	9.3	1.0714	0.999	10ng Cu	100
Mn55	2.73	1.0264	1.000	10ng Cu	100
Cu 63	7.74	N/A	N/A	N/A	N/A

(1) Detection limits

After optimizing the instrumental operating conditions for the DSI-ICP-MS, the detection limits for Fe, Co, Mn and Cu in solution aliquots were determined. The detection limit is defined as the analyte concentration corresponding to the signal intensity equal to three times the standard deviation of the blank. The post-insertions of the bare cups are used for the calculation of background standard deviation. The detection limits in Table 4.2 are given on the basis of peak height. The detection limits of these elements obtained by DSI-ICP-MS are in the low-pg range.

(2) Relative standard deviation (%RSD)

For the quantitative determination of Fe, Co and Mn in standard solution, Cu was chosen as an internal standard. The internal standard improves the precision of the measurements by decreasing the % RSD of the analytes from about 8% to about 4%. The amount of internal standard Cu is 10 ng (10 uL x 1 ppm) in each insertion. The relative intensity is the ratio of analyte peak area to Cu peak area.

(3) Calibration curve

The calibration curves for quantitative measurements of Fe, Co and Mn are shown in Fig. 4.3. All calibration curves were established with 10 ng Cu as the internal standard. Each point on the calibration curve represents an average value based on 5 replicates. It can be seen that excellent calibration curves were established over a dynamic range of at least two orders of magnitude, with correlation coefficients of 0.999-1.000. The calibration function slope is the slope of the log-log plot. Calibration curves without internal standard were also established for comparison (not shown), and their calibration function slope and correlation coefficient are all worse than those obtained with the use of an internal standard.

4.4. Conclusion

An important feature of the DSI technique used with ICP-MS is spectral simplicity. The background species containing oxygen and hydrogen are reduced or eliminated due to the complete elimination of water from the plasma. The relatively interference-free determination of Fe can be performed by DSI-ICP-MS at trace levels because of the low background level of ArO^+ in the "dry plasma". Good quantitative results were obtained for elements Fe, Co, Mn and Cu with good precision and low detection limits using 10 uL of solution sample. Excellent calibration curves were established for these elements with the use of an internal standard.

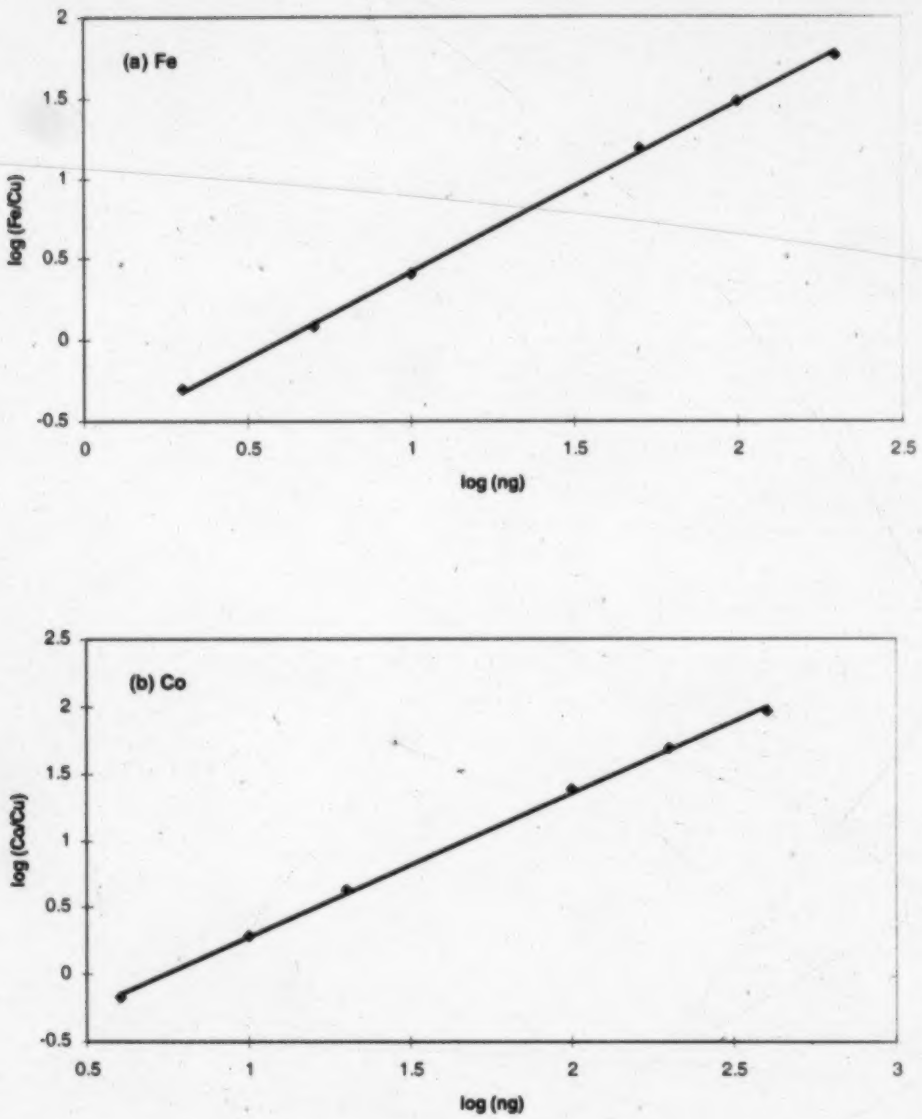

Fig. 4.3 Calibration curves (log-log) of Fe, Co, and Mn with 10 ng Cu as internal standard

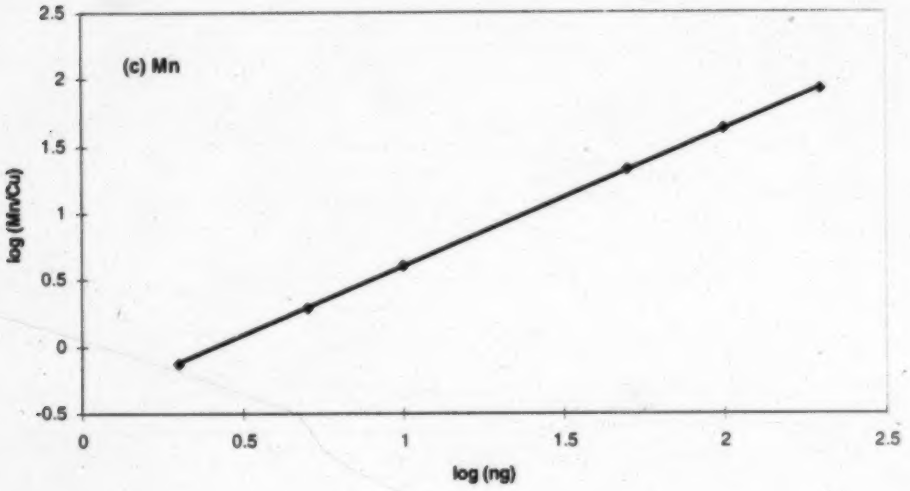

Fig. 4.3 (cont.) Calibration curves (log-log) of Fe, Co, and Mn with 10 ng Cu as internal standard

References

1. Houk, R. S., Fassel, V. A., Flesch, G. D., Svec, H. J., Gray, A. L., and Taylor, C. E., **Anal. Chem.**, 1980, *52*, 2283-2289
2. Vaughan, M. A., and Horlick, G., **Appl. Spectrosc.** 1986, *40*, 434-445
3. Tan, S. H., and Horlick, G., **Appl. Spectrosc.** 1986, *40*, 445-460
4. Smith, F. G., Wiederin, D. R., and Houk, R. S., **Anal. Chem.**, 1991, *63*, 1458-1462
5. Lam, J. W. H., and Horlick, G., **Spectrochim. Acta.**, 1990, *45B*, 1313-1325
6. Hill, S. J., ford, M. J., and Ebdon, L., **J. Anal. At. Spectrosc.**, 1992, *7*, 1157-1165
7. Tanner, S. D., **J. Anal. At. Spectrosc.**, 1995, *10*, 905-921
8. Jiang, S.-J., Houk, R. S., and stevens, M. A., **Anal Chem.**, 1988, *60*, 1217-1221
9. Sakata, K., and Kawabata, K., **Spectrochim. Acta.**, 1994, *49B*, 1027-1038
10. Hutton, R. C., and Eaton, A. N., **J. Anal. At. Spectrosc.**, 1987, *2*, 595-598
11. Zhu, G., and Browner, R. F., **J. Anal. At. Spectrosc.**, 1988, *3*, 781-789
12. Tsukahara, R., and Kubota, M., **Spectrochim. Acta.**, 1990, *45B*, 779-787
13. Whittaker, P. G., Lind, T., Williams, J. G., and Gray, A. L., **Analyst**, 1989, *114*, 675-678
14. Weast, R. C., and Astle, M. J., Eds, **Handbook of Chemitry and Physics**, *60th edn.*, C.R.C. Press, Cleveland, U.S.A.

Chapter 5
Measurement of As, Sb and Se by DSI-ICP-MS

5.1 Measurement of As, Sb and Se in Standard Solutions

5.1.1 Introduction

Inductively coupled plasma mass spectrometry (ICP-MS) has been developed into an accurate and sensitive technique for multi-element determinations over a range of sample matrices. However, because of the low resolution of the quadrupole mass filter used in most of the commercially available ICP-MS instruments, a number of spectroscopic interferences have been reported [1, 2]. The detection of both As and Se suffers from polyatomic spectral interferences. The combination of chlorine introduced via the sample with argon from the plasma can give rise to the formation of $^{40}Ar^{35}Cl^{+}$, which interferes with the monoisotopic $^{75}As^{+}$ and polyatomic ions such as $^{40}Ar^{37}Cl^{+}$, $^{38}Ar^{40}Ar^{+}$ and $^{40}Ar^{40}Ar^{+}$ may interfere with the determination of the selenium isotopes ^{77}Se, ^{78}Se and ^{80}Se.

Another problem for the determination of As, Sb and Se is that ICP-MS is less sensitive to As, Sb and Se compared to most elements and it is difficult to determine them accurately at trace levels by the conventional nebulizer method without preconcentration. Separation or preconcentration procedures, such as solvent extraction [3, 4], ion exchange [5, 6], and high-performance liquid chromatography [7, 8] tend to be time-consuming and may lead to contamination.

The most common way to determine As, Sb and Se has been in converting these elements to the gaseous hydrides and transporting the hydrides via an argon stream into the plasma [8, 9, 10]. Hydride generation (HG) involves acid-base reaction, oxidation-reduction, transportation, gas-liquid separation, and possible precipitation of hydrides with transition metals. The HG technique improves sample introduction efficiency, but continuous generation of the hydride introduces relatively large quantities of hydrogen as well as water into the plasma, both of which reduce the ionization efficiency and the stability of the argon plasma. Hydride generation also has severe and complicated chemical interference problems. The problems can come from major matrix components or transition metals.

Another method used to determine As, Sb and Se is electrothermal vaporization (ETV) coupled with ICP spectrometry [11, 12, 13]. In an ETV-ICP system, a measured weight or volume of sample (solid or liquid) is placed on the vaporizer surface and stepped through a controlled heating sequence that produces a highly dispersed dry aerosol. The aerosol is subsequently swept into the plasma by the injector gas, usually argon, where it undergoes decomposition, atomization, ionization, and excitation. ETV shows several advantages over conventional nebulization, such as the possibility of analyzing small samples, the capability to separate the analyte from the matrix using an appropriate temperature program, and the possibility of direct analysis of solid samples. The problem of ETV is analyte transport loss. Analyte vaporized within the ETV sampling cell may condense on passage from the ETV cell to the plasma, leading to a low transport efficiency, generally on the order of 60-80%. Change in transport efficiency will obviously reduce the precision of results obtained in ETV

studies. Severe memory effects can be encountered with some elements, such as As, and the severity may depend on the sample matrix. To solve this problem, some chemical modifiers (e.g. Pd/Mg modifier) are used to reduce the condensation of analytes. But the use of chemical modifiers may cause problems of contamination, spectroscopic interference and matrix suppression.

Compared to the methods mentioned above, direct sample insertion mass spectrometry (DSI-ICP-MS) shows some advantages for the direct analysis of liquid and solid samples, such as the capability to handle small quantities of samples, and removal of sample matrix before insertion, and 100% sample introduction efficiency (The entire sample is presented for vaporization in DSI). An absence of transport problems is a major advantage of DSI introduction over ETV. In this part, the capability of DSI-ICP-MS to simultaneously determine As, Sb and Se in standard solutions will be demonstrated, and the analytical curve figures of merit will be discussed.

5.1.2 Experimental

The Perkin-Elmer/SCIEX Elan 250 ICP-MS coupled with the DSI device described previously was used in this research. The operating parameters are summarized in Table 5.1.

The ionization energies (IE) of arsenic, antimony, and selenium are in the 9-11 eV range. They are known as hard-to-ionize elements under standard ICP-MS conditions and their degree of ionization has been estimated to be

Table 5.1 Summary of DSI-ICP-MS instrumental parameters

A. DSI device:	
Ashing Position:	45 mm below TOLC
Time:	5 s
Atomizing Position:	3 mm below TOLC
Time:	Depends on volatility
B. ICP-MS:	
Power :	2.0 kW
Sampling Depth:	10 mm
Carrier Gas Flow Rate:	1 L/min
Plasma Gas Flow Rate:	13 L/min
Auxiliary Gas Flow Rate:	0.2 L/min
Lens Setting:	Decided by pneumatic system
C. Transient Signal Acquisition	
Dwell Time:	100 ms
Measurement/peak:	1

less than 50% [14]. In order to obtain maximum signal sensitivity and better peak shape with less tailing, a high forward power of 2 kW was used. An atomizing time of 40 seconds was chosen by determining the time to completely evaporate the 10 uL multielement liquid solution residue of As, Sb and Se in the graphite cup. Again, samples were dried under an infrared lamp for 2-3 minutes before insertion. The drying and atomizing parameters are:

	Drying	Atomizing	Cooling
Position/mm (below TOLC)	45	3	180
Time/s	5	40	5

As mentioned previously, the ion lens settings used in DSI were established using a pneumatic nebulizer system, in this case, by running a 1 ppm multielement standard solution and by maximizing for the As signal. No further tuning was required when switching to the DSI system. The ion lens settings are:

Lens	Setting
Bessel Box Barrel (B)	99
Bessel Box Plates (P)	45
Einzel Lens (E1)	99
Photon Stops (S2)	60

The undercut graphite electrodes ASTM# S-15 were purchased from Bay Carbon, Inc., Bay City, Michigan. In order to reduce the amount of

impurities contained in the sample probe, the graphite electrodes were pre-burned in the plasma 3-5 times under regular insertion sequence prior to their use.

All solutions were prepared by serial dilution with distilled/deionized water from 1000 ppm standard stock solution (SPEX Industries Inc., Edison, NJ or LECO Instruments Ltd., Mississauga, ON) of the respective element. The distilled/deionized water was produced in a Millipore Super-Q apparatus (Millipore, Milford, MA).

5.1.3 Results and discussion

5.1.3.1 Signal time profiles

The DSI technique is considered to be particularly effective for the determination of elements such as As and Sb which are less sensitive with the conventional pneumatic nebulization method. The rapid heating and higher temperatures result in sharp and symmetric peak signals. The signals for of 1 ppm As and Sb, and 10 ppm Se measured with the DSI-ICP-MS are shown in Fig. 5.1 for the insertion of a desolvated multielement aqueous sample (10 uL), under the optimized running conditions. The analyte time behavior is element dependent. As shown in Fig. 5.1, Sb has higher sensitivity and a shorter evaporation time than As. For Se, the signal at mass 78 was measured, so as to have low spectral interference and relatively high

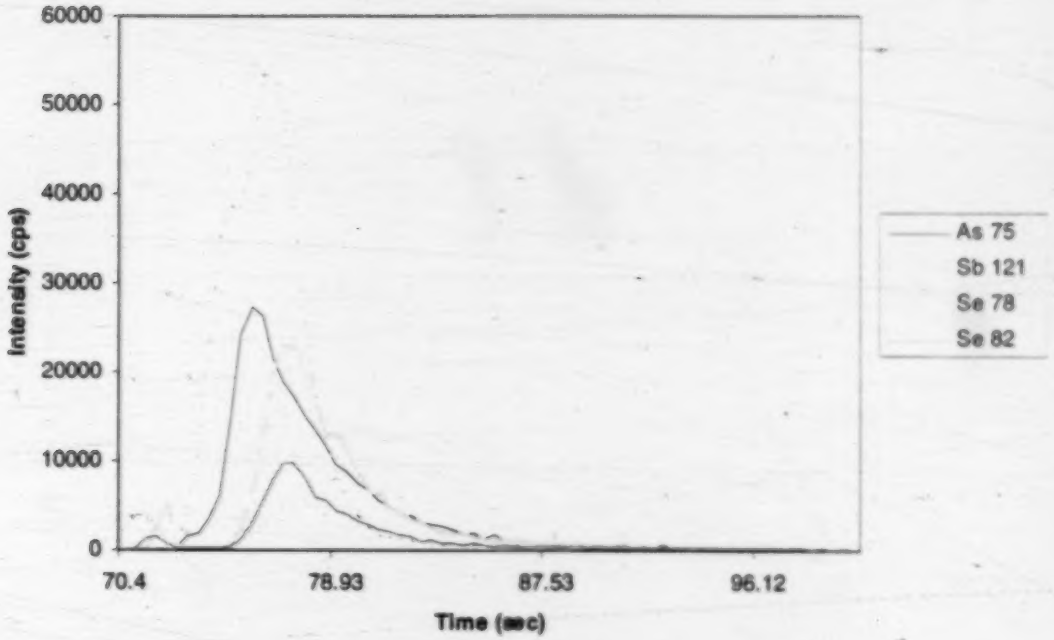

Figure 5.1 Signal time profiles of 1 ppm As, Sb and 10 ppm Se by DSI-ICP-MS

natural abundance. The most abundant ^{80}Se has a major interference caused by Ar_2^+. It should be mentioned that a tendency for a lower peak height was observed as the graphite cup aged in use. Typically, a 30-50% change in sensitivity could be experienced for As after 5 analyses. In order to obtain precise quantitative results, a new graphite electrode was used for each insertion in this study.

Low level signal time profiles for 100 pg As, 100 pg Sb and 1000 pg Se and their respective background time profiles are shown in Fig. 5.2. The background levels for As, Sb and ^{78}Se are about 100, 200, and 120 counts/sec respectively. The potential interference of $^{40}Ar^{35}Cl^+$ on $^{75}As^+$ was investigated by monitoring the background level for $^{75}As^+$. The experiments showed that even on addition of large amounts of Cl (up to 500 ng and 500 times higher than the As concentration) in a 10 uL sample, the background level of $^{75}As^+$ remains constant and low, indicating that the determination of As should not be deteriorated by the presence of Cl. The effect of removing the solvent from the plasma (dry plasma) leads to a significant reduction in the background signal at m/z 75 compared to a conventional nebulization system (wet plasma). It is believed that Cl is eliminated in part below 500 ^0C before the atomization stage of the As, which is a distinct advantage of the DSI sample introduction system. An essentially interference-free determination of As can be fulfilled by DSI-ICP-MS. This result agrees with that found in ETV-ICP-MS [11, 15] and in graphite furnace ICP-MS [16].

5.1.3.2 Effect of Pd/Mg chemical modifier

Chemical modifiers are essential in ETV-ICP-MS to determine elements

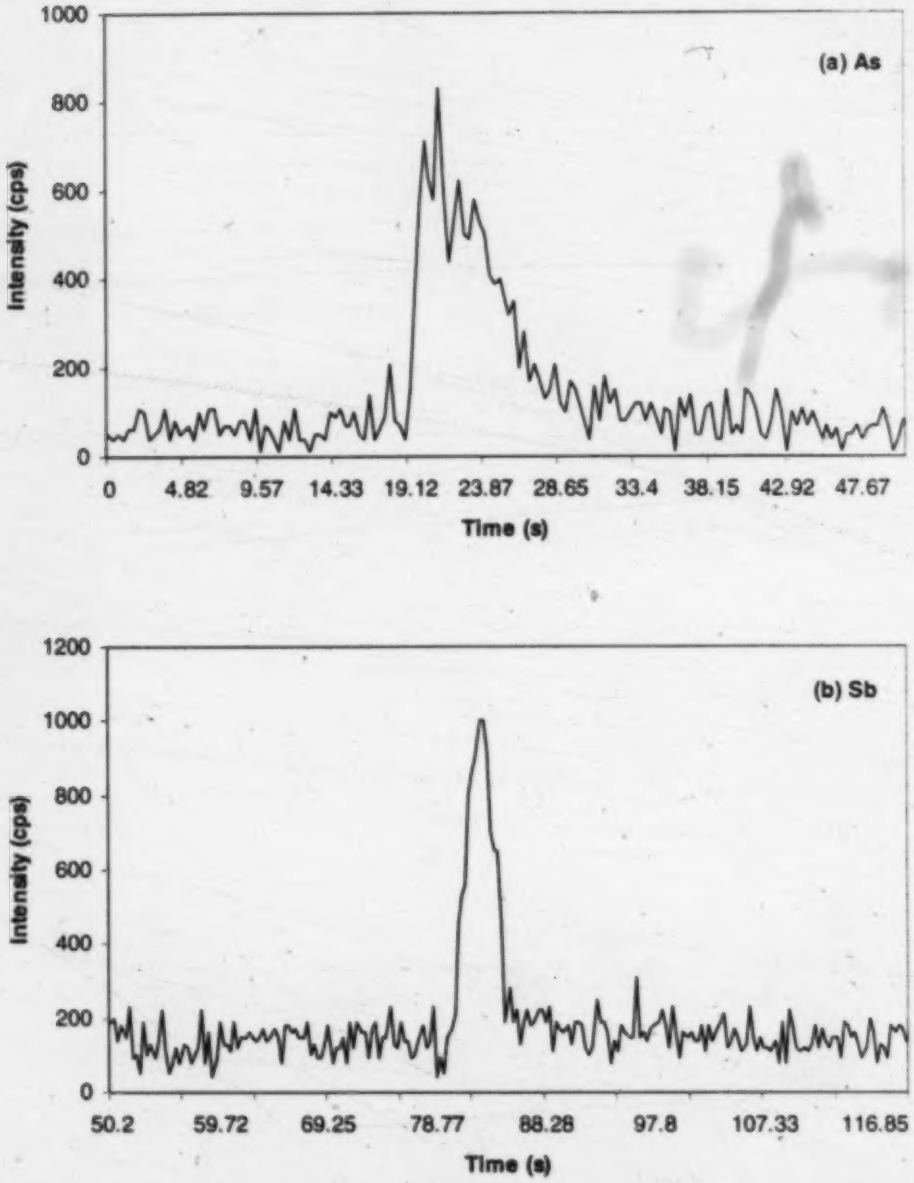

Fig. 5.2 Low level signal time profiles of (a) 100 pg As, (b) 100 pg Sb and (c) 1000 pg Se78

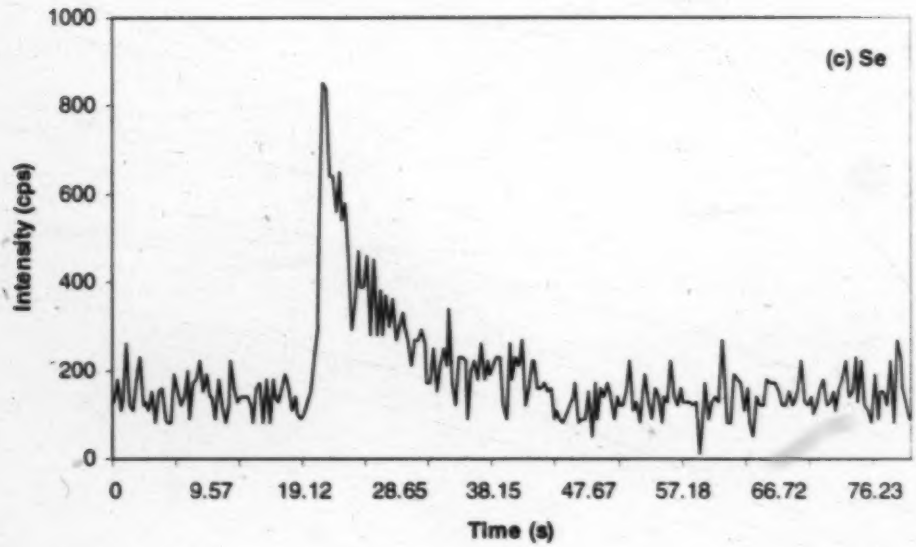

Fig. 5.2 (cont.) Low level signal time profiles of (a) 100 pg As, (b) 100 pg Sb and (c) 1000 pg Se78

like As, Sb and Se [11, 12, 13, 15, 17]. The condensation of the analyte vapor upon transport to the plasma commonly causes poor precision and memory effects from run to run. A chemical modifier can diminish the analyte transport loss, and thus, improve the mass transport efficiency. Chemical modifiers have also been reported to improve thermal stability of some analytes during the drying stage. A palladium and magnesium nitrate or chloride (Pd/Mg) mixed chemical modifier is the most common.

The effect of a Pd/Mg chemical modifier on the signals of As and Sb was investigated in DSI-ICP-MS as follows. The Pd/Mg modifier was prepared from 1000 ppm stock solutions. 10 uL of 1 ppm As and Sb solution was placed on the graphite cup together with 10 uL of the mixed chemical modifier. The mixture was dried and subsequently transported into the plasma for measurements. Fig. 5.3 shows the effect of different amounts of Pd/Mg modifier on the signal intensities (peak area) of 1 ppm As and Sb. The signal time profiles for As and Sb with and without the Pd/Mg modifier are shown in Fig. 5.4. It can be seen that the Pd/Mg modifier does not enhance the signal sensitivities of As and Sb in DSI, as it does commonly in ETV. On the contrary, the signal sensitivities are lower. The investigation shows that chemical modifiers are not necessary in DSI-ICP-MS. The 100% sample introduction efficiency and lack of transport loss problems are important advantages of DSI over ETV.

5.1.3.3 Analytical curve figures of merit

The analytical curve figures of merit obtained under the optimized

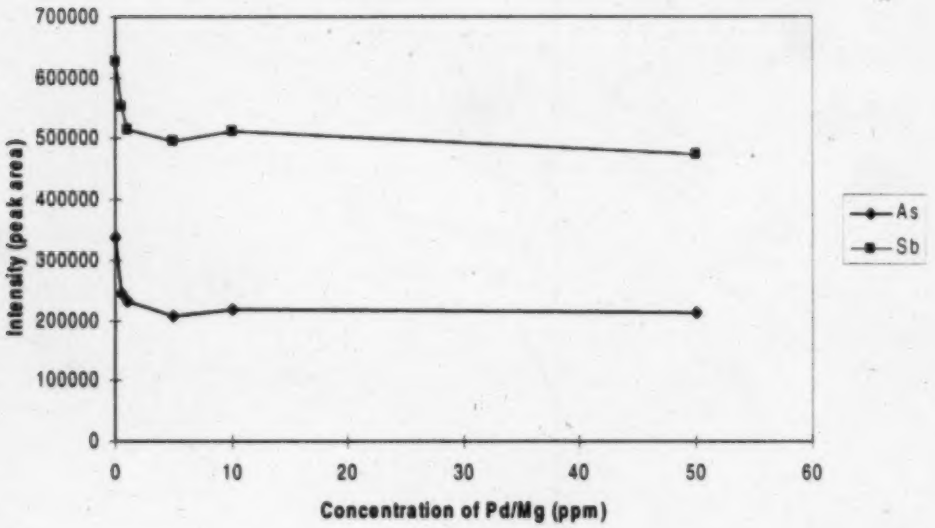

Fig. 5.3 Effect of Pd/Mg chemical modifier on the signal intensities (peak area) of 1 ppm As and Sb

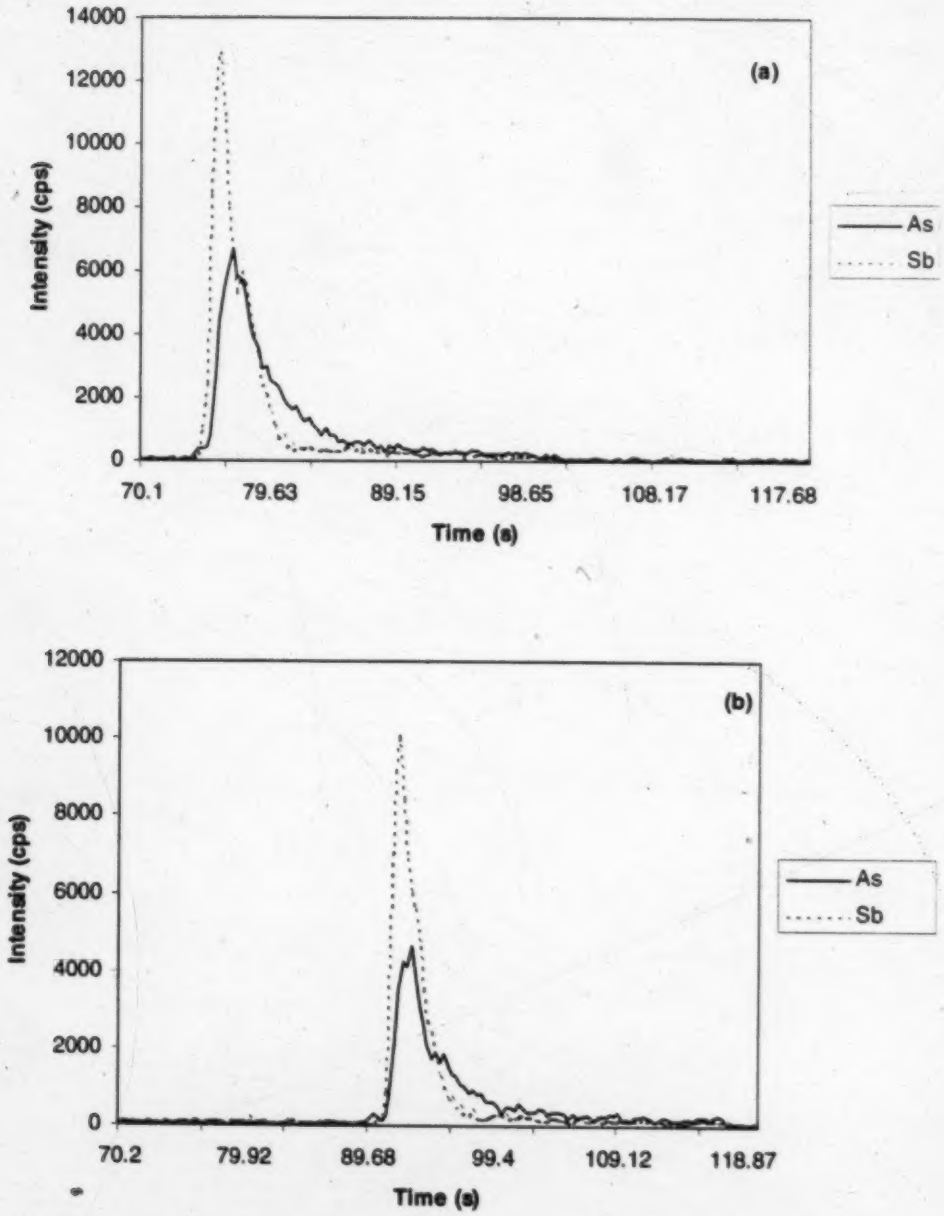

Fig. 5.4 Signal time profiles of 1 ng As and Sb (a) without modifier, and (b) with 500 ng Pd/Mg midifier

instrument conditions, with 10 uL aliquots of the multielement standard solution containing As, Sb and Se, are shown in Table 5.2.

Table 5.2 Summary of analytical curve figures of merit

Element	Detection limit (pg)	Calibration function slope	Correlation coefficient	Internal standard	linear range
As 75	17.2	1.0576	0.9994	5ng In	100
Sb 121	10.05	1.0096	0.9994	5ng In	100
Se 78	281.57	1.0502	0.9993	5ng In	100
Se 82	382.08	N/A	N/A	N/A	N/A

(1) Detection limits

After optimizing the instrumental operating conditions for the DSI-ICP-MS, the detection limits for As, Sb and Se in solution aliquots were determined. For Se, both m/z 78 and 82 were measured, and the detection limit calculated by isotope 78 is slightly better than isotope 82. The detection limit is defined as the analyte concentration corresponding to the signal intensity equal to three times the standard deviation of the blank. Post-insertions of the bare cups are used for the calculation of background standard deviation. The detection limits in Table 5.2 are given on the basis of peak height.

(2) Relative standard deviation (%RSD)

For the quantitative determination of As, Sb and Se in standard solution, Indium could be chosen as a suitable internal standard. The internal standard improves the precision of the measurements by decreasing the

%RSD of the analytes from about 8-10% to about 2-4%. The amount of In was 5 ng (10 uL x 0.5 ppm) in each insertion. The relative intensity is the ratio of analyte peak area to In peak area.

(3) Calibration curve

The calibration curves for As, Sb and ^{78}Se are shown in Fig. 5.5. All calibration curves were established with 5 ng In as the internal standard. Each point on the calibration curve represents an average value based on 5 replicates. It can be seen that excellent calibration curves were established over a dynamic range of at least two orders of magnitude, with correlation coefficients of at least 0.999. The calibration function slope is the slope of the log-log plot. Calibration curves without an internal standard were also established for comparison (not shown), and their calibration function slopes and correlation coefficients were all worse than those obtained with an internal standard.

5.1.4 Conclusion

A multi-element DSI-ICP-MS method for the determination of As, Sb and Se in standard liquid solutions has been tested. The DSI-ICP-MS method shows some important advantages over conventional nebulizer systems and ETV-ICP-MS, due to the dry plasma character and 100% transport efficiency of DSI. The effect of a chemical modifier on signal characters in DSI was also investigated. Good quantitative results were obtained with good precision and low detection limits using 10 uL of solution samples. Excellent calibration curves were established for these elements with the use of an internal standard.

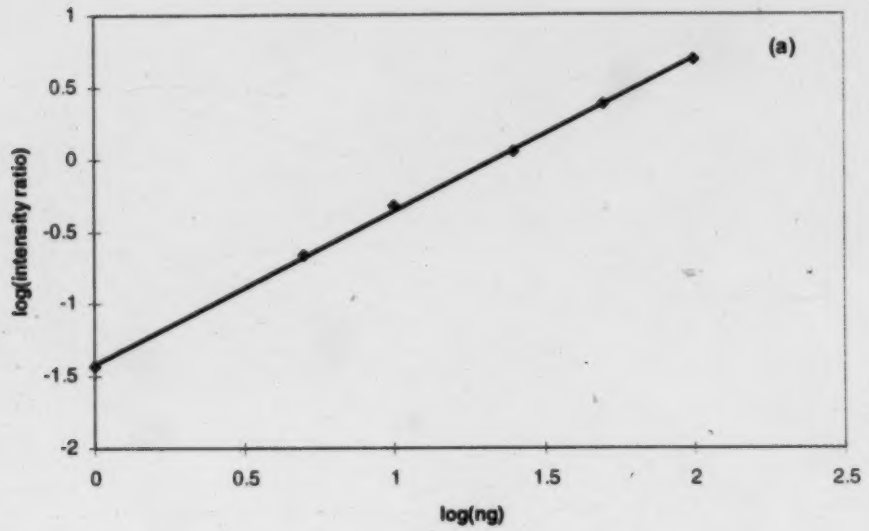

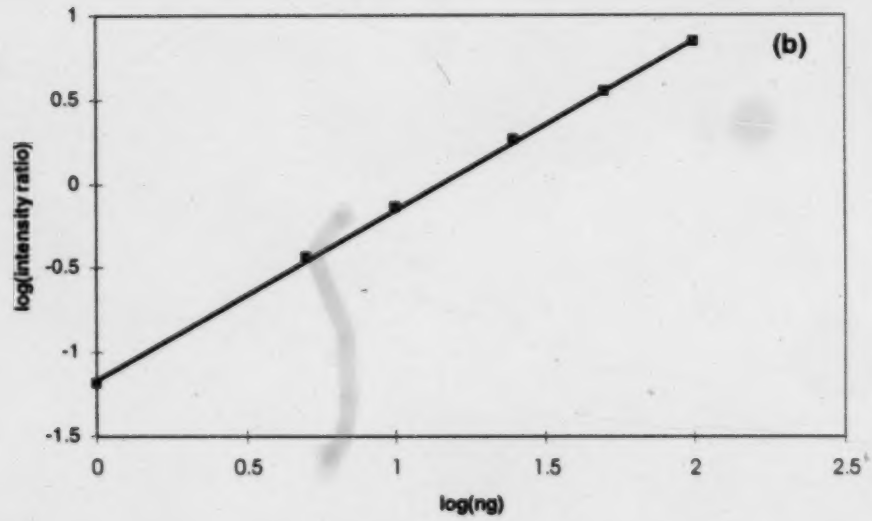

Fig. 5.5 Calibration curves (log-log) of (a) As, (b) Sb, and (c) Se78 with 5 ng In as internal standard

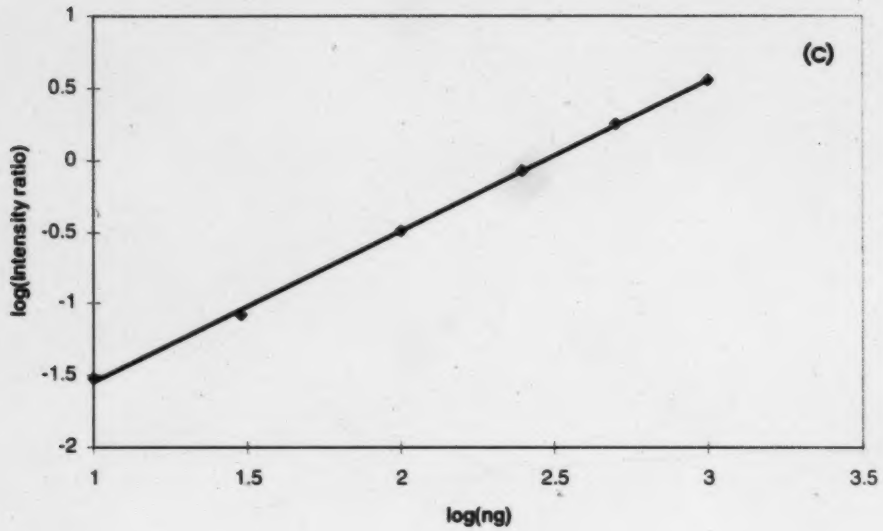

Fig. 5.5 (cont.) Calibration curves (log-log) of (a) As, (b) Sb, and (c) Se78
With 5 ng In as internal standard

5.2 Measurement of As and Sb in Solid Biological Samples

5.2.1 Introduction

There is an ever increasing demand in environmental and biological studies for the development of analytical methods to determine toxic elements such as arsenic and antimony.

The contamination of public water supplies by As is known to cause skin pigmentation changes, keratoses and carcinoma. Arsenic is also recognized as a cumulative poison and carcinogen. Antimony is a non-essential element in plants, animals and humans and its toxicity and biological effect is similar to that of arsenic. Since concentrations of these elements existing even in sub-ug/g or ng/g levels can exhibit significant effects on environmental and biological systems, highly sensitive and reliable methods for their determinations in various samples need to be developed.

In this part, an analytical procedure for the direct and simultaneous determination of As and Sb in powered plant materials by DSI-ICP-MS was developed. As and Sb were determined in a number of standard reference materials, so that by comparing the results obtained with the certified values, the accuracy could be evaluated. A discussion on the applicability of various methods of calibration (external calibration using both liquid and solid standards and standard addition) will be presented.

5.2.2 Experimental

The DSI-ICP-MS instrumentation was described previously. The undercut graphite electrodes ASTM# S-14 (Bay Carbon, Inc., Bay City, Michigan) were used for solid samples because their deep crater can hold more sample and reduce sample spattering. In order to reduce the amount of impurities in the sample probe, the graphite electrodes were pre-burned in the plasma 3-5 times under regular insertion sequence prior to their use.

The solid samples which included spinach SRM 1570, tomato leaves SRM 1573, pine needles SRM 1575, orchard leaves SRM 1571, and pepperbush NIES SRM No.1 were used directly without further treatment except for homogenization (by shaking). The solid samples were weighed using a micro-balance and placed in the graphite cup.

The addition of internal standard was performed by adding 10 uL of 0.5 ppm In (5 ng) standard solution onto a graphite cup, and drying it under a infrared lamp for 2-3 minutes, before weighing the solid sample.

One of the characteristics of DSI-ICP-MS instrumentation is the horizontal insertion of the sample probe required by the mass spectrometry interface. As mentioned previously, 20 uL of 1% sugar solution was applied on the top of the solid sample, and then dried under infrared lamp for 3 minutes. The sugar coating after drying prevents loss of sample during the insertion sequence.

The ashing and atomizing parameters are:

	Ashing	Atomizing	Cooling
Position/mm (below TOLC)	45	3	180
Time/s	30	40	5

With the ashing time of 30 seconds, most of the organic component of the powdered botanicals is removed before insertion.

5.2.3 Results and discussion

The As and Sb signals for 6.2 mg spinach SRM 1570, 6.0 mg tomato leaves SRM 1573, 6.1 mg pine needles SRM 1575, 2.2 mg orchard leaves SRM 1571, and 5.0 mg pepperbush NIES SRM No.1 are shown in Fig. 5.6. The measured As and Sb concentrations in SRMs are summarized in Table 5.3. The results are based on four calibration methods: external calibration by liquid standard solutions, standard addition, external calibration by different SRMs, and external calibration by same SRM with different masses.

(1) External calibration by liquid standard solutions

If completely reliable, external calibration using liquid standard solutions would be the most straightforward and fastest way to determine the As and Sb content in the materials analyzed. As recommended by many analysts, it is essential to use an internal standard to compensate the matrix effects. When using In as internal standard for the determination of As and Sb, an

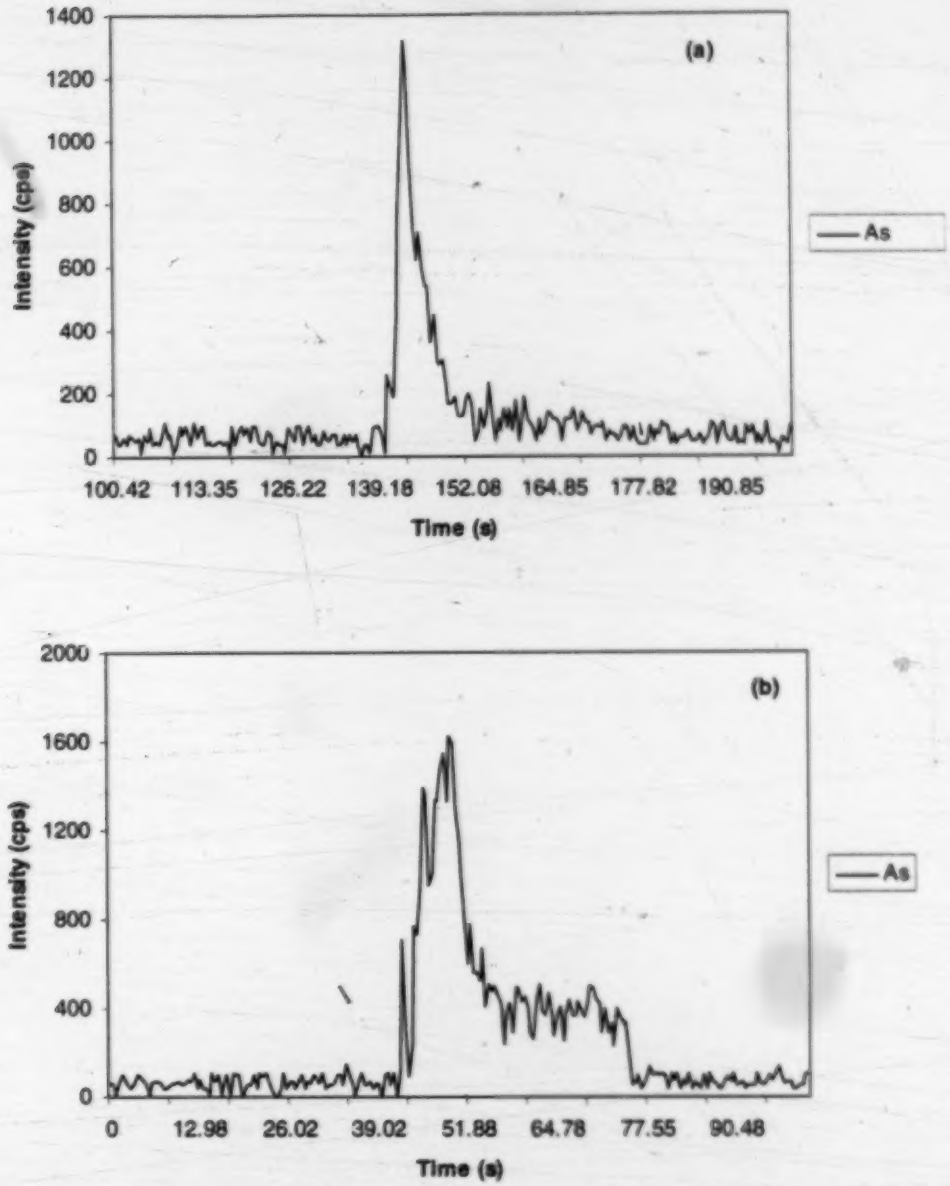

Fig. 5.6 As and Sb signal time profiles of (a) 6.2 mg spinach, (b) 6.0 mg tomato leaves, (c) 6.1 mg pine needles, (d) 2.2 mg orchard leaves and (e) 5.0 mg pepperbush

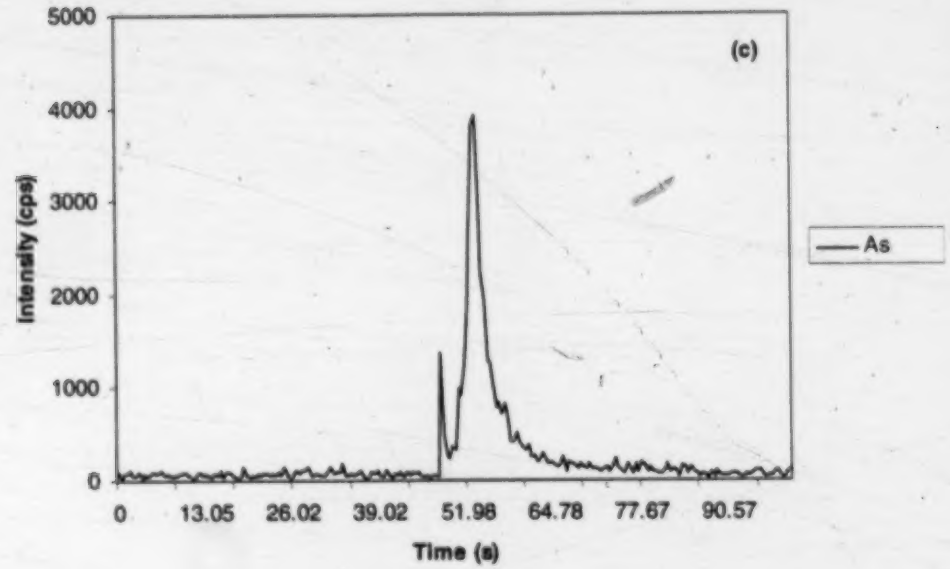

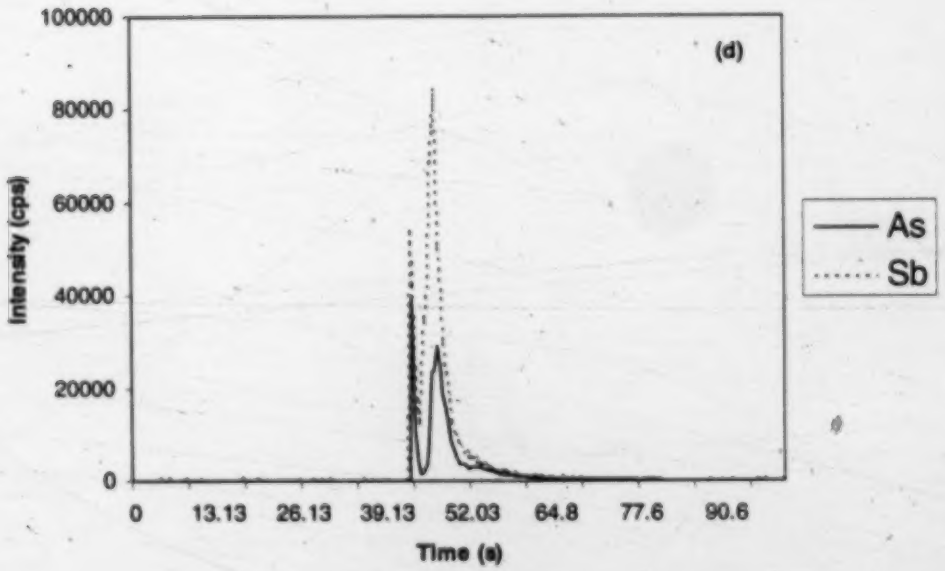

Fig. 5.6 (cont.) As and Sb signal time profiles of (a) 6.2 mg spinach, (b) 6.0 Mg tomato leaves, (c) 6.1 mg pine needles, (d) 2.2 mg orchard leaves and (e) 5.0 mg pepperbush

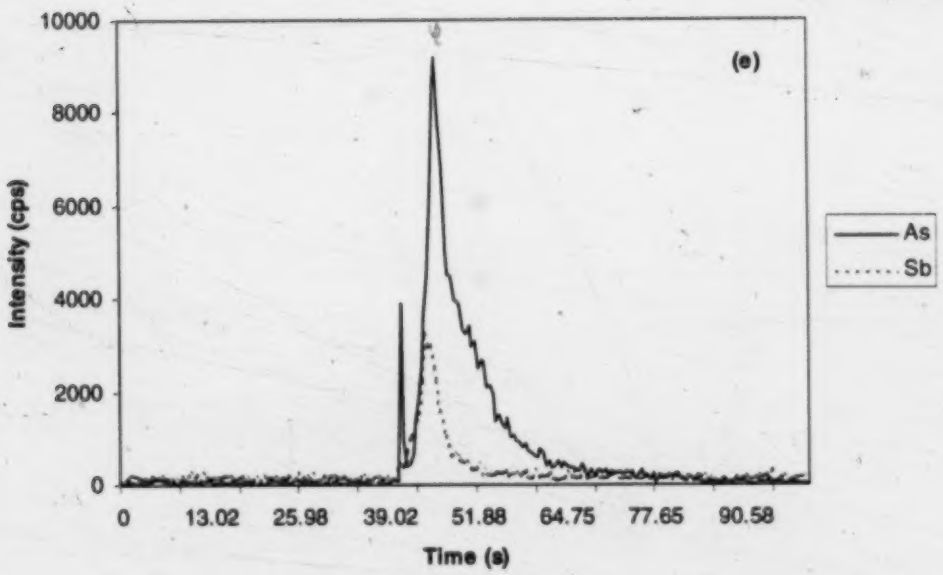

Fig. 5.6 (cont.) As and Sb signal time profiles of (a) 6.2 mg spinach, (b) 6.0 mg tomato leaves, (c) 6.1 mg pine needles, (d) 2.2 mg orchard leaves and (e) 5.0 mg pepperbush
(Note: no detectable Sb signal in spinach, tomato leaves and pine needles)

Table 5.2 Measurement of As and Sb in plant samples

Calibration method	Element	correlation coefficient	SRM	Certified value(ug/g)	Measured value(ug/g)	recovery%	RSD%
external calibration using standard solutions (In as internal standard)	As	0.9998	orchard leaves	10	4.0	40%	7.0%
	Sb	0.9998		2.9	2.9	99%	7.8%
external calibration using different mass of orchard leaves	As	0.9996	spinach	0.15	0.15	100%	17.7%
	Sb	0.9996		N/A	N/A	N/A	
	As		tomato leaves	0.27	0.28	105%	2.0%
	Sb			N/A	N/A	N/A	
	As		pepperbush	2.3	2.4	102%	8.7%
	Sb			N/A	0.1	N/A	7.8%
external calibration using SRMs	As	0.9999	pepperbush	2.3	2.0	86%	4.5%
standard addition	As	0.9992	orchard leaves	10	11	111%	2.8-23.8%
	Sb	0.9950		2.9	2.9	101%	8.1-14.3%
	As	0.9965	pepperbush	2.3	2.3	101%	1.0-9.2%
	Sb	0.9988		N/A	0.1	N/A	3.2-9.0%

aliquot of 10 uL of 0.5 ppm In solution was transferred into the sample probe using a micropipette, the probe was subsequently dried using an infrared lamp and was then loaded with solid sample as described. The concentrations of the aqueous standards containing internal standard were carefully chosen so that the values in the unknown solids are within the calibration curve range. From the results shown in Table 5.3, it can be seen that an accurate result was achieved for Sb, but a much lower value was obtained for As in orchard leaves. It is assumed that As experiences a much higher matrix effect (suppression) than Sb in plant tissues with similar origin. The internal standard works well for Sb, but not for As. Another internal standard (Te) was also tested, but the same results were obtained. The use of liquid standards may not allow for the adequate correction for matrix effects, even with the use of an internal standard. In order to measure As and Sb simultaneously in plant tissues, other calibration methods must be investigated for accurate results.

(2) Standard addition

The method of standard addition may be thought of as a more ideal method for the correction of matrix suppression effects since each analyte is essentially used as its own internal standard. For accurate quantification, the spike should contain at least the same absolute amount of analyte as the sample.

For calibration by standard addition, 10 uL of As and Sb solution of appropriate concentration was transferred into the sample probe and dried using an infrared lamp after solid sample loading. The method of adding

spikes before sample loading was also tested, but a non-linear calibration curve was obtained. The reason for this behavior is not clear and a detailed explanation would require more investigation. Fig. 5.7(a) shows the As and Sb signal time profiles for a 1 ppm liquid sample solution. Fig. 5.7(b) shows the signal profiles of As and Sb in 2.5 mg orchard leaves without a spike. Fig. 5.7(c) shows the signal profiles of As and Sb in 2.5 mg orchard leaves spiked with 60 ng As and 20 ng Sb. It can be seen that the sample with As and Sb spikes (added after the samples) gives rise to analogous analyte profiles as observed for the solid samples. Hence, under these conditions, a similar behavior between As and Sb coming from the solid samples and from the liquid spikes can be assumed.

The calibration curves for As and Sb constructed by the standard addition method for orchard leaves and pepperbush are shown in Fig. 5.8 and Fig. 5.9. For each data point, three or four replicate burns were made and the average intensity values were used. The %RSD of three or four measurements fell in the range of 3-15% (for orchard leaves) and 1-9% (for pepperbush). The As and Sb contents calculated by this method are shown in Table 5.3. The results agree well with the certified values, with the recovery ranging between 93% and 110%. It should be mentioned that the concentration of spikes chosen for orchard leaves is not suitable for pepperbush; but because it is a time-consuming method, no further work has been done on it.

The standard addition method is a relatively accurate method to analyze solid samples with a complex matrix. With a carefully chosen concentration

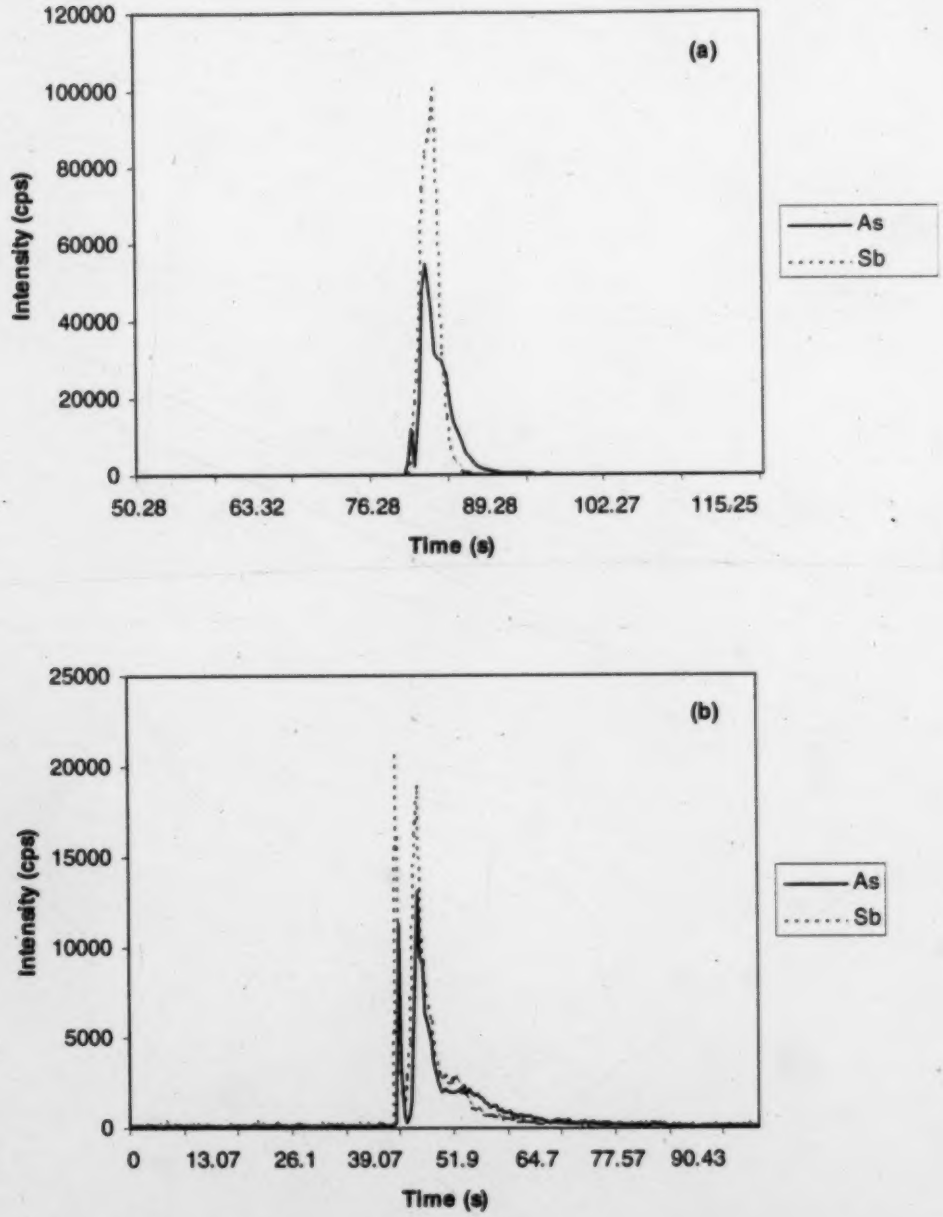

Fig. 5.7 As and Sb signal time profiles in (a) 1 ppm As and Sb liquid solution, (b) 2.5 mg orchard leaves, (c) 2.5 mg orchard leaves spiked with 60 ng As and 20 ng Sb

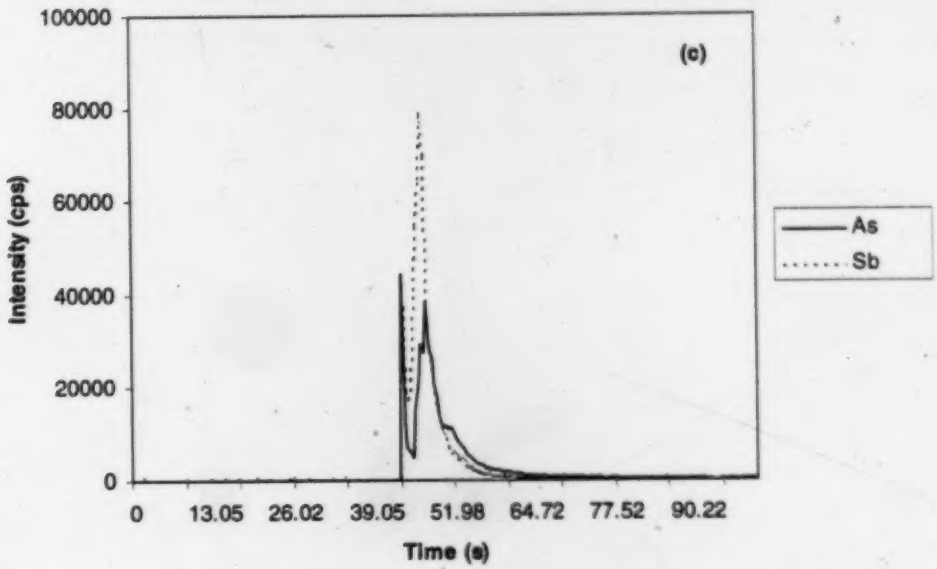

Fig. 5.7 (cont.) As and Sb signal time profiles in (a) 1 ppm As and Sb liquid solution, (b) 2.5 mg orchard leaves, (c) 2.5 mg orchard leaves spiked with 60 ng As and 20 ng Sb

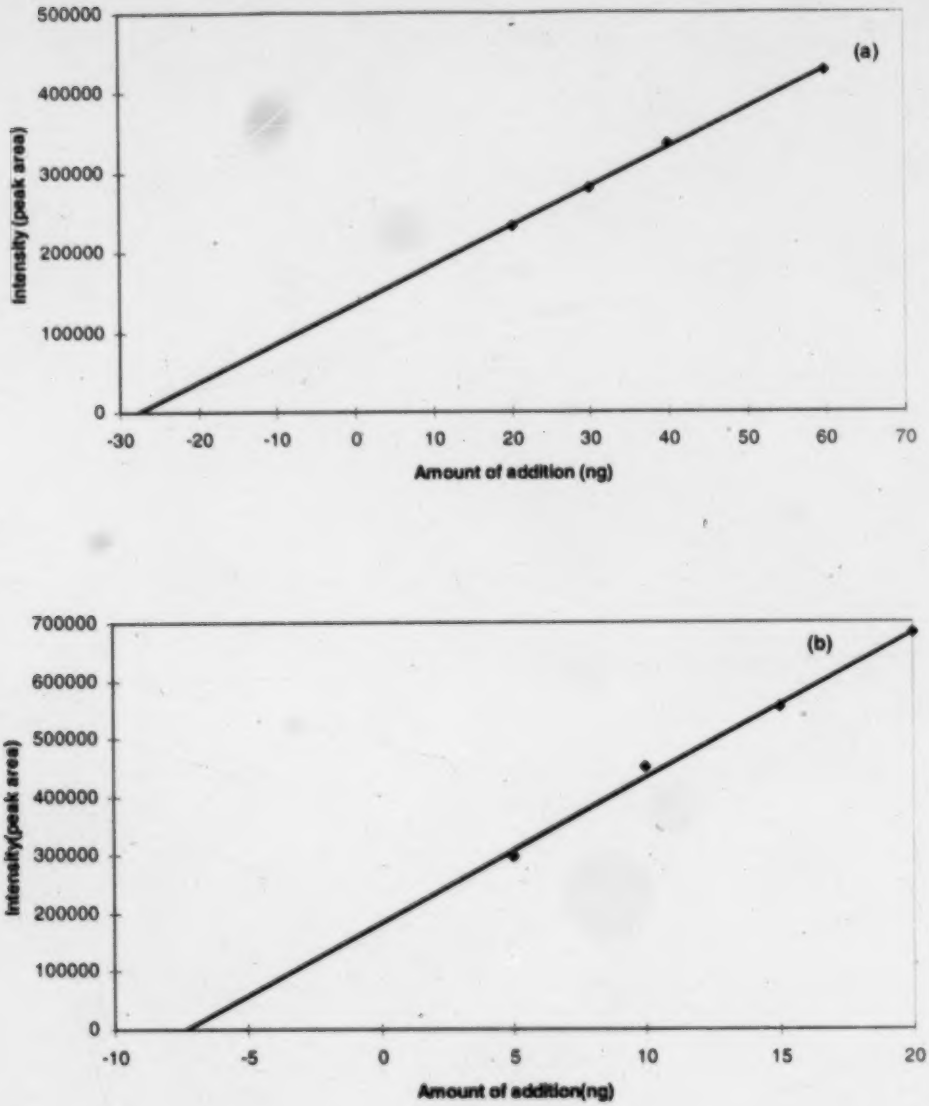

Fig. 5.8 Calibration curves of (a) As and (b) Sb in orchard leaves by standard addition method

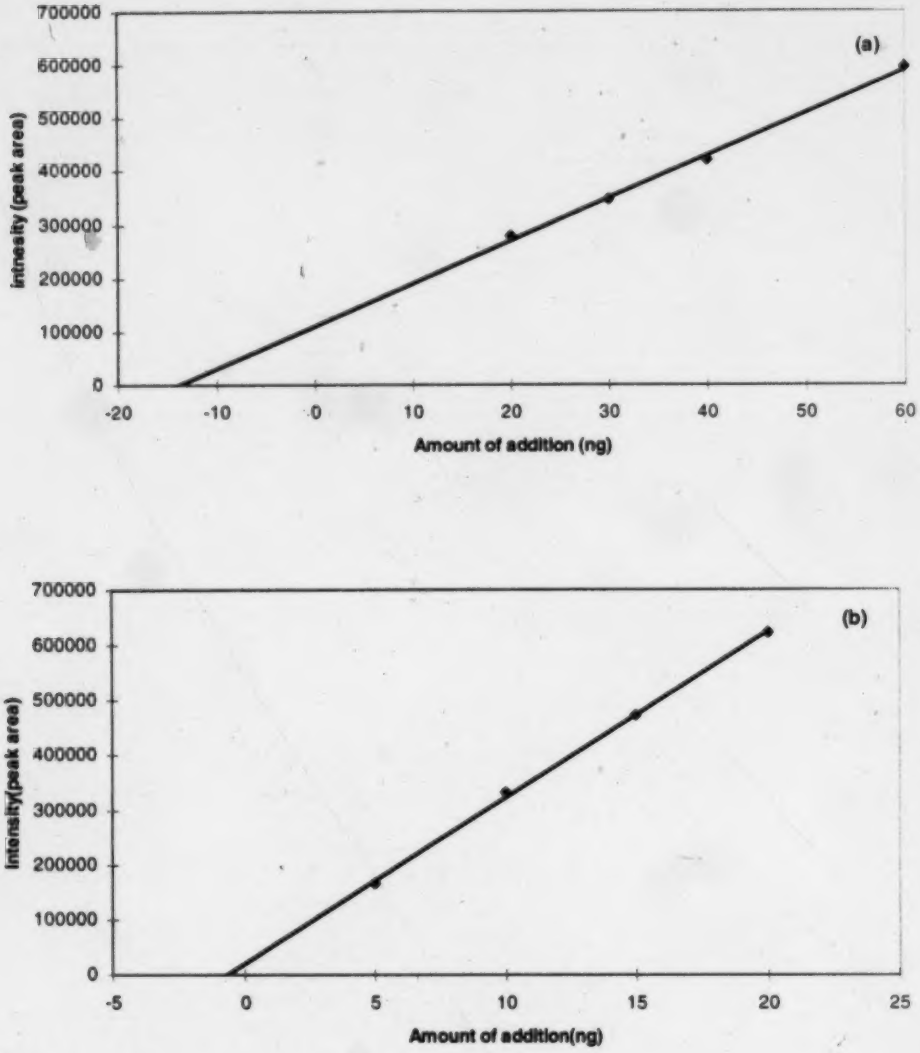

Fig. 5.9 Calibration curves of (a) As and (b) Sb in pepperbush by standard addition method

range of spikes, As and Sb can be determined simultaneously in plant tissues by this method. The drawback of this method is that it is very time-consuming, in that only one determination can be made for each calibration curve.

(3) External calibration by different SRMs

The use of SRMs as calibrants with similar matrix composition and analyte content to that of the sample to be analyzed is a well-known procedure in solid sampling, and the success of this method has been demonstrated in the measurement of lead in plant tissues in Chapter 3.

A calibration curve for As based on 6.2 mg spinach SRM 1570, 6.0 mg tomato leaves SRM 1573, 6.1 mg pine needles SRM 1575, and 2.2 mg orchard leaves SRM 1571 is shown in Fig. 5.10. Three random weighs of pepperbush sample (5.0 mg) were measured as an unknown sample. For each data point, three replicate runs were made and the average intensity values were used. The %RSD of the three measurements ranges between 4-16%. Because the As content in spinach (0.15 ug/g), tomato leaves (0.27 ug/g) and pine needles (0.21 ug/g) are quite close to each other, and much lower than that in orchard leaves (10 ug/g), an awkward calibration curve (i.e. basically two points) was obtained. The measured As concentration in pepperbush (recovery 86.4%) by this calibration curve, shown in Table 5.3, is worse than that obtained by the standard addition method (recovery 101%). On the other hand, because there are no certified values for Sb in spinach, tomato leaves and pine needles, the Sb calibration curve can not be established, and the Sb concentration in pepperbush can not be acquired.

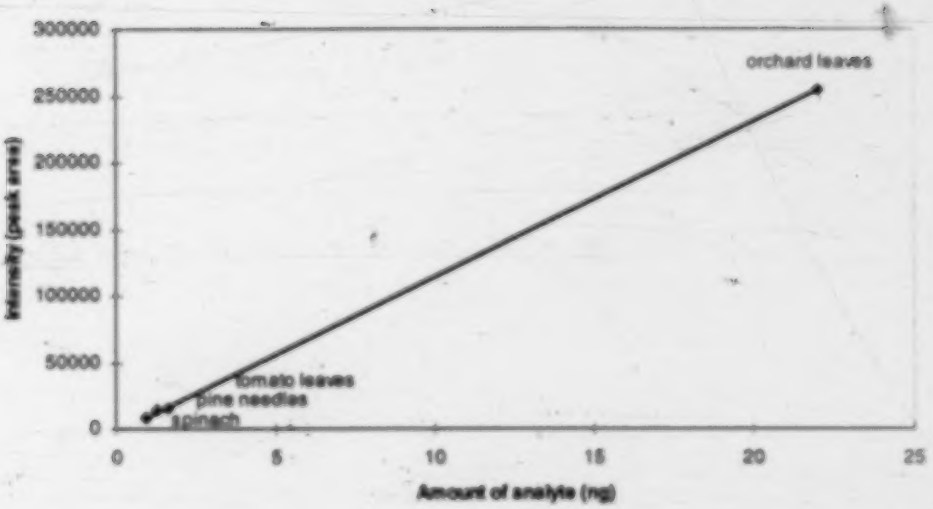

Fig. 5.10 Calibration curve of As containing four SRMs: spinach, pine needles, tomato leaves, and orchard leaves

(4) External calibration by same SRM with different masses

A final solution to measure As and Sb content in solid samples is the use of different weights of a standard reference material with a known analyte concentration with similar matrix to the samples to be determined. Essentially, it is another matrix-matching method, and has been investigated by some researchers [11, 18] in ETV-ICP-MS. In this study, orchard leaves with certified As and Sb values was chosen as the calibration standard, and spinach, tomato leaves and pepperbush were tested as unknown samples.

Two calibration curves, shown in Fig. 5.11, were constructed for As and Sb from a series of increasing weights of orchard leaves SRM whose elemental concentrations were calculated from the certified values. The quality of the linear curve fit to these data is shown by the correlation coefficient. For this analysis a value of 0.9996 (for both As and Sb) was obtained for 0.55-4.7 mg solid samples. For each data point, three replicate runs were made and the average intensity values were used. The results of spinach, tomato leaves and pepperbush obtained by this method are shown in Table 5.3. It can be seen that the results for As concentration agree well with the certified values, with recoveries 100% in spinach, 105% in tomato leaves, and 102% in pepperbush. The %RSD of the three measurements of the "unknown" samples is in the range of 3-18%, reasonable, considering the small amount of sample that was used. The Sb content in pepperbush agrees with the value obtained by the standard addition method (no certified value available), whereas the concentration of Sb in spinach and tomato leaves is too low to be detected. The excellent results obtained by this calibration

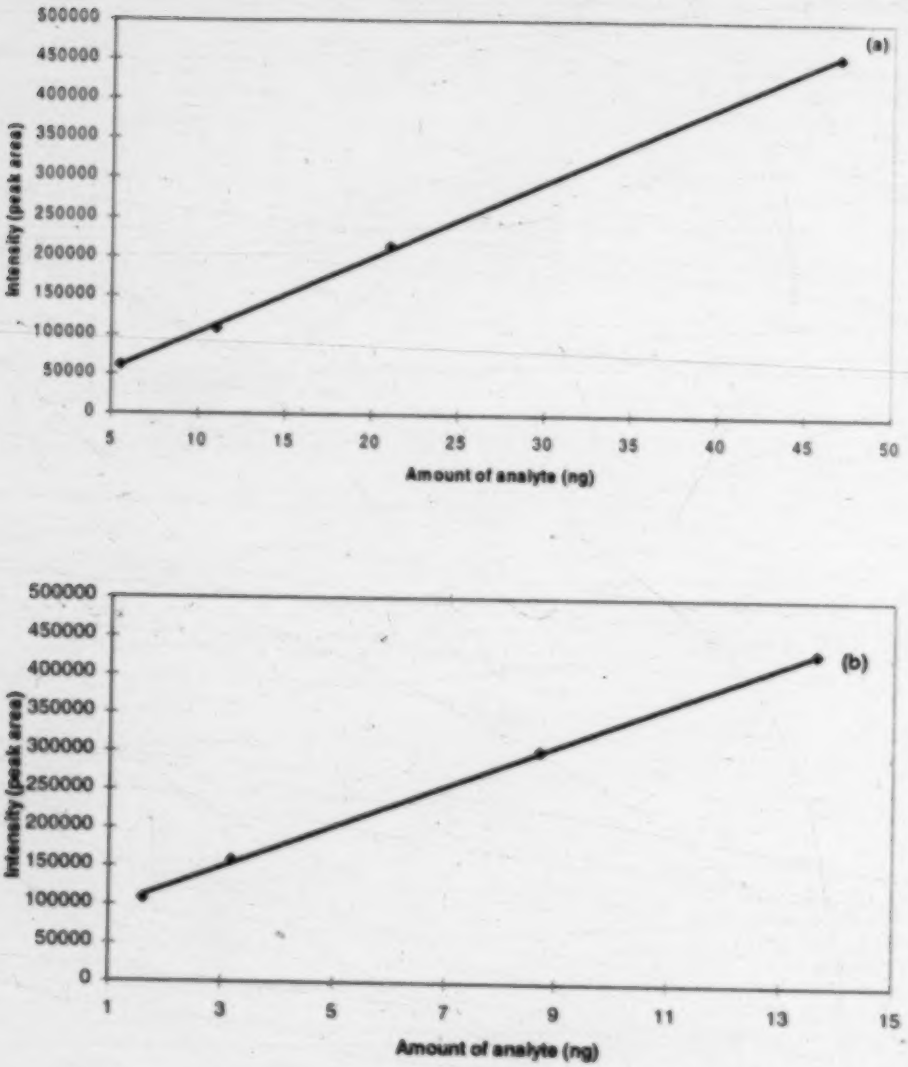

Fig. 5.11 Calibration curves of (a) As, and (b) Sb containing different weights of orchard leaves

method can be explained in that the solid standards and the solid unknowns are similar. Thus calibration by different weights of the same SRM has potential application for the direct analysis of solid materials if the solid samples are similar to the solid standard reference material.

5.2.4 Conclusion

The direct analysis of As and Sb in solid samples by DSI-ICP-MS has been demonstrated, yielding reasonable results for a variety of standard reference materials. This method provides a reliable alternative to traditional means of solid sample analysis, as the sample pre-treatment procedures are eliminated or minimized. Four calibration methods for the determination were investigated. External calibration using different weights of a solid standard reference material (SRM), when available, with a composition as similar as possible to that of the sample, provides the best performance, allowing accurate and simultaneous measurements of As and Sb in plant tissues.

References

1. Vaughan, M. A., and Horlick, G., **Appl. Spectrosc**. 1986, *40*, 434-445
2. Tan, S. H., and Horlick, G., **Appl. Spectrosc**. 1986, *40*, 445-460
3. McLeod, C.W., Otsuki, K., Okamoto, K., Haraguchi, H., and Fuwa, K., **Analyst**, 1981, *106*, 419-423
4. Wang, J., Tomlinson, M. J., and Caruso, J. A., **J. Anal. At. Spectrosc.**, 1995, *10*, 601-607
5. Crock, J. G., and Lichte, F. E., **Anal. Chem.**, 1982, *54*, 1329-1334
6. Ko, F.-H., and Yang, M.-H., **J. Anal. At. Spectrosc.**, 1996, *11*, 413-420
7. Thomas, P., and Sniatecki, K., **J. Anal. At. Spectrosc.**, 1995,*10*, 615-618
8. Smichowski, P., Madrid, Y., De La Calle Guntinas, M. B., and Camara, C., **J. Anal. At. Spectrosc.**, 1995, *10*, 815-821
9. Hahn, M. H., Wolnik, K. A., Fricke, F. L., and Caruso, J. A., **Anal. Chem.**, 1982, *54*, 1048-1054
10. Zhang, L. S., and Combs, S. M., **J. Anal. At. Spectrosc.**, 1996, *11*, 1049-1054
11. Vanhaecke, F., Boonen, S., moens, L., and Dams, R., **J. Anal. At. Spectrosc.**, 1995, *10*, 81-87
12. Boonen, S., Vanhaecke, F., Moens, L., Dams, R., **Spectrochim. Acta**, *51B*, 1996, 271-278
13. Fairman, B., and Catterick, T., **J. Anal. At. Spectrosc.**, 1997, *12*, 863-866
14. Jarvis, K. E., Gray, A. L., and Houk, R. S., **Handbook of Inductively Coupled Plasma Mass Spectrometry**, Blackie & Sons, Glasgow, 1992
15. Gregoire, D. C., and de Lourdes Ballinas, M., **Spectrochim. Acta**, 1997, *52B* , 75-82

16. Carey, J. M., Evans, E. H., and Caruso, A., **Spectrochim. Acta**, 1991, *46B*, 1711-1721

17. Pozebon, D., Dressler, V. L., and Curtius, A. J., **J. Anal. At. Spectrosc.** 1998, *13*, 7-11

18. Wang, J., Carey, J. M., and Caruso, J. A., **Spectrochim. Acta**, 1994, *49B*, 193-203

Chapter 6
Conclusion and Future Work

Solution nebulization has been and, for the foreseeable future, will continue to be the primary means of introducing samples into the ICP. However, a large percentage of samples which are analysed by ICP spectrometry originate as solids of various types (metals, soils, rocks, sediments, biological materials) or as liquids which are obtainable only in very limited volumes (biological fluids). Direct sample insertion (DSI), where the sample is place into a sample carrying probe which is subsequently inserted directly into the core of the plasma, is one of the alternative sample introduction techniques that can conveniently handle both solid samples and small volume solution samples. The analytical performance of DSI-ICP-MS has been studied in this thesis.

In order to use DSI-ICP-MS efficiently, it is necessary to know the effect of the instrumental operating parameters on the analytical signals. Characterising and optimising the parameters of both DSI and ICP-MS make up the first part of the thesis. Basically, a higher power (at least 1.5 kW) should be used in DSI because of the cooling effect of the sample carrying probe. The atomizing position is also critical for DSI signals, and a position of 3 mm below TOLC was found for this DSI-ICP-MS system. The transient signal acquisition parameters were also investigated in this part. The "peak-hopping" mode provides some multielement capacity, the extend of which depends upon dwell time and the elements (masses) scanned. In general, when four elements (masses) are determined simultaneously, a 100 ms dwell time is a suitable compromise to define the transient signal

behaviour properly with an adequate number of data points and low detection limits.

With the optimized instrumental conditions, the analytical performance of DSI-ICP-MS was demonstrated with liquid standard solutions containing Pb, Bi, In, Ag, Fe, Co, Mn, Cu, Ga, As, Sb and Se. The detection limits are in the low-pg range, except Se. With the use of internal standards, excellent calibration curves can be established for these elements, over a dynamic range of at least two orders of magnitude. The correlation coefficient of log-log plot is from 0.999 to 1.000, and the calibration function slope is about 1. The internal standard decreases the %RSD of the analyte signals from about 10% to less than 3%. In DSI, The effect of removing the solvent from the analyte before the final insertion ("dry plasma") leads to a significant reduction of background signals such as $^{40}Ar^{16}O^{+}$ and $^{40}Ar^{35}Cl^{+}$, and Fe and As can be determined at trace level with minimum interference.

On the basis of the excellent performance for liquid solutions, the DSI technique was extended to the direct analysis of real solid biological samples. The direct measurements of toxic element Pb, As and Sb were investigated in standard reference materials (SRMs), without any labour intensive sample pre-treatment. In comparing different calibration methods, external calibration by SRMs with similar organic origin was found to be a reliable method for the accurate measurement of Pb concentration in a similar sample. For the measurements of As and Sb, external calibration using different weights of a SRM with a composition as similar as possible to that of the sample provides the best performance, allowing accurate and simultaneous measurements of As and Sb in plant tissues. The measured

results agreed well with the certified values. The %RSD was in a range of 1%-15%, reasonable in consideration of run-to-run difference, instrument drift and solid sample inhomogeneity due to the small amount of sample (<10 mg) in use. DSI-ICP-MS provides a reliable alternative to traditional means of solid sample analysis, as the sample pre-treatment procedures are eliminated or minimized. /

The future work will focus on the direct analysis of other types of biological samples, including human and animal tissues, human blood. It is believed that DSI-ICP-MS will be particularly efficient for the analysis of these types of samples, because of the small sample amount required by DSI and the low detection limits of ICP-MS.

Additionally, the use of solid internal standard will be studied in the future work. The method of compensating for a matrix effect is effective only if the analyte and internal standard experience the same matrix effect. The liquid internal standards used in this thesis do not allow for the adequate correction for the matrix effect because of their different physical and chemical states. The use of synthetic solid internal standard may be a solution to this problem.

Finally, the rather slow scan speed with the current quadruple mass spectrometer limited the multielement capability of DSI technique. Time-of-flight mass analysers have been coupled to the ICP in recent years. These mass analysers are capable of measuring full mass spectra at rates of up to 20000 spectra per second with the ions of each spectrum being simultaneously extracted from the plasma. Consequently, such instruments

appear ideally adapted to the rapid transient sample introduction technique such as DSI. Interfacing the DSI-ICP to the time-of-flight mass spectrometer would be of great interest for future work.